

Diss ETH Nr. 14643

**Molecular mechanism of the ATP synthase's  
F<sub>o</sub> motor probed by  
mutational analyses of subunit a**

A dissertation submitted to the

SWISS FEDERAL INSTITUTE OF TECHNOLOGY ZÜRICH

for the degree of

DOCTOR OF NATURAL SCIENCES

presented by

FRANZISKA WEHRLE

Dipl. Natw. ETH

born May 10, 1972

from Muolen (SG)

accepted on the recommendation of

Prof. Dr. P. Dimroth, examiner

Prof. Dr. M. Aebi, co-examiner

PD Dr. G.Kaim, co-examiner

Zürich 2002



Was wir wissen, ist ein Tropfen,  
was wir nicht wissen, ein Ozean.

Isaac Newton



# DANK

Viele Leute haben in irgendeiner Weise zum Gelingen dieser Arbeit beigetragen. Allen möchte ich danken, auch dafür, dass mir diese Zeit in guter Erinnerung bleiben wird.

Mein Dank gilt Herrn Prof. P. Dimroth für die interessante Aufgabenstellung und dass er mir die Möglichkeit gegeben hat, diese Doktorarbeit in seiner Arbeitsgruppe auszuführen.

Ich danke Herrn Prof. M. Aebi für die Übernahme des Koreferates und die sorgfältige Durchsicht meiner Arbeit.

Georg möchte ich danken für die Betreuung während meiner Arbeit und die dabei gewährte Freiheit, sowie die Erweiterung meiner Kenntnisse in Bayrischer Kultur (i.e. Weisswurst, Weissbier, ..... und v.a. Brezen mit süssem Senf).

Ein grosser Dank gilt auch den Mitgliedern vom A-Team: Thomi, der mich auch während unseres Exiljahres im D11 unterstützt hat; Yvonne, die sich während ihrer Diss bereits mit der Reinigung der aUE rumgeschlagen hat; Diana, die in ihrer Diplomarbeit erste Mutanten hergestellt hat; Uli, der mich mit diversen "Koch"anleitungen versorgt hat. Ebenso ein herzlicher Dank an Christoph, Beni und Sandy, die mit beigetragen haben zur angenehmen Arbeitsatmosphäre.

Danke auch an alle jetzigen und ehemaligen Mitglieder der AG Dimroth für die kollegiale Arbeitsatmosphäre und die Hilfsbereitschaft bei kleineren und grösseren Steinen, die aus dem Weg geräumt werden mussten. In besonderer Erinnerung werde ich auch die unzähligen geselligen Abende und Skiwochenenden behalten.

Allen Mitgliedern des Instituts danke ich für das gute Arbeitsklima und die Hilfsbereitschaft – nicht zu vergessen die Guten Geister des Hauses, die immer dafür sorgen, dass alles gut läuft.

Schliesslich ein riesiges Dankeschön an meine Eltern und meine Geschwister, ohne deren Aufmunterung und Unterstützung diese Arbeit nicht möglich gewesen wäre. Und ganz besonders danke ich Markus für seine Motivation in schwierigen Situationen, und dass er mit im richtigen Augenblick gezeigt hat, dass es neben dem Labor noch andere wichtige Dinge gibt.



## TABLE OF CONTENTS

SUMMARY	1	
KURZFASSUNG	3	
CHAPTER 1:	GENERAL INTRODUCTION	6
	1.1 Molecular architecture of F <sub>1</sub> F <sub>o</sub> ATP synthases	6
	1.2 The catalytic F <sub>1</sub> domain	8
	1.3 Subunits of the F <sub>o</sub> part	12
	1.3.1 Subunit a	13
	1.3.2 Subunit b	14
	1.3.3 Subunit c	15
	1.4 The sodium-dependent F-ATPase of <i>Propionigenium modestum</i>	18
	1.4.1 Physiology of <i>P. modestum</i>	18
	1.4.2 Properties of the <i>P. modestum</i> F <sub>1</sub> F <sub>o</sub> -ATPase	19
	1.5 Operation principle of the <i>P. modestum</i> F <sub>1</sub> F <sub>o</sub> ATP synthase	21
	1.5.1 Ion translocation mechanism through F <sub>o</sub>	21
	1.5.2 Operation modes of the ATPase and the role of the membrane potential	22
	1.5.3 Model of torque generation in the F <sub>o</sub> motor	23
	1.6 Aim of this work	25
	1.7 References	27
CHAPTER 2:	RECONSTITUTION OF F <sub>o</sub> OF THE SODIUM TRANSLOCATING ATP SYNTHASE OF <i>PROPIONIGENIUM MODESTUM</i> FROM ITS HETEROLOGOUSLY EXPRESSED AND PURIFIED SUBUNITS	34
	2.1 Abstract	35
	2.2 Introduction	35
	2.3 Materials and Methods	37
	2.4 Results and Discussion	42
	2.5 References	48
CHAPTER 3:	MOLECULAR MECHANISM OF THE ATP SYNTHASE'S F <sub>o</sub> MOTOR PROBED BY MUTATIONAL ANALYSES OF SUBUNIT A	51
	3.1 Abstract	52
	3.2 Introduction	53
	3.3 Materials and Methods	54
	3.4 Results	60

---

	3.5	Discussion	69
	3.6	References	74
CHAPTER 4:		MUTATIONAL ANALYSIS OF ASP259 OF SUBUNIT A FROM <i>PROPIONIGENIUM MODESTUM</i> F <sub>1</sub> F <sub>0</sub> ATP SYNTHASE	77
	4.1	Abstract	78
	4.2	Introduction	78
	4.3	Materials and Methods	80
	4.4	Results and Discussion	84
	4.5	References	88
CHAPTER 5:		GENERAL DISCUSSION	91
	5.1	Rotary enzymes in biological membranes	91
	5.1.1	Bacterial flagellar motor	91
	5.1.2	V-type ATPases	95
	5.1.3	A-type ATPases	100
	5.2	Coupling mechanism of the F <sub>1</sub> F <sub>0</sub> -ATPases	101
	5.2.1	Coupling models of F <sub>1</sub> F <sub>0</sub> -ATPases	102
	5.2.2	<i>In vitro</i> re-assembled ATPase offers a powerful tool to investigate mutants of <i>P. modestum</i> ATPase	104
	5.3	Role of the positive stator charge in the coupling process of F <sub>1</sub> F <sub>0</sub> ATPase	105
	5.3.1	ATP synthesis	105
	5.3.2	ATP hydrolysis	107
	5.4	Outlook	108
	5.5	References	108
APPENDIX			113
CURRICULUM VITAE			116
LIST OF PUBLICATIONS			117



## SUMMARY

ATP is the main carrier of free energy in living cells and is primarily synthesised by  $F_1F_0$  ATP synthases. The strictly anaerobic, marine bacterium *Propionigenium modestum* grows by the degradation of succinate to propionate and  $CO_2$ . During fermentation, the free energy of a decarboxylation step generates an electrochemical  $Na^+$  gradient across the membrane, which is directly used by a  $Na^+$ -dependent  $F_1F_0$  ATP synthase. F-type ATPases are composed of a catalytically active headpiece ( $F_1$ ) protruding into the cytoplasm and a membrane embedded moiety ( $F_0$ ), which is responsible for ion translocation across the membrane. The mechanism of ion translocation and the coupling of the flux of  $Na^+$  across the membrane to the catalytic events at  $F_1$  are not completely elucidated. The current working model predicts that a ring of c subunits rotates relative to subunits a and b driven by the electrochemical  $Na^+$  gradient and that the torque generated by this rotation is transferred to the catalytic sites in order to synthesise ATP.

In the work presented here, the genes for  $F_0$  subunits a and b from *P. modestum* were cloned as His-tagged fusion proteins and expressed in *Escherichia coli* C43(DE3). The recombinant proteins were purified using  $Ni^{2+}$  affinity chromatography. By the use of the above *E. coli* strain, unsatisfactory yield and purity of subunit a after expression in *E. coli* PEF42(DE3) could be overcome to a great extent, and subunit b was purified to homogeneity. Subunits a and b were combined with purified subunit c and re-assembled to a functional  $F_0$  complex. The reconstituted  $F_0$  liposomes were able to perform  $^{22}Na^+_{out}/Na^+_{in}$  exchange and  $\Delta\Psi$ -driven  $^{22}Na^+$  uptake. Furthermore, by the incubation of these  $F_0$  liposomes with purified  $F_1$ -ATPase, a functional  $F_1F_0$  holoenzyme was reconstituted that was able to synthesise ATP and translocate  $Na^+$  upon addition of ATP. By this method we were also able to form an  $F_0$  chimera between *P. modestum* subunits a and b together with the c-oligomer of *Ilyobacter tartaricus* that showed  $^{22}Na^+$  transport activities comparable to the wild-type enzyme.

In order to analyse the function of the strictly conserved residue Arg227 on the *P. modestum* subunit a, site directed mutagenesis studies were performed. Previous investigations in *E. coli* describe this site as absolutely essential for a coupled enzyme.

However, we could give convincing evidence that ATP synthases harbouring the aArg227Lys or the aArg227His replacement perform ATP-driven  $^{22}\text{Na}^+$  transport, and  $F_o$  liposomes of these mutants catalyse  $^{22}\text{Na}^+_{\text{out}}/\text{Na}^+_{\text{in}}$  exchange and  $\Delta\Psi$ -driven  $^{22}\text{Na}^+$ -uptake. The pH optima were shifted compared to the wild-type enzyme to a more basic pH in case of the lysine mutant and to a more acidic pH for the histidine mutant. In addition, they do not cover a wide pH range like the wild-type enzyme but rather show narrow pH optima. Data obtained with mutant aArg227Ala displayed different characteristics. In first studies, it was found that  $F_o$  liposomes catalysed  $\Delta\Psi$ -driven  $^{22}\text{Na}^+$  uptake and  $F_1F_o$  liposomes showed  $\text{Na}^+$ -dependent ATP hydrolysis that, however, was not coupled to sodium translocation. The latter result indicated that dissociation of  $\text{Na}^+$  from the rotor sites might be impaired. Further studies revealed that aArg227Ala was able to synthesise ATP only if the  $\text{Na}^+$  concentration in the buffer was low. Interestingly, unlike wild-type  $F_o$  complexes, those with the aArg227Ala mutation were able to catalyse  $\Delta p\text{Na}^+$ -driven  $^{22}\text{Na}^+$  uptake. This transport was also sensitive to elevated sodium concentrations in the lumen of the proteoliposomes. Our data indicate that aArg227 is not essential for coupling the ion flux to rotation, but rather promotes the dissociation of the sodium ions from their binding sites on subunit c. They also do not support earlier suggestions that aArg227 cannot be replaced by other amino acids without loss of function.

A second group of important residues of *E. coli* subunit a are Glu219 and His245. It was demonstrated that these two sites can be functionally interchanged. In *P. modestum* Met236 and Asp259 reside at the equivalent positions. We replaced aAsp259 by glutamate, glycine or lysine. All tested mutants were able to hydrolyse ATP in a  $\text{Na}^+$ -coupled manner and could perform ATP synthesis in presence of a membrane potential. The mutant  $F_o$  complexes catalysed  $^{22}\text{Na}^+_{\text{out}}/\text{Na}^+_{\text{in}}$  exchange and  $\Delta\Psi$ -driven  $^{22}\text{Na}^+$  uptake. The transport rates were reduced compared to the wild-type in the order wild-type $\geq$ Glu>Gly>Lys, thus clearly depending on charge and polarity of the substitution. Asp259 is not likely to be an essential residue for a functional enzyme, but it seems to be involved in the ion translocation process.

## KURZFASSUNG

Energie in Form von ATP ist für alle Organismen von zentraler Bedeutung, um lebensnotwendige Prozesse aufrecht zu erhalten. Sie wird hauptsächlich von  $F_1F_0$  ATP Synthasen bereitgestellt. *Propionigenium modestum* ist ein strikt anaerobes, marines Bakterium, das seinen Energiebedarf durch den Abbau von Succinat zu Propionat und  $CO_2$  deckt. Während der Fermentation von Succinat wird die freie Energie aus der Decarboxylierung von Methylmalonyl-CoA in einem elektrochemischen Natrium-Gradienten konserviert, der direkt von einer  $Na^+$ -abhängigen  $F_1F_0$  ATP Synthase genutzt wird. F-Typ ATPasen bestehen aus einem katalytisch aktiven  $F_1$ -Teil, der auf der cytoplasmatischen Seite an den membrangebundenen  $F_0$ -Teil assoziiert ist. Der Mechanismus der Ionentranslokation durch den  $F_0$ -Teil und die Kopplung des Ionenflusses an die Synthese von ATP sind noch nicht vollständig aufgeklärt. Das gängige Arbeitsmodell besagt, dass sich ein Ring von 11 c-Untereinheiten relativ zur a-Untereinheit und den zwei b-Untereinheiten dreht. Dabei werden  $Na^+$  Ionen über die Membran transportiert. Die Triebkraft für diese Rotation ist die Energie, die im elektrochemischen  $Na^+$ -Gradienten gespeichert ist. Das Drehmoment wird mittels der  $\gamma$ -Untereinheit zu den katalytisch aktiven  $\beta$ -Untereinheiten übertragen, wo schlussendlich ATP synthetisiert wird.

In der vorliegenden Arbeit wurde das Protein für die a-Untereinheit von *Propionigenium modestum* mit einem N-terminalen-, und dasjenige der b-Untereinheit mit einem C-terminalen Polyhistidin-Rest modifiziert. Die rekombinanten Proteine wurden in *Escherichia coli* C43(DE3) überexprimiert und mittels  $Ni^{2+}$ -Affinitätschromatographie gereinigt. Durch die Verwendung dieses Expressionsstammes konnte die geringe Ausbeute und unvollständige Reinigung der a-Untereinheit im Vergleich zur Expression in *E. coli* PEF42(DE3) deutlich verbessert werden. Die b-Untereinheit konnte bis zur Homogenität gereinigt werden. Zusammen mit gereinigter c-Untereinheit wurden die a- und die b-Untereinheiten zu einem  $F_0$ -Teil zusammengesetzt und in Liposomen rekonstituiert. Die Funktionalität des rekonstituierten  $F_0$ -Teils wurde anhand von  $^{22}Na^+_{out}/Na^+_{in}$ -Austausch- und

$\text{Na}^+$ -Aufnahme-Experimenten nachgewiesen. Darüber hinaus konnte durch Inkubation der  $\text{F}_0$ -Liposomen mit gereinigtem  $\text{F}_1$ -Teil eine aktive  $\text{F}_1\text{F}_0$ -ATPase generiert werden. Diese war in der Lage, ATP zu hydrolysieren und in Anwesenheit eines Membranpotentials ATP zu synthetisieren. Diese Methode wurde auch eingesetzt, um funktionelle  $\text{F}_0$ -Hybride zwischen den a- und b-Untereinheiten von *P. modestum* und dem c-Oligomer von *Ilyobacter tartaricus* zu bilden. Die dabei erhaltenen Transportraten waren vergleichbar mit den Werten des  $\text{F}_0$  Teils von *P. modestum*.

Die Funktion vom hoch konservierten Arg227 der a-Untereinheit der *P. modestum* ATPase wurde mittels Mutagenese-Versuche untersucht. Frühere Studien an aArg210 der *E. coli* ATPase (homologer Rest zu aArg227 aus *P. modestum*) ergaben, dass diese Aminosäure essentiell ist für ein funktionelles Enzym. Es konnte jedoch stichhaltig gezeigt werden, dass das Arginin funktionell durch ein Lysin oder ein Histidin ersetzt werden kann.  $\text{F}_0$ -Liposomen mit den jeweiligen Mutanten katalysieren  $^{22}\text{Na}^+_{\text{out}}/\text{Na}^+_{\text{in}}$ -Austausch und Potential-getriebene  $\text{Na}^+$ -Aufnahme. Die pH Optima der beiden Mutanten waren allerdings im Vergleich zum Wildtyp-Enzym verschoben, im Falle der Lysin-Mutante zu einem basischeren pH und im Falle der Histidin-Mutante zu einem saureren pH. Die beiden Mutanten waren zudem über einen kleineren pH Bereich aktiv als das Wildtyp-Enzym. Eine Mutante, bei der das Arginin 227 durch ein Alanin ausgetauscht wurde, zeigte ganz andere Charakteristika.  $\text{F}_0$ -Liposomen mit der aArg227Ala Mutante waren in Anwesenheit eines Membranpotentials in der Lage,  $^{22}\text{Na}^+$  aufzunehmen.  $\text{F}_1\text{F}_0$  Liposomen zeigten  $\text{Na}^+$ -stimulierbare ATP Hydrolyse, die jedoch nicht an einen  $\text{Na}^+$ -Transport gekoppelt war. Dieses Ergebnis deutet darauf hin, dass die Dissoziation der  $\text{Na}^+$ -Ionen von den Bindungsstellen der c-Untereinheit beeinträchtigt sein könnte. Weitere Studien zeigten, dass die aArg227Ala Mutante in der Lage war, ATP zu synthetisieren, wenn die Natriumkonzentration im Umgebungspuffer niedrig war. Interessanterweise katalysierte aArg227Ala im Gegensatz zum Wildtyp-Enzym eine  $\Delta\text{pNa}^+$ -getriebene  $^{22}\text{Na}^+$ -Aufnahme. Dieser  $^{22}\text{Na}^+$ -Transport reagierte ebenfalls empfindlich auf ansteigende  $\text{Na}^+$ -Konzentrationen. Unsere Daten weisen hin auf eine mögliche Rolle der positiven Ladung vom aArg227 bei der Dissoziation der  $\text{Na}^+$ -Ionen, die sich, gebunden an die c-Untereinheiten, nähern. Die Daten stehen ausserdem im Gegensatz zu früheren Arbeiten, die besagten, dass aArg227 nicht ohne Verlust der Funktionalität durch andere Aminosäuren ausgetauscht werden kann.

Eine zweite Gruppe von wichtigen Resten auf der  $\alpha$ -Untereinheit der *E. coli* ATPase sind Glu219 und His245. Es wurde gezeigt, dass diese zwei Reste gegenseitig funktionell ausgetauscht werden können. In *P. modestum* befinden sich Met236 und Asp259 an den äquivalenten Positionen. In dieser Arbeit wurde  $\alpha$ Asp259 durch Glutamat, Glycin oder Lysin ausgetauscht. Alle untersuchten Mutanten waren in der Lage, ATP zu synthetisieren und zeigten  $\text{Na}^+$ -stimulierbare ATP Hydrolyse. Die gemessenen Aktivitäten waren im Vergleich zum Wildtyp reduziert. Der Aktivitätsverlust war abhängig von der Ladung und Polarität der Aminosäure-Substitutionen, und zwar in der Folge Wildtyp $\geq$ Glu>Gly>Lys. Dieses Ergebnis deutet darauf hin, dass  $\alpha$ Asp259 nicht essentiell ist für ein funktionelles Enzym. Trotzdem ist dieser Rest am Ionen-Translokations Prozess beteiligt.

## CHAPTER 1: GENERAL INTRODUCTION

Adenosine triphosphate (ATP) is the universal carrier of free energy in living cells. The energy released from the hydrolysis of ATP to ADP and inorganic phosphate is used in all cells to carry out numerous biological processes, e.g. biosynthetic reactions, mechanical work or solute transport. As membranes are impermeable to ATP, this compound needs to be synthesised continuously within the cell from ADP and inorganic phosphate. Accordingly, the ATP turnover is enormous in living organisms: a resting adult synthesises and consumes an ATP amount that roughly corresponds to half of his body weight per day. The main pathways for ATP synthesis are substrate chain phosphorylation, oxidative phosphorylation or photophosphorylation. Substrate chain phosphorylation involves the formation of intermediates with highly energetic phosphoryl-groups during degradation of organic substrates. The phosphoryl-group is subsequently transferred to ADP to yield ATP. During oxidative phosphorylation or photophosphorylation, chemical or light energy is converted into an electrochemical ion gradient across the membrane ( $\Delta\mu\text{H}^+$  or  $\Delta\mu\text{Na}^+$ ). The energy stored in this gradient is used by  $\text{F}_1\text{F}_0$  ATP synthases, which are located in the inner membrane of mitochondria, the thylakoid membrane of chloroplasts or the cytoplasmic membrane of bacteria to synthesise ATP.

### 1.1 Molecular architecture of $\text{F}_1\text{F}_0$ ATP synthases

All known F-type ATP synthases share a common general overall structure comprising a membrane-embedded  $\text{F}_0$  moiety and a water-soluble  $\text{F}_1$  portion (Figure 1A).

Many initial studies have been performed with the ATP synthase from *Escherichia coli* mainly because this enzyme is readily amenable to studies using molecular biology techniques. The  $\text{F}_1$  domain harbouring the catalytic sites for ATP synthesis has the universal subunit composition  $\alpha_3\beta_3\gamma\delta\epsilon$ , which in *E. coli* results in a mass of 382 kDa. The  $\text{F}_0$  part mediates proton translocation across the cytoplasmic membrane and comprises subunits  $\text{ab}_2\text{c}_{9-12}$  in *E. coli* (Foster & Fillingame, 1982;

Jiang *et al.*, 2001) with molecular masses of 30.3 kDa (a), 17.2 kDa (b) and 8.3 kDa (c), respectively.

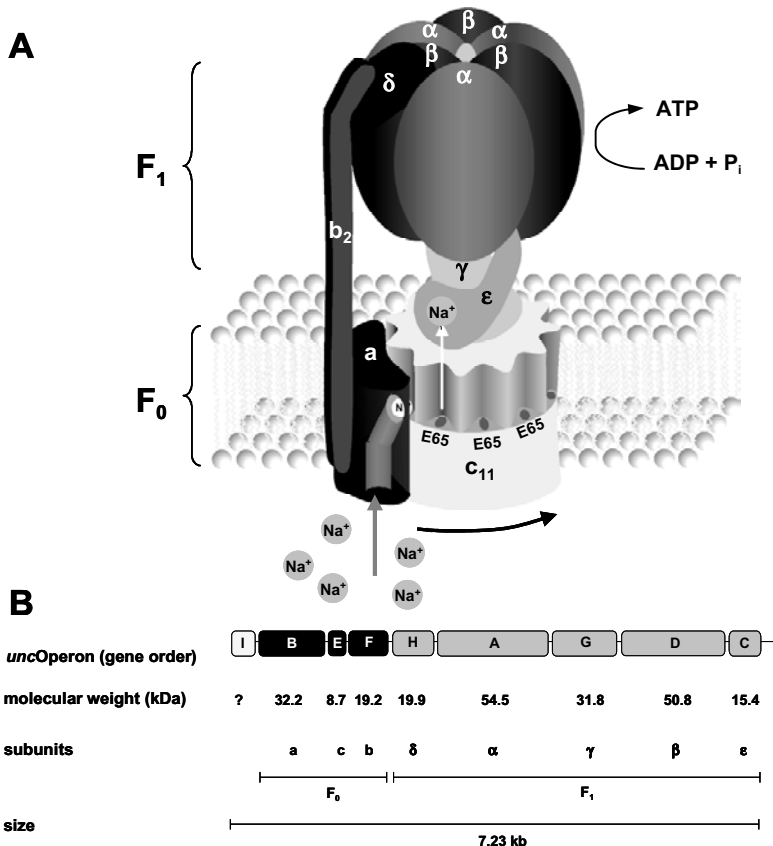


**Figure 1: A Model showing the structure and function of the ATP synthase of *Propionigenium modestum*.** The water-soluble F<sub>1</sub> domain with the catalytic sites on the three  $\beta$  subunits is connected *via* the  $\gamma$  and  $\epsilon$  subunits to the c<sub>11</sub> oligomer of the F<sub>0</sub> domain, and *via* the  $\delta$  and b<sub>2</sub> subunits to subunit a. The rotor (light grey) consists of subunits c<sub>11</sub> $\gamma\epsilon$  and the stator (dark grey) is assembled from subunits a $\beta_2\alpha_3\beta_3\delta$ . **B Organisation of the *P. modestum unc* operon.** Genes coding for F<sub>0</sub> are coloured black and genes coding for F<sub>1</sub> subunits are depicted in grey. The gene coding for the i-protein is drawn in light grey.

The coding regions for the eight subunits are clustered in a single operon, termed *unc* (*uncoupled*) or *atp* operon. The genes are arranged in the sequence

*unc1BEFHAGDC*, transcribed and translated into the *i*-protein, the  $F_0$  subunits a, c, b and the  $F_1$  subunits  $\delta$ ,  $\alpha$ ,  $\gamma$ ,  $\beta$  and  $\epsilon$ , respectively (Figure 1B). The role of the *i*-gene is still not known. The *uncI* gene product is a small membrane protein and can be co-purified with  $F_0$  or  $F_1F_0$  in substoichiometric amounts (Schnepppe *et al.*, 1991). Deletion of *uncI* did not interfere with the synthesis of an active enzyme complex, but bacteria with this deletion grew to a lower yield and the ATPase activity in isolated membranes was reduced to about 80 % of the wild-type activity (Gay, 1984).

## 1.2 The catalytic $F_1$ domain

The structure of a major part of  $F_1$  of bovine heart mitochondria was determined by X-ray crystallography to atomic resolution (Abrahams *et al.*, 1994). Around 85 % of the amino acids were assigned in the structure, representing nearly all residues of subunits  $\alpha$  and  $\beta$ . Major parts of subunit  $\gamma$  could also be resolved in this structure, whereas no electron densities could be obtained for subunits  $\delta$  and  $\epsilon$ . Three  $\alpha$  and three  $\beta$  subunits are arranged in an alternating fashion to form a cylindrical hexamer around the central  $\gamma$  subunit (Figure 2).

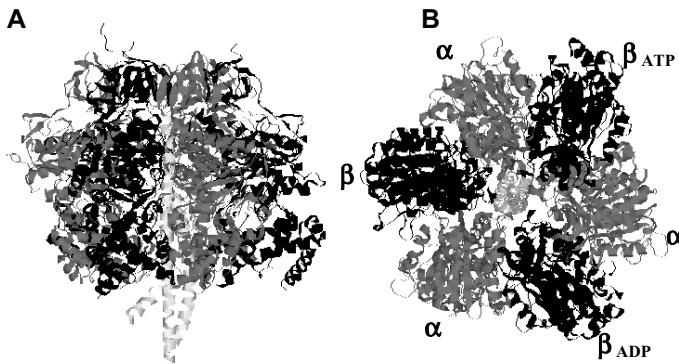


**Figure 2: Structure of the  $F_1$ -ATPase from bovine mitochondria.** Side view (A) and cross section viewed from the membrane side (B) of the  $F_1$  structure as determined by Abrahams *et al.* (1994). The three pairs of subunits  $\alpha$  (dark grey) and  $\beta$  (black) are arranged around the central  $\gamma$  subunit (light grey). Subunit  $\beta$  appears in three different conformations, depending on the bound nucleotides.



The  $\alpha$  and  $\beta$  subunits share a similar fold, as one might expect from their sequence similarity (24 % identity and 51 % similarity among the  $\alpha$  and  $\beta$  subunits from *E. coli* (Nakamoto *et al.*, 1999)). At their N-terminus on top of  $F_1F_0$ , the two proteins form a  $\beta$ -barrel domain, followed by a central  $\alpha\beta$  sector harbouring the nucleotide binding sites, and a C-terminal  $\alpha$ -helix bundle. All  $\alpha$  subunits are found in similar conformations with a bound ATP analogue (the non-hydrolysable derivative AMP-PNP). However, the  $\beta$  subunits appear in three different conformational states: one is empty, the second contains ADP and the third has AMP-PNP bound. The inner shape of each nucleotide-binding site is determined by the asymmetry of the  $\gamma$  subunit, which forms a coiled-coil shaft structure within the cavity of the  $\alpha_3\beta_3$  hexamer (Abrahams *et al.*, 1994; Gibbons *et al.*, 2000).

The structure of the major part of the  $\delta$  subunit was elucidated by NMR spectroscopy (Wilkens *et al.*, 1997a; Wilkens *et al.*, 1997b). The main structural feature of this protein is a six  $\alpha$ -helix bundle at its N-terminal domain. This domain binds to the top of the  $\alpha_3\beta_3$  hexamer through interactions with the N-terminal part of the  $\alpha$  subunit (Lill *et al.*, 1996; Ogilvie *et al.*, 1997). The C-terminal domain of subunit  $\delta$  is less well defined. Evidence from crosslinking studies showed that subunit  $\delta$  and the two b subunits are in close proximity. Removal of the C-terminal 43 residues from subunit  $\delta$  prevented binding to the C-terminal fragment of subunit b (Wilkens *et al.*, 1997b).

The structure of the  $\epsilon$  subunit was determined by X-ray crystallography (Uhlin *et al.*, 1997) and NMR spectroscopy (Wilkens *et al.*, 1995; Wilkens, 1998). The crystal structure closely resembles the data determined in solution by NMR spectroscopy and can be divided into two major domains. The N-terminal 10-stranded  $\beta$ -sandwich is in the vicinity of subunit  $\gamma$  and is in contact with the c-multimer (Zhang & Fillingame, 1995; Tang & Capaldi, 1996; Hermolin *et al.*, 1999; Rodgers & Wilce, 2000). The C-terminus is arranged in a helix-loop-helix motif that is close to the  $\beta$  subunit interacting with the "DELSEED" motif (Dallmann *et al.*, 1992; Aggeler *et al.*, 1995; Wilkens, 1998; Hara *et al.*, 2001).

More details about the overall structure of  $F_1$  were brought into focus by crystals of a subcomplex of the yeast mitochondrial ATPase (Stock *et al.*, 1999; Figure 3). This structure contains subunits  $\alpha$ ,  $\beta$ ,  $\gamma$ ,  $\delta$ ,  $\epsilon$ , and a  $c_{10}$ -multimer. Six to seven of the c

subunits are in close contact with the  $\gamma$  and  $\delta$  subunits of the central stalk. Please consider that subunit  $\delta$  of the mitochondrial enzyme is the equivalent to the bacterial subunit  $\epsilon$ . However, the structure from the yeast ATPase subcomplex could not be resolved to atomic level due to the relatively poor resolution of the electron density map. The  $\alpha$  and  $\beta$  subunits are well defined in the electron density and have similar conformations as their bovine counterparts. A new feature in the structure of the yeast central stalk was the resolution of the part of subunit  $\gamma$  protruding towards the  $F_0$  domain. Subunit  $\gamma$  consists of a five-stranded  $\beta$ -sheet and six  $\alpha$ -helices. The first and the sixth  $\alpha$ -helix are associated in the coiled coil shaft, which is located in the core of the  $\alpha_3\beta_3$  hexamer.

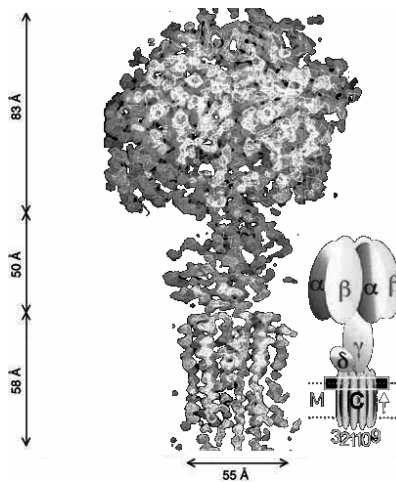


**Figure 3: Electron density map of the yeast  $F_1$  complex associated with a ring of ten c subunits from the  $F_0$  domain.** In the cartoon on the right: the presumed membrane boundaries are intuitively indicated by a dotted line.

The asymmetric feature of the  $\beta$  subunits seen in the high resolution structure of  $F_1$  corresponds well to the binding change mechanism worked out by Boyer (1993). This model suggested a rotational mechanism where the rotation of the  $\gamma$  subunit induces the sequential conformational changes of the  $\beta$  subunits. During the past few years, several approaches were developed to demonstrate that the  $\gamma$  subunit rotates relative to the  $\alpha_3\beta_3$  hexamer (Figure 4).

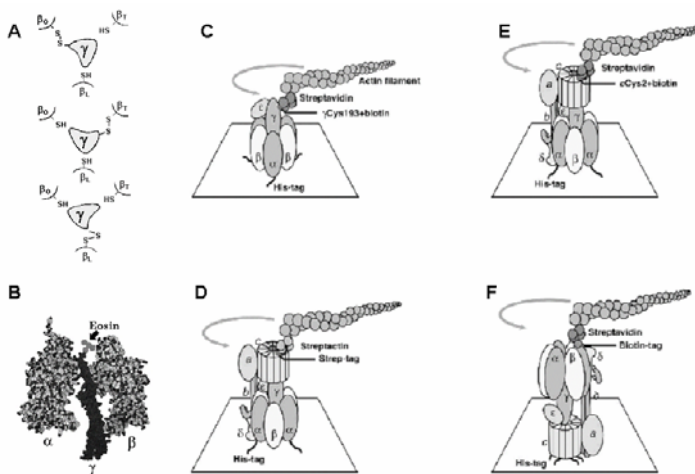


**Figure 4: Experimental systems for the verification of the rotation of subunit  $\gamma$  within the  $\alpha_3\beta_3$  hexamer.** **A** A crosslink product of subunits  $\beta$  and  $\gamma$  was reconstituted with radioactively labelled  $\beta$  subunits to yield a  $\alpha_3\beta_3\gamma$  subcomplex. After reduction of the disulfide bond, addition of ATP and reoxidation of the crosslink, new  $\beta\gamma$  pairs were identified containing the radioactively labelled subunit  $\beta$  (Duncan *et al.*, 1995). **B** An eosin label was attached to subunit  $\gamma$  and ATP-induced rotation of the label was observed by polarised absorption recovery after photobleaching (Sabbert *et al.*, 1996). **C-D** Direct observation of the rotation of a fluorescently labelled actin filament after immobilisation of either  $F_1$  or  $F_1F_0$  through a His-tag. System for the  $\gamma$  subunit rotation (**C**) (Noji *et al.*, 1997), systems for the c subunit rotation (**D/E**) (Sambongi *et al.*, 1999; Pänke *et al.*, 2000) and a system for  $\alpha$  subunit rotation (**F**) (Tanabe *et al.*, 2001).

First evidence has been obtained by Cys-crosslinking of the  $\beta/\gamma$  subunits in soluble *E. coli*  $F_1$ -ATPase (Duncan *et al.*, 1995) and the  $F_1F_0$  holoenzyme (Zhou *et al.*, 1996; Zhou *et al.*, 1997) (Figure 4A). Another approach giving evidence for  $\gamma$  rotation in  $F_1$  was performed using polarised absorption relaxation after photobleaching of eosin-labelled subunit  $\gamma$  (Sabbert *et al.*, 1996) (Figure 4B). The most elegant experiment, however, was the direct visualisation of the rotation *via* fluorescent actin filaments attached to the  $\gamma$  subunit (Noji *et al.*, 1997) (Figure 4C-E). In this study,  $F_1$  was immobilised *via* N-terminal His-tags at subunit  $\beta$  and a micron-sized actin filament was fixed at the  $\gamma$  subunit. Upon ATP-addition, rotation of the

filament was observed under a microscope. Extending this setup to the  $\epsilon$  subunit and the oligomeric c-ring allowed the direct observation of a rotating  $\epsilon\gamma c_n$  assembly, giving additional evidence for the subdivision of F-type enzymes into rotor ( $\epsilon\gamma c_n$ ) and stator ( $ab_2\alpha_3\beta_3\delta$ ) subcomplexes (Sambongi *et al.*, 1999; Pänke *et al.*, 2000). The simultaneous rotation of subunits  $\gamma$ ,  $\epsilon$  and c was additionally corroborated by crosslinking studies. Disulfide crosslinks of the rotor subunits  $\gamma$  and c or  $\gamma$  and  $\epsilon$  had little effect on ATPase activity (Watts *et al.*, 1995; Watts *et al.*, 1996). On the other hand disulfide crosslinks between stator subunit  $\beta$  and rotor subunit  $\epsilon$  led to the inhibition of the enzyme (Aggeler & Capaldi, 1996; Bulygin *et al.*, 1998).

In a more recent approach  $F_1F_0$  was immobilised by His-tags fused to the N-terminal end of subunit c and the actin filament was attached to subunit  $\alpha$  or  $\beta$  (Figure 4F). The filament rotated upon the addition of ATP and generated similar torque as the rotating  $\gamma$  subunit. These results indicated that rotor and stator can be interchanged experimentally (Tanabe *et al.*, 2001).

### 1.3 Subunits of the $F_0$ part

Compared to the detailed structural information available for  $F_1$ , the structure of the membrane integral  $F_0$  domain is much less characterised. Electron microscopy and image analysis provide only a low-resolution structural overview and show the general shape, dimension and mass distribution in the  $F_0$  complex. These micrographs suggested that the c subunits form a ring-like complex, whereas subunits a and b are located at the periphery of the subunit c oligomer (Birkenhäger *et al.*, 1995; Singh *et al.*, 1996; Takeyasu *et al.*, 1996).

The  $F_0$  moiety is responsible for the translocation of the coupling ions through the membrane. The ion pathway is thought to involve subunits a and c only. Subunit b is presumably essential for connecting  $F_1$  to  $F_0$  together with the  $\delta$  subunit, but is not likely to participate directly in ion translocation. However, the presence of all  $F_0$  subunits is required for a functional enzyme complex as subcomplexes harbouring only two of the three subunits in any possible combination were not active in the ion translocation process (Schneider & Altendorf, 1984; Schneider & Altendorf, 1985; Wehrle *et al.*, 2002).

### 1.3.1 Subunit a

Subunit a, the largest of the  $F_0$  subunits, comprises 271 residues and is a particularly hydrophobic protein. It is not thought to be essential in  $F_1$  binding, but has been postulated to play a key role in ion translocation (Fillingame, 1990; Deckers-Hebestreit & Altendorf, 1996; Howitt *et al.*, 1996; Nakamoto, 1996). Site directed mutagenesis has revealed that three residues seem to be important in the *E. coli* subunit a: Arg210, Glu219 and His245 (Cain & Simoni, 1986; Lightowers *et al.*, 1987; Cain & Simoni, 1988; Lightowers *et al.*, 1988, Hatch *et al.*, 1995; Cain & Simoni, 1989). However, only the highly conserved residue Arg210 has proven to be critical for energy coupled proton transport. Any amino acid replacement, except Arg210Ala, caused a complete loss of function (Valiyaveetil & Fillingame, 1997). The Arg210Ala mutant was not able to grow by oxidative phosphorylation and its membranes exhibited no ATPase-coupled proton translocation, either. Interestingly, upon removal of  $F_1$  from the membrane, the  $F_0$  sector with the Arg210Ala mutation allowed passive proton translocation (Valiyaveetil & Fillingame, 1997), indicating that Arg210 is important for ATP-driven  $H^+$  pumping but not for passive proton conductance.

In order to understand the role of subunit a in the ion translocation process, knowledge on the relative location of important residues is a significant prerequisite. For the determination of the topological arrangement of subunit a, different labelling techniques have been used taking advantage of the reactivity or accessibility of hydrophilic regions at the cytoplasmic or periplasmic surface of the membrane. Since the results of the different approaches were controversial, no concise topology model for subunit a could be established so far. All models suggest similar C-termini but the location of the N-terminus remains uncertain. In consequence of these divergences, the different secondary structure models predict five (Hatch *et al.*, 1995; Long *et al.*, 1998; Valiyaveetil & Fillingame, 1998; Wada *et al.*, 1999) or six transmembrane regions (Yamada *et al.*, 1996; Jäger *et al.*, 1998; Deckers-Hebestreit *et al.*, 2000). The arrangement of the two C-terminal helices, harbouring most of the conserved residues, is similar in all models, whereas major differences occur in the positioning of the N-terminal three or four helices and the connecting loops, respectively. Crosslinking studies indicated close contacts between the penultimate helix of subunit a and the C-terminal helix of subunit c. It was also suggested that the two C-terminal helices of

subunit a are directly involved in ion translocation by interactions with the c subunits (Jiang & Fillingame, 1998).

### 1.3.2 Subunit b

Subunit b is an amphipathic polypeptide with a molecular mass of 17.2 kDa. The hydrophobic N-terminus is anchored in the membrane, whereas the highly charged remainder of the protein protrudes into the cytoplasm. Detailed structural information of the entire b subunit is not available so far. The N-terminal part (residues 1-34) was analysed by NMR in an organic solvent mixture (Fillingame *et al.*, 1998). Residues 4-22 form an  $\alpha$ -helix, which is likely to span the membrane. The helical structure is interrupted by a rigid bend between residues 23-26 with the helical structure proceeding from residue 27 to 32, thus connecting the transmembrane helix to the cytoplasmic domain.

The secondary structure of the soluble moiety (residues 25-146) has been determined by circular dichroism (CD) and was found to be mostly  $\alpha$ -helical (Dunn, 1992). The hydrophilic part as well as the native protein form a homodimer with an elongated shape. As a consequence, cysteine mutants showed strong tendencies to form disulfide bridges linking the two monomers together (McLachlin & Dunn, 1997; Rodgers *et al.*, 1997). These disulfide crosslinks between two b subunits did not affect the ATPase activity. Dimerisation also occurred at the N-terminus after introduction of cysteines at residues 2-11, but not between residues 12-21 (Fillingame *et al.*, 1998). The dimerisation of the b subunits was found to be crucial for the interaction with the  $F_1$  part (Dunn & Chandler, 1998; Sorgen *et al.*, 1998).

Proteolysis experiments and antibody binding studies have shown that the hydrophilic part of subunit b is essential for the association of  $F_1$  and  $F_0$  (Hermolin *et al.*, 1983; Perlin & Senior, 1985; Steffens *et al.*, 1987). To fulfil this requirement, the cytoplasmic part of subunit b must span a distance of over 100 Å to contact subunit  $\delta$ , another essential subunit for binding  $F_1$  to  $F_0$  (Jounouchi *et al.*, 1992). The two proteins were shown to interact with their C-terminal regions, even in the absence of the other ATPase subunits (Rodgers *et al.*, 1997; Sawada *et al.*, 1997; Dunn & Chandler, 1998; McLachlin *et al.*, 1998). Therefore the  $b_2\delta$  complex seems to have a shape consistent with its role to act as the peripheral stalk of ATP synthase and linking subunit a to  $\alpha_3\beta_3$  (Dunn *et al.*, 2000).

Further evidence for the long extension of subunit b from the bilayer to the top of the  $F_1$  moiety derived from crosslinking studies (Rodgers & Capaldi, 1998). A disulfide crosslink was formed between residue 156 of subunit b to the N-terminal region of subunit  $\alpha$ . This linkage between  $\alpha$  and b did not affect ATPase activity, but proton pumping was markedly reduced. An explanation for this finding would be, that the torque generated by rotation of the  $\gamma\epsilon$  domain within the  $\alpha_3\beta_3$  hexamer could require compensation by conformational flexibility presented by the connection between the peripheral stalk and  $F_1$  (Rodgers & Capaldi, 1998).

### 1.3.3 Subunit c

Subunit c consists of 79 mostly hydrophobic amino acids. It plays a key role in the ion translocation reaction. A conserved carboxyl group (Asp61 in *E. coli*) serves as binding site for the protons during their translocation across the membrane. In the sodium-dependent F-type ATPase of *Propionigenium modestum* the equivalent residue is Glu65. Additional ligands for sodium binding are Ser66 and Gln32 (Kaim *et al.*, 1997). The protein folds like a hairpin with two transmembrane-spanning  $\alpha$ -helices separated by a polar loop region, which is exposed to the cytoplasm. Such an arrangement is supported by biochemical and genetic experiments (reviewed in Deckers-Hebestreit & Altendorf, 1996) as well as by NMR data of subunit c monomers (see below).

Structure determination of *P. modestum* subunit c was performed by NMR spectroscopy with protein solubilised in dodecyl sulfate micelles (Matthey *et al.*, 1999). The secondary structure was found to comprise four well defined  $\alpha$ -helices connected by short loops. The helical structure is interrupted in the region of the  $\text{Na}^+$  binding site. Due to the lack of long range NOEs, it was not possible to assign a tertiary structure. The solution structure of the *E. coli* c-monomer was determined using NMR in a chloroform/methanol/water (4:4:1) mixture at pH 8.0 and 5.0 (Girvin *et al.*, 1998; Rastogi & Girvin, 1999a). At these pH values the protein folds into two extended, slightly bent  $\alpha$ -helices of 38 and 33 amino acids in length, which are connected by a polar loop. The two structures adopt different conformations at low or high pH, the major distinction being a  $140^\circ$  turn of helix II with respect to helix I. It is assumed that this conformational change is elicited by the protonation or deprotonation of Asp61. With the aid of this structural basis, a mechanistic model was

proposed describing how proton translocation across  $F_0$  could be coupled to the generation of torque, which is essential for ATP synthesis (Rastogi & Girvin, 1999b). In this mechanism, torque generation is assumed to be driven by the clockwise rotation of helix II of subunit c (as viewed from the cytoplasm) when Asp61 becomes protonated. The interface between subunits a and c is stabilised *via* electrostatic interactions, and thus helix II of subunit c moves in a ratchet-like manner versus the penultimate helix of subunit a. This promotes the movement of the c-oligomer versus subunit a. After deprotonation of Asp61 from the following c subunit the starting position is regenerated. However, serious discrepancies to crosslink experiments and mutagenesis studies question the physiological relevance of the pH-dependent conformational change of subunit c. In particular, crosslinking data obtained for helix II of subunit c and the penultimate helix of subunit a are not in accordance with the structure obtained at pH 5.0, but perfectly match the results obtained for the pH 8.0 structure (Jiang & Fillingame, 1998). Furthermore, the fully functional suppression of cD61 mutants by placing an aspartate residue on position cAla24 on helix I is not conceivable with a rotating helix II (Miller *et al.*, 1990; Zhang *et al.*, 1994). And at last, the rotation of helix II versus helix I would cause a major structural change in the loop region of a c subunit and is not consistent with recent experimental data indicating that the c- $\epsilon$  connection remains fixed as the c-oligomer rotates (Schulenberg *et al.*, 1999; Jones *et al.*, 2000).

It was supposed that the subunit c oligomer is arranged in  $F_0$  as a ring-like structure. This assumption was based on crosslinking studies (Jones *et al.*, 1998), tryptophane scanning mutagenesis (Groth *et al.*, 1998; Schnick *et al.*, 2000), electron microscopy (Birkenhäger *et al.*, 1995; Singh *et al.*, 1996; Takeyasu *et al.*, 1996) and X-ray crystallography (Stock *et al.*, 1999). However, the stoichiometry (Foster & Fillingame, 1982; Jones & Fillingame, 1998; Dmitriev *et al.*, 1999; Schnick *et al.*, 2000; Jiang *et al.*, 2001) and the helix packing were discussed controversially (Groth *et al.*, 1998; Jones & Fillingame, 1998). Recently, this was settled and both, structure and stoichiometry of the c-ring have been elucidated in more detail for several organisms. Strikingly, the number of c subunits was found to be variable among species. A first structural model was obtained from crystals of a yeast  $F_1c_{10}$  complex (Stock *et al.*, 1999) (see Figure 3). The electron densities of individual c subunits show that they consist of two  $\alpha$ -helices, linked by a loop. However, the side chain



orientation in the c-oligomer could not be resolved. Recently, the c-rings of chloroplast and *I. tartaricus* ATPase were analysed by atomic force microscopy and *cryo* electron microscopy of 2D-crystals (Seelert *et al.*, 2000; Stahlberg *et al.*, 2001). Chloroplast c-oligomers are composed of 14 monomers, whereas *I. tartaricus* ATPase comprises 11 c subunits. In the structure of the *I. tartaricus* c-oligomer the two helices forming one c subunit are identified by the connecting loop (Figure 5A; Vonck *et al.*, 2002). The inner helices are packed very tightly. This tight helix packing leaves no space for large side chains, and therefore the most likely residues at the helix interface are glycines. This allowed the assignment of the inner helices to the N-terminal half of the c subunit sequence. In this model a Na<sup>+</sup> binding pocket is formed in a space flanked by three helices. The binding site includes Glu65 from one c subunit and Ser66 and Gln32 from the neighbouring c subunit (Figure 5B).

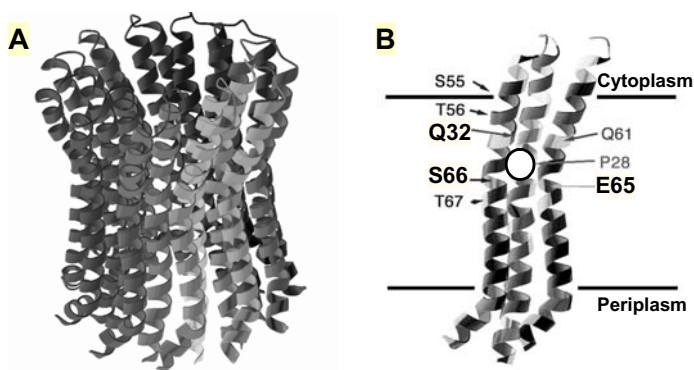


**Figure 5: A Model of the *Hyobacter tartaricus* c-oligomer.** The model was calculated from electron crystallography pictures of two dimensional crystals of the c-oligomer. The loops on the top of the model reflect the cytoplasmic surface of the membrane. **B** This cartoon shows two c-monomers generating the Na<sup>+</sup> binding site (white circle) with residues Ser66 and Gln32 from the first monomer and Glu65 from the second monomer.

According to this model the Na<sup>+</sup> binding site is located within the core of the membrane, which is in good agreement with recent crosslinking data (von Ballmoos *et al.*, 2002).

## 1.4 The sodium-dependent F-ATPase of *Propionigenium modestum*

### 1.4.1 Physiology of *P. modestum*

*P. modestum* is a strictly anaerobic gram negative bacterium isolated from the marine sediment from the Canale Grande in Venice, Italy (Schink & Pfennig, 1982). It appears as a small, rod-shaped cell with a length of 0.5 - 2.0  $\mu\text{m}$  and a diameter of 0.5 - 0.6  $\mu\text{m}$ . In growing cultures chains of several cells can be observed.

This bacterium grows on the degradation of succinate to propionate and  $\text{CO}_2$  (Figure 6). The first step in the fermentation pathway is the activation of succinate *via* CoA transfer from propionyl-CoA to yield succinyl-CoA and propionate. The next steps are the rearrangement of the carbon chain to (*R*)-methylmalonyl-CoA and its isomerisation to (*S*)-methylmalonyl-CoA. (*S*)-Methylmalonyl-CoA is subsequently decarboxylated to propionyl-CoA, which is used to activate the next succinate molecule to succinyl-CoA. All enzymes involved in the fermentation process have been identified in cell-free extracts (Hilpert *et al.*, 1984); however, the mechanism of succinate uptake and propionate secretion still needs to be elucidated.

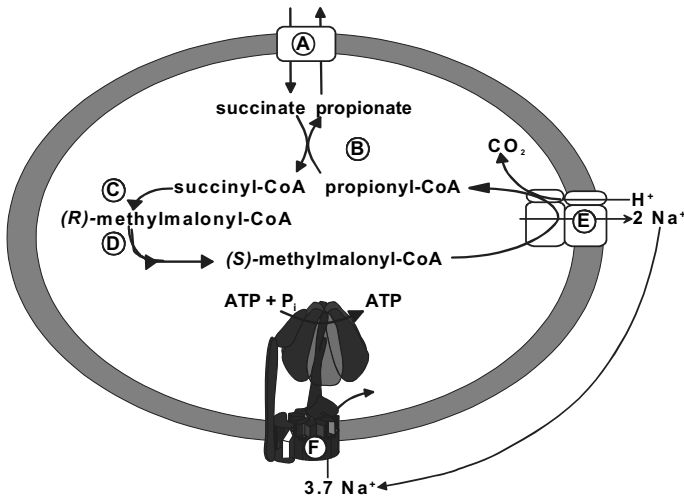


**Figure 6:** Energy metabolism of *Propionigenium modestum* with a sodium cycle coupling the decarboxylation of (*S*)-methylmalonyl-CoA to ATP synthesis. (A) hypothetical succinate uptake/propionate release system; (B) succinate propionyl-CoA:CoA transferase; (C) (*R*)-methylmalonyl-CoA mutase; (D) (*R*)-methylmalonyl-CoA epimerase; (E) (*S*)-methylmalonyl-CoA decarboxylase; (F)  $\text{Na}^+$ -translocating  $\text{F}_1\text{F}_0$  ATP synthase (adapted from Dimroth, 1997).

The free energy of the (*S*)-methylmalonyl-CoA decarboxylation is converted into an electrochemical sodium ion gradient, which can be directly used by a Na<sup>+</sup>-dependent F-type ATP synthase to synthesise ATP from ADP and phosphate (Hilpert *et al.*, 1984; Laubinger & Dimroth, 1987; Laubinger & Dimroth, 1988). This coupling of a decarboxylation reaction to ATP synthesis is termed decarboxylation phosphorylation and was discovered in *P. modestum* (Hilpert *et al.*, 1984; Laubinger & Dimroth, 1988).

#### 1.4.2 Properties of the *P. modestum* F<sub>1</sub>F<sub>o</sub>-ATPase

Biochemical characterisation allowed the assignment of the *P. modestum* ATP synthase to the family of F<sub>1</sub>F<sub>o</sub> ATP synthases (Laubinger & Dimroth, 1987). The genes for this enzyme were sequenced and shown to be organised in a single operon with the sequence *atpIBEFHAGDC* (Esser *et al.*, 1990; Kaim *et al.*, 1990; Ludwig *et al.*, 1990; Kaim *et al.*, 1992). They encode the i protein and subunits a, c, b, δ, α, γ, β and ε, respectively. This gene arrangement is also evident in other eubacteria, e.g. *E. coli*, *Bacillus firmus* or *Vibrio alginolyticus*. Compared to *E. coli*, the sequence conservation within subunits is low, with the exception of the catalytically active subunits α and β.

A remarkable feature of the *P. modestum* ATPase complex is the specific stimulation of the enzyme by sodium ions. The degree of activation by Na<sup>+</sup> was dependent on pH and increased at more basic pH values. At low Na<sup>+</sup> concentrations (<1 mM) H<sup>+</sup> or Li<sup>+</sup> act as alternative coupling ions. However, the K<sub>m</sub> for Li<sup>+</sup> is about ten times higher than for Na<sup>+</sup>, and for H<sup>+</sup> translocation the pH optimum is shifted from pH 8.7 to the more acidic pH 6.8 (Laubinger & Dimroth, 1989; Kluge & Dimroth, 1993a). Proton pumping activity into proteoliposomes continuously decreased with increasing Na<sup>+</sup> concentrations indicating a competition of both coupling ions in a common ion translocation mechanism.

Upon dissociation of the F<sub>1</sub> moiety from the membrane-bound F<sub>o</sub> part, the activation of ATP hydrolysis by Na<sup>+</sup> was lost (Laubinger & Dimroth, 1987). This implies that the cation specificity is localised on the F<sub>o</sub> moiety, which was confirmed by *in vitro* chimeras between *P. modestum* F<sub>o</sub> and *E. coli* F<sub>1</sub> (Laubinger *et al.*, 1990). Furthermore, hybrid strains containing different combinations of *atp* genes from *P. modestum* and *E. coli* were constructed for *in vivo* and *in vitro* studies (Kaim *et al.*,

1992; Kaim & Dimroth, 1993; Kaim & Dimroth, 1994; Gerike *et al.*, 1995). The only two functional chimeras consisted of subunits a, b, c, and  $\delta$  from *P. modestum* and the remaining F<sub>1</sub> subunits from *E. coli* (Kaim & Dimroth, 1993; Kaim & Dimroth, 1994). The hybrid ATPases were either expressed from plasmid pHEP100 or from the genome of *E. coli* strain PEF42 (Figure 7) and showed similar biochemical characteristics as the wild-type *P. modestum* ATP synthase.

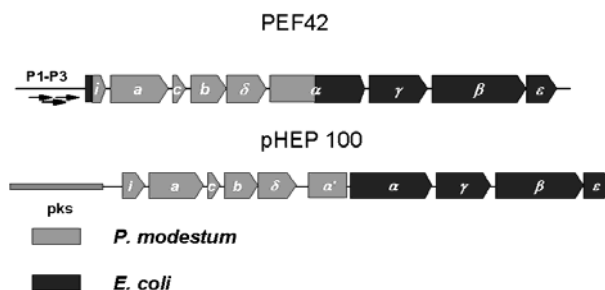


**Figure 7: Structure of the *P. modestum*/*E. coli* hybrid *atp* operons encoded either on a plasmid (pHEP100) or on the chromosome (*E. coli* PEF42).** The genes from *P. modestum* are drawn in light grey and the genes from *E. coli* are depicted in dark grey. Strain PEF42 contains the genes of *P. modestum* F<sub>0</sub> and subunit  $\delta$ , the genes for subunits  $\gamma$ ,  $\beta$  and  $\epsilon$  from *E. coli* and a hybrid subunit  $\alpha$  and a hybrid *i*-protein. Plasmid pHEP100 encodes the *P. modestum* genes from the *i*-protein to a truncated  $\alpha$  subunit and the residual *E. coli* F<sub>1</sub> genes.

Biochemical studies revealed that the *P. modestum* ATPase is specifically inhibited by DCCD in a pH-dependent manner. Furthermore the presence of sodium or lithium ions prevented the modification of the enzyme with the inhibitor. Therefore, it was concluded that Na<sup>+</sup> and H<sup>+</sup> compete for a common binding site at the DCCD-reactive site (Glu65) in the C-terminal transmembrane helix of subunit c (Kluge & Dimroth, 1993a; Kluge & Dimroth, 1993b).

To identify amino acid residues involved in sodium binding, a random mutagenesis approach was performed (Kaim & Dimroth, 1995). Mutants were selected for sodium-independent growth on succinate as sole carbon source. Under these conditions the wild-type grows only at Na<sup>+</sup> concentrations >1 mM. Therefore, Na<sup>+</sup>-independent growth indicated a phenotype with altered coupling ion specificity. By this procedure, a class of mutants was obtained harbouring two mutations at the

C-terminal end of subunit c (Phe84Leu and Leu87Val). These mutants were no longer able to translocate sodium ions, whereas  $\text{Li}^+$  and  $\text{H}^+$  transport was not inhibited. The location of the two amino acid replacements at a considerable distance to cGlu65 suggested that the binding pocket for  $\text{Na}^+$  might be indirectly affected by minor conformational changes. In addition, site directed mutagenesis was used to identify the  $\text{Na}^+$  coordinating amino acid residues. Three residues (cGlu65, cSer66 and cGln32) are required for  $\text{Na}^+$  binding, two (cGlu65 and cSer66) for  $\text{Li}^+$  binding and one (cGlu65) is sufficient for  $\text{H}^+$  binding (Figure 5B) (Kaim *et al.*, 1997).

The same screening procedure led to the isolation of mutants in subunit a, showing  $\text{Na}^+$ -independent growth on succinate. The signature of these clones was a triple mutation on subunit a (aLys220Arg, aVal264Glu, aIle278Asn). Interestingly, growth of *E. coli* MPA762 harbouring these three amino acid substitutions was inhibited by  $\text{Na}^+$  ions. This inhibition correlated with the inhibition of the ATPase activity by  $\text{Na}^+$  and with the lack of any  $\text{Na}^+$  transport activity by the mutant enzyme (Kaim & Dimroth, 1998b). However, the mutant retained its  $\text{Li}^+$  and  $\text{H}^+$  transport activity. The  $K_i$  for NaCl in the triple mutant correlated with the  $K_m$  in the wild-type enzyme at pH 6.5 indicating that the sodium binding site on subunit c is not affected by these mutations. The inhibitory effect could be interpreted by an ion selective channel on subunit a, which has become impermeable for sodium ions in the triple mutant. These data suggest that the coupling ion selectivity of  $\text{F}_1\text{F}_0$ -ATPase is determined by structural elements of both subunit a and subunit c.

## 1.5 Operation principle of the *P. modestum* $\text{F}_1\text{F}_0$ ATP synthase

### 1.5.1 Ion translocation mechanism through $\text{F}_0$

Recent data showed that the sodium binding site is located within the core of the lipid bilayer (von Ballmoos *et al.*, 2002). Therefore, ion selective channels are required to ensure the accessibility for the coupling ions to their binding sites. The structure of the c-oligomer suggests a half channel protruding from the cytoplasm to the sodium binding site (Vonck *et al.*, 2002). Bulky, hydrophobic amino acids seal the channel towards the periplasm (Figure 5B). To complete the ion pathway across the membrane, the current working model predicts the presence of a second ion selective half-channel on subunit a, connecting the ion binding sites on subunit c to the periplasm (Kaim & Dimroth, 1998b). This model is supported by  $^{22}\text{Na}^+$  occlusion

experiments with mutant MPA762 comprising a triple mutation in subunit a. In this mutant one  $^{22}\text{Na}^+$  ion was entrapped per ATPase molecule in a strictly ATP-dependent manner (Kaim *et al.*, 1998). This result can be explained with the following scenario:  $^{22}\text{Na}^+$  can bind from the aqueous environment to the binding site on subunit c and ATP-driven rotation moves the occupied rotor site into the interface with the a subunit. Since the mutant a subunit channel does not allow  $\text{Na}^+$  ions to pass to the periplasmic surface, ATP-driven rotation stops, and the occupied c subunit is kept in the rotor-stator interface. In contrast, in the wild-type enzyme  $^{22}\text{Na}^+$  is released into the subunit a channel and can exit to the periplasmic side of the membrane. The stoichiometry of one entrapped  $\text{Na}^+$  ion per ATPase indicated that all binding sites on subunit c are freely accessible for the  $\text{Na}^+$  ions from the cytoplasm, except the one at the subunit a interface. This free accessibility of the sodium binding sites is in agreement with mechanistic models proposing one channel on subunit a.

### 1.5.2 Operation modes of the ATPase and the role of the membrane potential

In absence of an external driving force, the  $F_o$  motor is in its idling mode, and the rotor performs Brownian back and forth movements against the stator within a narrow angle. A characteristic of this operation mode is the exchange of external  $^{22}\text{Na}^+$  with internal, unlabelled  $\text{Na}^+$  after reconstitution of  $F_1F_o$  proteoliposomes (Kaim & Dimroth, 1998c).  $^{22}\text{Na}^+_{\text{out}}/\text{Na}^+_{\text{in}}$  exchange was catalysed with an initial rate that was comparable to the initial rate observed for ATP-driven  $\text{Na}^+$  pumping, and hence idling appears to be a highly significant option of the motor. Interestingly,  $^{22}\text{Na}^+_{\text{out}}/\text{Na}^+_{\text{in}}$  exchange was not significantly affected by the modification of single rotor sites with DCCD. This finding corroborates that the  $F_o$  motor allows ion transfer across the membrane only by minor back and forth movements of the rotor versus the stator and does not need a full rotation to perform ion translocation. In contrast, models comprising two stator half channels (Junge *et al.*, 1997) would require an almost complete turn of the rotor relative to the stator to carry out exchange. These revolutions would undoubtedly be stopped by a single DCCD modified rotor subunit. Thus, in the two channel model, idling would be abolished by DCCD modification, which is not in agreement with the experimental data.

In order to perform work, the motor has to switch from  $^{22}\text{Na}^+_{\text{out}}/\text{Na}^+_{\text{in}}$  exchange into a torque generating operation mode. This can be achieved by ATP hydrolysis in

the  $F_1$  part, which turns the rotor assembly and leads to  $\text{Na}^+$  translocation across the membrane. Conversely, ATP synthesis requires rotary torque, which is generated by the movement of ions across the  $F_0$  moiety. Interestingly enough, as indicated by the  $^{22}\text{Na}^+_{\text{out}}/\text{Na}^+_{\text{in}}$  exchange experiments, a  $\text{Na}^+$  concentration gradient was unable to generate torque. Upon application of a membrane potential ( $\Delta\Psi$ ), however, the motor switched from idling into the torque generating operation mode (Kaim & Dimroth, 1998c).

In summary, these data gave good evidence that the membrane potential ( $\Delta\Psi$ ) is an obligatory driving force for ATP synthesis. This was further corroborated by ATP synthesis studies on  $F_1F_0$ -ATPases from chloroplasts, mitochondria and bacteria (Thayer & Hinkle, 1975; Kaim & Dimroth, 1998a; Kaim & Dimroth, 1999). It could be demonstrated that ATP synthesis occurred only in the presence of a membrane potential ( $\Delta\Psi$ ) and no ATP synthesis was observed with the chemical gradient alone. According to Mitchell's chemiosmotic theory  $\Delta\Psi$  and  $\Delta\text{pH}/\Delta\text{pNa}^+$  are thermodynamically equivalent driving forces for ATP synthesis. Kinetically, they are distinct, however, so that ATP synthesis can be driven by  $\Delta\Psi$  only or by  $\Delta\Psi$  in combination with  $\Delta\text{pH}$  or  $\Delta\text{pNa}^+$ , but not by  $\Delta\text{pH}$  or  $\Delta\text{pNa}^+$  alone.

### 1.5.3 Model of torque generation in the $F_0$ motor

Oster and colleagues (Dimroth *et al.*, 1999) designed a model of the  $F_0$  motor based on the experimental data obtained with the *P. modestum* ATPase. The  $F_0$  motor is composed of the rotor comprising 11 copies of subunit c in a ring-like assembly and the stator subunit a (Figure 8). Each rotor subunit harbours a  $\text{Na}^+$  binding site (Q32, E65, S66) within the core of the membrane (Kaim *et al.*, 1997; von Ballmoos *et al.*, 2002). This site is freely accessible from the cytoplasm *via* putative half-channels in the c-oligomer (Vonck *et al.*, 2002). The stator subunit a flanks the c-ring laterally and constitutes an ion selective half-channel conducting the  $\text{Na}^+$  ions from the periplasm to the rotor binding sites. To prevent ion leakage from the periplasm to the cytoplasm, the rotor-stator interface does not provide an uninterrupted ion path connecting the periplasm with the cytoplasm, but rather generates a hydrophobic barrier.

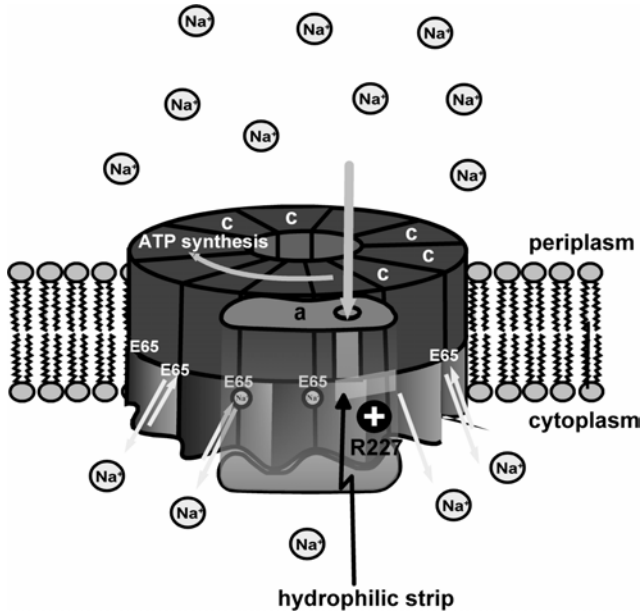


**Figure 8: Model of the rotor-stator assembly of the *P. modestum* ATP synthase.** Rotation during ATP synthesis is clockwise as viewed from the periplasm (indicated by the arrow). The rotor harbours 11  $\text{Na}^+$  binding sites at the centre of the bilayer, which are freely accessible from the cytoplasm. The stator subunit a contains an aqueous half channel, which conducts the ions from the periplasm to the rotor sites on the level of the hydrophilic strip. The positive stator charge (aR227) prevents leakage of ions along this strip to the cytoplasm and facilitates the dissociation of  $\text{Na}^+$  from rotor sites approaching this residue (Wehrle *et al.*, 2002). Coupling ions from the periplasm can only exit to the cytoplasm by binding to a rotor site and passing through the hydrophobic barrier forming the left wall of the channel.

During ATP synthesis the symmetrical rotor turns clockwise if viewed from the periplasm. Therefore the asymmetry required for this unidirectional rotation must be provided by the stator. In this model, the fundamental asymmetry defining the direction of rotation is given by a horizontal hydrophilic strip at the rotor-stator interface. This hydrophilic strip enables negatively charged, empty rotor sites to enter the rotor-stator interface from the right and pass as far to the left as to the edge of the stator channel. The strictly conserved positive stator charge (aR227) was placed close to the strip to fulfil a duplicate task: (i) the positive charge prevents ion leakage through the hydrophilic strip and (ii) unoccupied rotor sites are attracted when they enter the rotor-stator interface. A further structural element contributing to the stator



asymmetry is the hydrophobic barrier on the left side of the rotor-stator interface. Having bound an ion from the stator channel, the rotor sites are neutralised and can pass to the left through the rotor-stator interface. Thus, the flux of ions from the periplasm through the stator to the cytoplasm works as follows: sodium ions enter the stator channel from the periplasm, bind to an empty rotor site and from there they can dissociate into the cytoplasm after the rotor has turned and passed the hydrophobic barrier.

We now have to rise the question what the role of the membrane potential in the torque generating process might be. Basically, the rotor moves owing to random Brownian motion and the progression is stochastic. A negatively charged rotor site, which is electrostatically attracted by the positive charge of aR227 is kept within its potential well and might escape to either side with equal probability. The membrane potential is thought to create an electrostatic gradient along the hydrophilic strip facilitating the escape of this rotor site from the positive stator charge (aR227) to the left. Once in contact with the channel the rotor site binds an ion, which prevents it from being attracted backwards by the stator charge. Consequently, the membrane potential elicits the directed diffusion of the rotor to the left, which is the key reaction for the generation of torque, essential for ATP synthesis.

## 1.6 Aim of this work

Mutational studies are a vital tool for the investigation of biochemical processes. Since there are no genetic tools available in *P. modestum*, it was indispensable to establish a genetic system in *E. coli* that allows the examination of the ion translocation mechanism through the  $F_0$  part of *P. modestum*. Two possibilities to express a sodium translocating ATP synthase were already available by chimeras harbouring the  $F_0$  part and subunit  $\delta$  from *P. modestum* and the remaining  $F_1$  subunits from *E. coli* (Kaim & Dimroth, 1993; Kaim & Dimroth, 1994). These ATPase hybrids are less stable than the wild-type enzyme and did not allow the purification to homogeneity. Thus, to perform careful biochemical studies on *P. modestum*  $F_0$ , a novel strategy was requested. A first goal of this thesis was to develop a method to assemble *P. modestum*  $F_0$  of individually expressed and purified subunits. A purification protocol for subunit c was already amenable (Matthey *et al.*, 1997). An expression system for the *uncB* and *uncF* genes had to be built up allowing the

synthesis of considerable amounts of recombinant *P. modestum* subunits a and b. The overexpressed subunits were purified and re-assembled *in vitro* to functional  $F_0$  complexes. By means of this technique the mutational analysis of individually synthesised *P. modestum*  $F_0$  subunits becomes feasible, and residues involved in sodium translocation can be identified. This method could encourage approaches for structural investigations of subunit a and offers a powerful tool for further characterising *P. modestum*  $F_0$ . It was already successfully adopted for single molecule spectroscopy since it is the only method to modify specifically single c subunits within the c-oligomer.

Mutational analyses on the *E. coli* ATPase attribute a very important role to residue Arg210 on subunit a (Lightowers *et al.*, 1987; Cain & Simoni, 1989; Howitt & Cox, 1992; Hatch *et al.*, 1995; Valiyaveetil & Fillingame, 1997). It was found that in all tested mutants of this site ATP synthesis was entirely abolished and ATP hydrolysis was not coupled to proton translocation. Not even the conservative replacement of the arginine by a lysine was tolerated. Since lysine is expected to carry a positive charge at physiological pH, such a deleterious effect of mutant aArg210Lys is not compatible with functional models of the  $F_0$  motor, which only demand the presence of a positive charge to couple the proton flux to the rotor motion (Elston *et al.*, 1998). The second part of this thesis focuses on this intriguing inconsistency. We scrutinised the role of the positive stator charge with the aid of the sodium translocating *P. modestum* ATPase. Therefore Arg227 on *P. modestum* subunit a (the homologue of aArg210 of *E. coli*) was investigated by thorough mutational analysis. Mutant  $F_0$  complexes were re-assembled *in vitro* by the above newly established method and sodium transport measurements with reconstituted  $F_0$  liposomes were performed. In addition, ATP synthesis and sodium ion activation of ATP hydrolysis were studied on mutant  $F_1F_0$  liposomes to elucidate the coupling of ion translocation through the  $F_0$  part to ATP synthesis/hydrolysis in the  $F_1$  part. The results obtained by the aR227 mutants are essential to clarify the role of the positive stator and allow better insights into the mechanism of the  $F_0$  motor.

Besides aArg210 of the *E. coli* ATPase, aGlu219 and aHis245 were identified as important residues and assumed to be involved in the proton transport process across the membrane (Lightowers *et al.*, 1987; Cain & Simoni, 1988; Eya *et al.*, 1991). There is experimental evidence that these two amino acids are interchangeable. By sequence alignment, Met236 and Asp259 were found to be the equivalent residues in

*P. modestum*. Since charged residues within a transmembrane span are promising candidates to be functionally relevant, in the third part of this thesis Asp259 on the C-terminal helix of *P. modestum* subunit a was investigated. It was of special interest, whether aAsp259 is directly involved in Na<sup>+</sup> binding or if it contributes to the hydrophilic environment required for the gating of the sodium ions from the periplasm to their binding sites on the c-oligomer. During this study mutational and kinetic analyses of this site were performed to elucidate its function.

## 1.7 References

- ABRAHAMS, J. P., LESLIE, A. G., LUTTER, R. & WALKER, J. E. (1994). Structure at 2.8 Å resolution of F<sub>1</sub>-ATPase from bovine heart mitochondria. *Nature* 370, 621-628.
- AGGELER, R. & CAPALDI, R. A. (1996). Nucleotide-dependent movement of the epsilon subunit between alpha and beta subunits in the *Escherichia coli* F<sub>1</sub>F<sub>o</sub>-type ATPase. *J. Biol. Chem.* 271(23), 13888-13891.
- AGGELER, R., WEINREICH, F. & CAPALDI, R. A. (1995). Arrangement of the epsilon subunit in the *Escherichia coli* ATP synthase from the reactivity of cysteine residues introduced at different positions in this subunit. *Biochim. Biophys. Acta* 1230(1-2), 62-68.
- BIRKENHÄGER, R., HOPPERT, M., DECKERS-HEBESTREIT, G., MAYER, F. & ALTENDORF, K. (1995). The F<sub>o</sub> complex of the *Escherichia coli* ATP synthase. Investigation by electron spectroscopic imaging and immunoelectron microscopy. *Eur. J. Biochem.* 230(1), 58-67.
- BOYER, P. D. (1993). The binding change mechanism for ATP synthase - some probabilities and possibilities. *Biochim. Biophys. Acta* 1140(3), 215-250.
- BULYGIN, V. V., DUNCAN, T. M. & CROSS, R. L. (1998). Rotation of the ε subunit during catalysis by *Escherichia coli* F<sub>o</sub>F<sub>1</sub>-ATP synthase. *J. Biol. Chem.* 273(48), 31765-31769.
- CAIN, B. D. & SIMONI, R. D. (1986). Impaired proton conductivity resulting from mutations in the a subunit of F<sub>1</sub>F<sub>o</sub>-ATPase in *Escherichia coli*. *J. Biol. Chem.* 261(22), 10043-10050.
- CAIN, B. D. & SIMONI, R. D. (1988). Interaction between Glu-219 and His-245 within the a subunit of F<sub>1</sub>F<sub>o</sub>-ATPase in *Escherichia coli*. *J. Biol. Chem.* 263(14), 6606-6612.
- CAIN, B. D. & SIMONI, R. D. (1989). Proton translocation by the F<sub>1</sub>F<sub>o</sub>-ATPase of *Escherichia coli*. Mutagenic analysis of the a subunit. *J. Biol. Chem.* 264(6), 3292-3300.
- DALLMANN, H. G., FLYNN, T. G. & DUNN, S. D. (1992). Determination of the 1-ethyl-3-[[3-(dimethylamino)propyl]-carbodiimide-induced cross-link between the b and ε subunits of *Escherichia coli* F<sub>1</sub>-ATPase. *J. Biol. Chem.* 267(26), 18953-18960.
- DECKERS-HEBESTREIT, G. & ALTENDORF, K. (1996). The F<sub>o</sub>F<sub>1</sub>-type ATP synthase of bacteria: Structure and function of the F<sub>o</sub> complex. *Annu. Rev. Microbiol.* 50, 791-824.
- DECKERS-HEBESTREIT, G., GREIE, J., STALZ, W. & ALTENDORF, K. (2000). The ATP synthase of *Escherichia coli*: structure and function of F<sub>o</sub> subunits. *Biochim. Biophys. Acta* 1458(2-3), 364-373.
- DIMROTH, P. (1997). Primary sodium ion translocating enzymes. *Biochim. Biophys. Acta* 1318(1-2), 11-51.
- DIMROTH, P., WANG, H., GRABE, M. & OSTER, G. (1999). Energy transduction in the sodium F-ATPase of *Propionigenium modestum*. *Proc. Natl. Acad. Sci. USA* 96(9), 4924-4929.

- DMITRIEV, O. Y., JONES, P. C. & FILLINGAME, R. H. (1999). Structure of the subunit c oligomer in the  $F_1F_0$  ATP synthase: model derived from solution structure of the monomer and cross-linking in the native enzyme. *Proc. Natl. Acad. Sci. USA* 96(14), 7785-7790.
- DUNCAN, T. M., BULYGIN, V. V., ZHOU, Y., HUTCHEON, M. L. & CROSS, R. L. (1995). Rotation of subunits during catalysis by *Escherichia coli*  $F_1$ -ATPase. *Proc. Natl. Acad. Sci. USA* 92(24), 10964-10968.
- DUNN, S. D. (1992). The polar domain of the b subunit of *Escherichia coli*  $F_1F_0$ -ATPase forms an elongated dimer that interacts with the  $F_1$  sector. *J. Biol. Chem.* 267(11), 7630-7636.
- DUNN, S. D. & CHANDLER, J. (1998). Characterization of a  $b_2\delta$  complex from *Escherichia coli* ATP synthase. *J. Biol. Chem.* 273(15), 8646-8651.
- DUNN, S. D., MCLACHLIN, D. T. & REVINGTON, M. (2000). The second stalk of *Escherichia coli* ATP synthase. *Biochim. Biophys. Acta* 1458(2-3), 356-363.
- ELSTON, T., WANG, H. & OSTER, G. (1998). Energy transduction in ATP synthase. *Nature* 391, 510-513.
- ESSER, U., KRUMHOLZ, L. R. & SIMONI, R. D. (1990). Nucleotide sequence of the  $F_0$  subunits of the sodium-dependent  $F_1F_0$ -ATPase of *Propionigenium modestum*. *Nucl. Acids Res.* 18(19), 5887.
- EYA, S., MAEDA, M. & FUTAI, M. (1991). Role of the carboxyl terminal region of  $H^+$ -ATPase ( $F_0F_1$ ) a subunit from *Escherichia coli*. *Arch. Biochem. Biophys.* 284(1), 71-77.
- FILLINGAME, R. H. (1990). Molecular mechanism of ATP synthesis by  $F_1F_0$ -Type  $H^+$ -transporting ATP synthases. — In: *The Bacteria*, p. 345-391.
- FILLINGAME, R. H., JONES, P. C., JIANG, W., VALIYAVEETIL, F. I. & DMITRIEV, O. Y. (1998). Subunit organization and structure in the  $F_0$  sector of *Escherichia coli*  $F_1F_0$  ATP synthase. *Biochim. Biophys. Acta* 1365(1-2), 135-142.
- FOSTER, D. L. & FILLINGAME, R. H. (1982). Stoichiometry of subunits in the  $H^+$ -ATPase complex of *Escherichia coli*. *J. Biol. Chem.* 257(4), 2009-2015.
- GAY, N. J. (1984). Construction and characterisation of an *Escherichia coli* strain with a *uncI* mutation. *J. Bacteriol.* 158(3), 820-825.
- GERIKE, U., KAIM, G. & DIMROTH, P. (1995). In vivo synthesis of ATPase complexes of *Propionigenium modestum* and *Escherichia coli* and analysis of their function. *Eur. J. Biochem.* 232(2), 496-602.
- GIBBONS, C., MONTGOMERY, M. G., LESLIE, A. G. & WALKER, J. E. (2000). The structure of the central stalk in bovine  $F_1$ -ATPase at 2.4 Å resolution. *Nat. Struct. Biol.* 7(11), 1055-1061.
- GIRVIN, M. E., RASTOGI, V. K., ALBILDGAARD, F., MARKLEY, J. L. & FILLINGAME, R. H. (1998). Solution structure of the transmembrane  $H^+$ -transporting subunit c of the  $F_1F_0$  ATP synthase. *Biochemistry* 37, 8817-8824.
- GROTH, G., TILG, Y. & SCHIRWITZ, K. (1998). Molecular architecture of the c-subunit oligomer in the membrane domain of F-ATPases probed by tryptophan substitution mutagenesis. *J. Mol. Biol.* 281(1), 49-59.
- HARA, K. Y., KATO-YAMADA, Y., KIKUCHI, Y., HISABORI, T. & YOSHIDA, M. (2001). The role of the  $\beta$ DELSEED motif of  $F_1$ -ATPase: propagation of the inhibitory effect of the e subunit. *J. Biol. Chem.* 276(26), 23969-23973.
- HATCH, L. P., COX, G. B. & HOWITT, S. M. (1995). The essential arginine residue at position 210 in the a subunit of the *Escherichia coli* ATP synthase can be transferred to position 252 with partial retention of activity. *J. Biol. Chem.* 270(49), 29407-29412.
- HERMOLIN, J., DMITRIEV, O. Y., ZHANG, Y. & FILLINGAME, R. H. (1999). Defining the domain of binding of  $F_1$  subunit e with the polar loop of  $F_0$  subunit c in the *Escherichia coli* ATP synthase. *J. Biol. Chem.* 274(23), 17011-17016.
- HERMOLIN, J., GALLANT, J. & FILLINGAME, R. H. (1983). Topology, organization, and function of the psi subunit in the  $F_0$  sector of the  $H^+$ -ATPase of *Escherichia coli*. *J. Biol. Chem.* 258(23), 14550-14555.

- HILPERT, W., SCHINK, B. & DIMROTH, P. (1984). Life by a new decarboxylation-dependent energy conservation mechanism with  $\text{Na}^+$  as coupling ion. *EMBO J.* 3(8), 1665-1670.
- HOWITT, S. M. & COX, G. B. (1992). Second-site revertants of an arginine-210 to lysine mutation in the a subunit of the  $\text{F}_1\text{F}_0$ -ATPase from *Escherichia coli*: implications for structure. *Proc. Natl. Acad. Sci. USA* 89(20), 9799-9803.
- HOWITT, S. M., RODGERS, A. J., HATCH, L. P., GIBSON, F. & COX, G. B. (1996). The coupling of the relative movement of the a and c subunits of the  $\text{F}_0$  to the conformational changes in the  $\text{F}_1$ -ATPase. *J. Bioenerg. Biomembr.* 28(5), 415-420.
- JÄGER, H., BIRKENHÄGER, R., STALZ, W.-D., ALTENDORF, K. & DECKERS-HEBESTREIT, G. (1998). Topology of subunit a of the *Escherichia coli* ATP synthase. *Eur. J. Biochem.* 251(1-2), 122-132.
- JIANG, W. & FILLINGAME, R. H. (1998). Interacting helical faces of subunits a and c in the  $\text{F}_1\text{F}_0$  ATP synthase of *Escherichia coli* defined by disulfide cross-linking. *Proc. Natl. Acad. Sci. USA* 95(12), 6607-6612.
- JIANG, W., HERMOLIN, J. & FILLINGAME, R. H. (2001). The preferred stoichiometry of c subunits in the rotary sector of *Escherichia coli* ATP synthase is 10. *Proc. Natl. Acad. Sci. USA* 98(9), 4966-4971.
- JONES, P. C. & FILLINGAME, R. H. (1998). Genetic fusions of subunit c in the  $\text{F}_0$  sector of the  $\text{H}^+$ -transporting ATP synthase. Functional dimers and trimers and determination of stoichiometry by crosslinking analysis. *J. Biol. Chem.* 273(45), 29701-29705.
- JONES, P. C., HERMOLIN, J. & FILLINGAME, R. H. (2000). Mutations in single hairpin units of genetically fused subunit c provide support for a rotary catalytic mechanism in  $\text{F}_0\text{F}_1$  ATP synthase. *J. Biol. Chem.* 275(15), 11355-11360.
- JONES, P. C., JIANG, W. & FILLINGAME, R. H. (1998). Arrangement of the multicopy  $\text{H}^+$ -translocating subunit c in the membrane sector of the *Escherichia coli*  $\text{F}_1\text{F}_0$  ATP synthase. *J. Biol. Chem.* 273(27), 17178-17185.
- JOUNOUCHI, M., TAKEYAMA, M., CHAI PRASERT, P., NOUMI, T., MORIYAMA, Y., MAEDA, M. & FUTAI, M. (1992). *Escherichia coli*  $\text{H}^+$ -ATPase: Role of the  $\delta$  subunit in binding  $\text{F}_1$  to the  $\text{F}_0$  sector. *Arch. Biochem. Biophys.* 292(2), 376-381.
- JUNGE, W., LILL, H. & ENGELBRECHT, S. (1997). ATP synthase: An electrochemical transducer with rotary mechanics. *Trends Biochem. Sci.* 22(11), 420-423.
- KAIM, G. & DIMROTH, P. (1993). Formation of a functionally active sodium-translocating hybrid  $\text{F}_1\text{F}_0$ -ATPase in *Escherichia coli* by homologous recombination. *Eur. J. Biochem.* 218(3), 937-944.
- KAIM, G. & DIMROTH, P. (1994). Construction, expression and characterization of a plasmid-encoded  $\text{Na}^+$ -specific ATPase hybrid consisting of *Propionigenium modestum*  $\text{F}_0$ -ATPase and *Escherichia coli*  $\text{F}_1$ -ATPase. *Eur. J. Biochem.* 222(2), 615-623.
- KAIM, G. & DIMROTH, P. (1995). A double mutation in subunit c of the  $\text{Na}^+$ -specific  $\text{F}_1\text{F}_0$ -ATPase of *Propionigenium modestum* results in a switch from  $\text{Na}^+$  to  $\text{H}^+$ -coupled ATP synthesis in the *Escherichia coli* host cells. *J. Mol. Biol.* 253(5), 726-738.
- KAIM, G. & DIMROTH, P. (1998a). ATP synthesis by the  $\text{F}_1\text{F}_0$  ATP synthase of *Escherichia coli* is obligatorily dependent on the electric potential. *FEBS Lett.* 434(1-2), 57-60.
- KAIM, G. & DIMROTH, P. (1998b). A triple mutation in the a subunit of the *Escherichia coli*/*Propionigenium modestum*  $\text{F}_1\text{F}_0$ -ATPase hybrid causes a switch from  $\text{Na}^+$  stimulation to  $\text{Na}^+$  inhibition. *Biochemistry* 37(13), 4626-4634.
- KAIM, G. & DIMROTH, P. (1998c). Voltage-generated torque drives the motor of the ATP synthase. *EMBO J.* 17(20), 5887-5895.
- KAIM, G. & DIMROTH, P. (1999). ATP synthesis by F-type ATP synthases is obligatorily dependent on the transmembrane voltage. *EMBO J.* 18(15), 4118-4127.

- KAIM, G., LUDWIG, W., DIMROTH, P. & SCHLEIFER, K. (1992). Cloning, sequencing and in vivo expression of genes encoding the  $F_0$  part of the sodium-ion-dependent ATP synthase of *Propionigenium modestum* in *Escherichia coli*. Eur. J. Biochem. 207(2), 463-470.
- KAIM, G., LUDWIG, W., DIMROTH, P. & SCHLEIFER, K. H. (1990). Sequence of subunits a and b of the sodium ion translocating adenosine triphosphate synthase of *Propionigenium modestum*. Nucl. Acids Res. 18(22), 6697.
- KAIM, G., MATTHEY, U. & DIMROTH, P. (1998). Mode of interaction of the single a subunit with the multimeric c subunits during the translocation of the coupling ions by  $F_1F_0$ -ATPases. EMBO J. 17(3), 688-695.
- KAIM, G., WEHRLE, F., GERIKE, U. & DIMROTH, P. (1997). Molecular basis for the coupling ion selectivity of  $F_1F_0$  ATP synthases: Probing the liganding groups for  $Na^+$  and  $Li^+$  in the c subunit of the ATP synthase from *Propionigenium modestum*. Biochemistry 36(30), 9185-9194.
- KLUGE, C. & DIMROTH, P. (1993a). Kinetics of inactivation of the  $F_1F_0$ -ATPase of *Propionigenium modestum* by dicyclohexylcarbodiimide in relationship to  $H^+$  and  $Na^+$  concentration: Probing the binding site for the coupling ions. Biochemistry 32(39), 10378-10386.
- KLUGE, C. & DIMROTH, P. (1993b). Specific protection by  $Na^+$  or  $Li^+$  of the  $F_1F_0$ -ATPase of *Propionigenium modestum* from the reaction with dicyclohexylcarbodiimide. J. Biol. Chem. 268(20), 14557-14560.
- LAUBINGER, W., DECKERS-HEBESTREIT, G., ALTENDORF, K. & DIMROTH, P. (1990). A hybrid adenosinetriphosphatase composed of  $F_1$  of *Escherichia coli* and  $F_0$  of *Propionigenium modestum* is a functional sodium ion pump. Biochemistry 29(23), 5458-5463.
- LAUBINGER, W. & DIMROTH, P. (1987). Characterization of the  $Na^+$ -stimulated ATPase of *Propionigenium modestum* as an enzyme of the  $F_1F_0$  type. Eur. J. Biochem. 168(168), 475-480.
- LAUBINGER, W. & DIMROTH, P. (1988). Characterization of the ATP synthase of *Propionigenium modestum* as a primary sodium pump. Biochemistry 27(19), 7531-7537.
- LAUBINGER, W. & DIMROTH, P. (1989). The sodium ion translocating adenosinetriphosphatase of *Propionigenium modestum* pumps protons at low sodium ion concentrations. Biochemistry 28(18), 7194-7198.
- LIGHTOWLERS, R. N., HOWITT, S. M., HATCH, L., GIBSON, F. & COX, G. (1988). The proton pore in the *Escherichia coli*  $F_0F_1$ -ATPase: Substitution of glutamate by glutamine at position 219 of the alpha-subunit prevents  $F_0$ -mediated proton permeability. Biochim. Biophys. Acta 933(2), 241-248.
- LIGHTOWLERS, R. N., HOWITT, S. M., HATCH, L., GIBSON, F. & COX, G. B. (1987). The proton pore in *Escherichia coli*  $F_0F_1$ -ATPase: A requirement of arginine at position 210 of the a-subunit. Biochim. Biophys. Acta 894(3), 399-406.
- LILL, H., HENSEL, F., JUNGE, W. & ENGELBRECHT, S. (1996). Cross-linking of engineered subunit  $\delta$  to ( $\alpha\beta$ )<sub>3</sub> in chloroplast F-ATPase. J. Biol. Chem. 271(51), 32737-32742.
- LONG, J. C., WANG, S. & VIK, S. B. (1998). Membrane topology of subunit a of the  $F_1F_0$  ATP synthase as determined by labelling of unique cysteine residues. J. Biol. Chem. 273(26), 16235-16240.
- LUDWIG, W., KAIM, G., LAUBINGER, W., DIMROTH, P., HOPPE, J. & SCHLEIFER, K. H. (1990). Sequence of subunit c of the sodium ion translocating adenosine triphosphate synthase of *Propionigenium modestum*. Eur. J. Biochem. 193(2), 395-399.
- MATTHEY, U., KAIM, G., BRAUN, D., WÜTHRICH, K. & DIMROTH, P. (1999). NMR studies of subunit c of the ATP synthase from *Propionigenium modestum* in dodecylsulfate micelles. Eur. J. Biochem. 261(2), 459-467.
- MATTHEY, U., KAIM, G. & DIMROTH, P. (1997). Subunit c from the sodium-ion-translocating  $F_1F_0$ -ATPase of *Propionigenium modestum*. Production, purification and properties of the protein in dodecylsulfate solution. Eur. J. Biochem. 247(3), 820-825.
- MCLACHLIN, D. T., BESTARD, J. A. & DUNN, S. D. (1998). The b and  $\delta$  subunits of the *Escherichia coli* ATP synthase interact via residues in their C-terminal regions. J. Biol. Chem. 273(24), 15162-15168.

- MCLACHLIN, D. T. & DUNN, S. D. (1997). Dimerization interactions of the b-subunit of the *Escherichia coli* F<sub>1</sub>F<sub>o</sub>-ATPase. *J. Biol. Chem.* 272(34), 21233-21239.
- MILLER, M. J., OLDENBURG, M. & FILLINGAME, R. H. (1990). The essential carboxyl group in subunit c of the F<sub>1</sub>F<sub>o</sub> ATP synthase can be moved and H<sup>+</sup>-translocating function retained. *Proc. Natl. Acad. Sci. USA* 87(13), 4900-4904.
- NAKAMOTO, R. K. (1996). Mechanisms of active transport in the F<sub>o</sub>F<sub>1</sub> ATP synthase. *J. Membrane Biol.* 151(2), 101-111.
- NAKAMOTO, R. K., KETCHUM, C. J. & AL-SHAWI, M. K. (1999). Rotational coupling in the F<sub>1</sub>F<sub>o</sub> ATP synthase. *Annu. Rev. Biophys. Biomol. Struct.* 28, 205-234.
- NOJI, H., YASUDA, R., YOSHIDA, M. & KINOSITA, K. (1997). Direct observation of the rotation of F<sub>1</sub>-ATPase. *Nature* 386, 299-302.
- OGILVIE, I., AGGELER, R. & CAPALDI, R. A. (1997). Cross-linking of the delta subunit to one of the three alpha subunits has no effect on functioning, as expected if delta is a part of the stator that links the F<sub>1</sub> and F<sub>o</sub> parts of the *Escherichia coli* ATP synthase. *J. Biol. Chem.* 272(26), 16652-16656.
- PÄNKE, O., GUMBIOWSKI, K., JUNGE, W. & ENGELBRECHT, S. (2000). F-ATPase: specific observation of the rotating c subunit oligomer of EF<sub>o</sub>EF<sub>1</sub>. *FEBS Lett.* 472(1), 34-38.
- PERLIN, D. S. & SENIOR, A. E. (1985). Functional effects and cross-reactivity of antibody to purified subunit b (UncF protein) of *Escherichia coli* proton-ATPase. *Arch. Biochem. Biophys.* 236(2), 603-611.
- RASTOGI, V. K. & GIRVIN, M. E. (1999a). <sup>1</sup>H, <sup>13</sup>C, and <sup>15</sup>N assignments and secondary structure of the high pH form of subunit c of the F<sub>1</sub>F<sub>o</sub> ATP synthase. *J. Biomol. NMR* 13(1), 91-92.
- RASTOGI, V. K. & GIRVIN, M. E. (1999b). Structural changes linked to proton translocation by subunit c of the ATP synthase. *Nature* 402, 263-268.
- RODGERS, A. J. & WILCE, M. C. (2000). Structure of the γ-ε complex of ATP synthase. *Nat. Struct. Biol.* 7(11), 1051-1054.
- RODGERS, A. J., WILKENS, S., AGGELER, R., MORRIS, M. B., HOWITT, S. M. & CAPALDI, R. A. (1997). The subunit delta-subunit b domain of the *Escherichia coli* F<sub>1</sub>F<sub>o</sub>-ATPase. The b subunits interact with F<sub>1</sub> as a dimer and through the δ subunit. *J. Biol. Chem.* 272(49), 31058-31064.
- RODGERS, A. J. W. & CAPALDI, R. A. (1998). The second stalk composed of the b- and δ-subunits connects F<sub>o</sub> to F<sub>1</sub> via an α-subunit in the *Escherichia coli* ATP synthase. *J. Biol. Chem.* 273(45), 29406-29410.
- SABBERT, D., ENGELBRECHT, S. & JUNGE, W. (1996). Intersubunit rotation in active F-ATPase. *Nature* 381, 623-625.
- SAMBONGI, Y., IKO, Y., TANABE, M., OMOTE, H., IWAMOTO-KIHARA, A., UEDA, I., YANAGIDA, T., WADA, Y. & FUTAI, M. (1999). Mechanical rotation of the c subunit oligomer in ATP synthase F<sub>1</sub>F<sub>o</sub>: direct observation. *Science* 286, 1722-1724.
- SAWADA, K., KURODA, N., WATANABE, H., MORITANI-OTSUKA, C. & KANAZAWA, H. (1997). Interaction of the δ and b subunits contributes to F<sub>1</sub> and F<sub>o</sub> interaction in *Escherichia coli* F<sub>1</sub>F<sub>o</sub>-ATPase. *J. Biol. Chem.* 272(48), 30047-30053.
- SCHINK, B. & PFENNIG, N. (1982). *Propionigenium modestum* gen. nov. sp. nov. a new strictly anaerobic, nonsporing bacterium growing on succinate. *Arch. Microbiol.* 133, 209-216.
- SCHNEIDER, E. & ALTENDORF, K. (1984). Subunit b of the membrane moiety (F<sub>o</sub>) of ATP synthase (F<sub>1</sub>F<sub>o</sub>) from *Escherichia coli* is indispensable for H<sup>+</sup> translocation and binding of the water-soluble F<sub>1</sub> moiety. *Proc. Natl. Acad. Sci. USA* 81(23), 7279-7283.
- SCHNEIDER, E. & ALTENDORF, K. (1985). All three subunits are required for the reconstitution of an active proton channel (F<sub>o</sub>) of *Escherichia coli* ATP synthase (F<sub>1</sub>F<sub>o</sub>). *EMBO J.* 4(2), 515-518.
- SCHNEPPE, B., DECKERS-HEBESTREIT, G. & ALTENDORF, K. (1991). Detection and localization of the *i* protein in *Escherichia coli* cells using antibodies. *FEBS Lett.* 292(1,2), 145-147.

- SCHNICK, C., FORREST, L. R., SANSOM, M. S. & GROTH, G. (2000). Molecular contacts in the transmembrane c-subunit oligomer of F-ATPases identified by tryptophan substitution mutagenesis. *Biochim. Biophys. Acta* 1459(1), 49-60.
- SCHULENBERG, B., AGGELER, R., MURRAY, J. & CAPALDI, R. A. (1999). The  $\gamma$ -c subunit interface in the ATP synthase of *Escherichia coli*. *J. Biol. Chem.* 274(48), 34233-34237.
- SEELERT, H., POETSCH, A., DENCHER, N. A., ENGEL, A., STAHLBERG, H. & MÜLLER, D. J. (2000). Proton-powered turbine of a plant motor. *Nature* 405, 418-419.
- SINGH, S., TURINA, P., BUSTAMANTE, C. J., KELLER, D. J. & CAPALDI, R. (1996). Topographical structure of membrane-bound *Escherichia coli* F<sub>1</sub>F<sub>o</sub> ATP synthase in aqueous buffer. *FEBS Lett.* 397(1), 30-34.
- SORGEN, P. L., CAVISTON, T. L., PERRY, R. C. & CAIN, B. D. (1998). Deletions in the second stalk of the F<sub>1</sub>F<sub>o</sub>-ATPase in *Escherichia coli*. *J. Biol. Chem.* 273(43), 27873-27878.
- STAHLBERG, H., MÜLLER, D. J., SUDA, K., FOTIADIS, D., ENGEL, A., MEIER, T., MATTHEY, U. & DIMROTH, P. (2001). Bacterial Na<sup>+</sup>-ATP synthase has an undecameric rotor. *EMBO reports* 2(3), 229-233.
- STEFFENS, K., SCHNEIDER, E., DECKERS-HEBESTREIT, G. & ALTENDORF, K. (1987). F<sub>o</sub> portion of *Escherichia coli* ATP synthase. Further resolution of trypsin-generated fragments from subunit b. *J. Biol. Chem.* 262(12), 5866-5869.
- STOCK, D., LESLIE, A. G. & WALKER, J. E. (1999). Molecular architecture of the rotary motor in ATP synthase. *Science* 286, 1700-1705.
- TAKEYASU, K., OMOTE, H., NETTIKADAN, S., TOKUMASU, F., IWAMOTU-KIHARA, A. & FUTAI, M. (1996). Molecular imaging of *Escherichia coli* F<sub>1</sub>F<sub>o</sub>-ATPase in reconstituted membranes using atomic force microscopy. *FEBS Lett.* 392(2), 110-113.
- TANABE, M., NISHIO, K., IKO, Y., SAMBONGI, Y., IWAMOTO-KIHARA, A., WADA, Y. & FUTAI, M. (2001). Rotation of a complex of the gamma subunit and c ring of *Escherichia coli* ATP synthase. The rotor and stator are interchangeable. *J. Biol. Chem.* 276(18), 15269-15274.
- TANG, C. & CAPALDI, R. A. (1996). Characterization of the interface between gamma and epsilon subunits of *Escherichia coli* F<sub>1</sub>-ATPase. *J. Biol. Chem.* 271(6), 3018-3024.
- THAYER, W. S. & HINKLE, P. C. (1975). Synthesis of adenosine triphosphate by an artificially imposed electrochemical proton gradient in bovine heart submitochondrial particles. *J. Biol. Chem.* 250(14), 5330-5335.
- UHLIN, U., COX, G. B. & GUSS, J. M. (1997). Crystal structure of the epsilon subunit of the proton-translocating ATP synthase from *Escherichia coli*. *Structure* 5(9), 1219-1230.
- VALIYAVEETIL, F. I. & FILLINGAME, R. H. (1997). On the role of Arg-210 and Glu-219 of subunit a in proton translocation by the *Escherichia coli* F<sub>o</sub>F<sub>1</sub>-ATP synthase. *J. Biol. Chem.* 272(51), 32635-32641.
- VALIYAVEETIL, F. I. & FILLINGAME, R. H. (1998). Transmembrane topography of subunit a in the *Escherichia coli* F<sub>1</sub>F<sub>o</sub> ATP synthase. *J. Biol. Chem.* 273(26), 16241-16247.
- VON BALLMOOS, C., APPOLDT, Y., BRUNNER, J., GRANIER, T., VASELLA, A. & DIMROTH, P. (2002). Membrane topography of the coupling ion binding site in Na<sup>+</sup>-translocating F<sub>1</sub>F<sub>o</sub> ATP synthase. *J. Biol. Chem.* 277(5), 3504-3510.
- VONCK, J., KRUG V. NIDDA, T., MEIER, T., MATTHEY, U., MILLS, D. J., KÜHLBRANDT, W. & DIMROTH, P. (2002). Molecular architecture of the undecameric rotor of a bacterial Na<sup>+</sup>-ATP synthase. *J. Mol. Biol.* 321(2), 307-316.
- WADA, W., LONG, J. C., ZHANG, D. & VIK, S. B. (1999). A novel labelling approach supports the five-transmembrane model of subunit a of the *Escherichia coli* ATP synthase. *J. Biol. Chem.* 274(24), 17353-17357.
- WATTS, S. D., TANG, C. & CAPALDI, R. A. (1996). The stalk region of the *Escherichia coli* ATP synthase. Tyrosine 205 of the gamma subunit is in the interface between the F<sub>1</sub> and F<sub>o</sub> parts and can interact with both the epsilon and c oligomer. *J. Biol. Chem.* 271(45), 28341-28347.



- WATTS, S. D., ZHANG, Y., FILLINGAME, R. H. & CAPALDI, R. A. (1995). The gamma subunit in the *Escherichia coli* ATP synthase complex (ECF<sub>1</sub>F<sub>o</sub>) extends through the stalk and contacts the c subunits of the F<sub>o</sub> part. FEBS Lett. 368(2), 235-238.
- WEHRLE, F., APPOLDT, Y., KAIM, G. & DIMROTH, P. (2002). Reconstitution of F<sub>o</sub> of the ATP synthase of *Propionigenium modestum* from its heterologously expressed and purified subunits. Eur. J. Biochem. 269(10), 2567-2573.
- WEHRLE, F., KAIM, G. & DIMROTH, P. (2002). Molecular mechanism of the ATP synthase's F<sub>o</sub> motor probed by mutational analysis. J. Mol. Biol. 322(2), 369-381.
- WILKENS, S. (1998). Solution structure of the ε subunit of the F<sub>1</sub>-ATPase from *Escherichia coli* and interactions of this subunit with b subunits in the complex. J. Biol. Chem. 273(41), 26645-26651.
- WILKENS, S., DAHLQUIST, F. W., MCINTOSH, L. P., DONALDSON, L. W. & CAPALDI, R. A. (1995). Structural features of the epsilon subunit of the *Escherichia coli* ATP synthase determined by NMR spectroscopy. Nat. Struct. Biol. 2(11), 961-967.
- WILKENS, S., DUNN, S. D., CHANDLER, J., DAHLQUIST, F. W. & CAPALDI, R. A. (1997a). Solution structure of the N-terminal domain of the delta subunit of the *E. coli* ATP synthase. Nat. Struct. Biol. 4(3), 198-201.
- WILKENS, S., RODGERS, A., OGILVIE, I. & CAPALDI, R. A. (1997b). Structure and arrangement of the δ subunit in the *Escherichia coli* ATP synthase (ECF<sub>1</sub>F<sub>o</sub>). Biophys. Chem. 68(1-3), 95-102.
- YAMADA, H., MORIYAMA, Y., MAEDA, M. & FUTAI, M. (1996). Transmembrane topology of *Escherichia coli* H<sup>+</sup>-ATPase (ATP synthase) subunit a. FEBS Lett. 390(1), 34-38.
- ZHANG, Y. & FILLINGAME, R. H. (1995). Subunits coupling H<sup>+</sup> transport and ATP synthesis in the *Escherichia coli* ATP synthase. Cys-Cys cross-linking of F<sub>1</sub> subunit epsilon to the polar loop of F<sub>o</sub> subunit c. J. Biol. Chem. 270(41), 24609-24614.
- ZHANG, Y., OLDENBURG, M. & FILLINGAME, R. H. (1994). Suppressor mutations in F<sub>1</sub> subunit epsilon recouple ATP-driven H<sup>+</sup> translocation in uncoupled Q42E subunit c mutant of *Escherichia coli* F<sub>1</sub>F<sub>o</sub> ATP synthase. J. Biol. Chem. 269(14), 10221-10224.
- ZHOU, Y., DUNCAN, T. M., BULYGIN, V. V., HUTCHEON, M. L. & CROSS, R. L. (1996). ATP hydrolysis by membrane-bound *Escherichia coli* F<sub>o</sub>F<sub>1</sub> causes rotation of the gamma subunit relative to the beta subunits. Biochim. Biophys. Acta 1275(1-2), 96-100.
- ZHOU, Y., DUNCAN, T. M. & CROSS, R. L. (1997). Subunit rotation in *Escherichia coli* F<sub>o</sub>F<sub>1</sub>-ATP synthase during oxidative phosphorylation. Proc. Natl. Acad. Sci. USA 94(20), 10583-10587.

## CHAPTER 2

### **Reconstitution of F<sub>0</sub> of the sodium ion translocating ATP synthase of *Propionigenium modestum* from its heterologously expressed and purified subunits**

Franziska Wehrle, Yvonne Appoldt, Georg Kaim and Peter Dimroth

Institut für Mikrobiologie, Eidgenössische Technische Hochschule  
CH-8092 Zürich, Switzerland

*European Journal of Biochemistry* (2002), 269(10):2567-2573

## 2.1 Abstract

The *atpB* and *atpF* genes of *Propionigenium modestum* were cloned as His-tag fusion constructs and expressed in *Escherichia coli*. Both recombinant subunits a and b were purified *via* Ni<sup>2+</sup> chelate affinity chromatography. A functionally active F<sub>o</sub> complex was re-assembled *in vitro* from subunits a, b and c, and incorporated into liposomes. The F<sub>o</sub> liposomes catalysed <sup>22</sup>Na<sup>+</sup> uptake in response to an inside negative potassium diffusion potential, and the uptake was prevented by modification of the c subunits with DCCD. In absence of a membrane potential the F<sub>o</sub> complexes catalysed <sup>22</sup>Na<sup>+</sup><sub>out</sub>/Na<sup>+</sup><sub>in</sub> exchange. After F<sub>1</sub> addition the F<sub>1</sub>F<sub>o</sub> complex was formed and the holoenzyme catalysed ATP synthesis, ATP-dependent Na<sup>+</sup> pumping, and ATP hydrolysis, which was inhibited by DCCD. Functional F<sub>o</sub> hybrids were reconstituted with recombinant subunits a and b from *P. modestum* and c<sub>11</sub> from *Ilyobacter tartaricus*. These F<sub>o</sub> hybrids had Na<sup>+</sup> translocation activities that were not distinguishable from that of *P. modestum* F<sub>o</sub>.

*Abbreviations:* DCCD, *N,N'*-dicyclohexylcarbodiimide; IPTG, isopropyl-2-D-thiogalactopyranoside; DTT, 1,4-dithio-DL-threitol; DFP, diisopropylfluoro-phosphate; PCR, polymerase chain reaction; SDS-PAGE, sodium-dodecyl-sulfate-polyacrylamide gel electrophoresis; Tris, tris-(hydroxymethyl)-aminomethane; Tricine, N-(tris-(hydroxymethyl)-methyl)-glycine; PEG, polyethylene glycol; Bistris-propane, 1,3-bis-[tris-(hydroxymethyl)-methylamino]-propane; ΔΨ, trans-membrane electrical potential.

## 2.2 Introduction

F<sub>1</sub>F<sub>o</sub> type ATP synthases are widely distributed among eukaryotes, plants and bacteria. Utilising the energy stored in an electrochemical ion gradient, these enzymes catalyse the synthesis of ATP from ADP and inorganic phosphate. In bacteria, the enzyme can also operate in reverse as an ATP-driven ion pump (Weber & Senior, 1997; Capaldi *et al.*, 2000; Yoshida *et al.*, 2001). Detailed structural knowledge is

available for the water-soluble F<sub>1</sub> headpiece with the subunit composition  $\alpha_3\beta_3\gamma\delta\epsilon$ . Alternating  $\alpha$  and  $\beta$  subunits form a cylinder around subunit  $\gamma$ . Part of the  $\gamma$  subunit protrudes from the bottom of the cylinder and forms the central stalk together with the  $\epsilon$  subunit. At its foot, this stalk is connected with an oligomeric ring of c subunits (Abrahams *et al.*, 1994; Stock *et al.*, 1999). The  $\gamma$ ,  $\epsilon$ , and c<sub>n</sub> assembly represents the rotor, which rotates against the stator consisting of subunits  $a_2\alpha_3\beta_3\delta$  upon ATP hydrolysis. The membrane-bound F<sub>0</sub> subunit a is connected laterally with the c-ring, where it is held in place by the two b subunits, which form the peripheral stalk connecting subunit a and an  $\alpha$  subunit of F<sub>1</sub> with the help of the  $\delta$  subunit (Ogilvie *et al.*, 1997; Rodgers *et al.*, 1997; Dunn & Chandler, 1998; McLachlin *et al.*, 1998; Wilkens & Capaldi, 1998; Dunn *et al.*, 2000). Recent structural work has shown that the number of c subunits within the ring varies among species, being 10, 11 or 14 for the ATP synthases from yeast mitochondria, from the bacterium *Ilyobacter tartaricus*, or from spinach chloroplasts, respectively (Stock *et al.*, 1999; Seelert *et al.*, 2000; Stahlberg *et al.*, 2001). Subunit c plays a key role in binding the coupling ions during their translocation across the membrane. Each c subunit contains either a glutamate (cE65 in *P. modestum*) or aspartate (cD61 in *E. coli*) residue that contributes to ion binding. This strictly conserved carboxylate side chain can be covalently modified with DCCD, and thereby ATPase activity is inhibited (Kluge & Dimroth, 1993a). Besides c<sub>n</sub>, subunit a is an essential part of the F<sub>0</sub> motor, which uses the electrochemical ion gradient to generate rotary torque. As the structure of the a subunit is not known in any detail, its precise function in the ion translocation and torque-generating mechanism remains speculative.

On the other hand, the mechanism of F<sub>0</sub> has been intensively studied biochemically. For this purpose, the Na<sup>+</sup>-translocating ATP synthase from *P. modestum* is particularly well suited (Dimroth, 2000; Kaim, 2001). It was discovered that the motor in its idling mode performs back and forth rotations of the rotor versus the stator thereby shuffling Na<sup>+</sup> ions back and forth across the membrane. The switch from idling into torque generation is strictly dependent on the membrane potential and consequently this driving force is kinetically indispensable for ATP synthesis (Kaim & Dimroth, 1998b; Kaim & Dimroth, 1998a; Kaim & Dimroth, 1999).

In this communication we describe the overproduction of the a and b subunits from *P. modestum* in *E. coli* together with purification and reconstitution of functional F<sub>0</sub> complexes. These methods open new avenues for biochemical and mutational studies on individual F<sub>0</sub> subunits in the future.

## 2.3 Materials and Methods

### **Cloning of *atpB* and *atpF* from *P. modestum* ATPase**

*AtpB* was amplified from chromosomal *P. modestum* DNA (DSM2376) by PCR using primers Pma1V (5'-TAAATGGAGACCATATGAAAAAAATGG-3' (*NdeI*)) and Pma889R (5'-TGTTTAAACTGGATCCAACTAATCTTC-3' (*Bam*HI)). The resulting 902 bp fragment was cloned into vector pET16b yielding plasmid pPmaHisN. *AtpF* was cloned by a similar approach into vector pET23a using oligonucleotides Pmb1V 5'-GAGGTAGACCATATG CACCAC-3' (*NdeI*) and Pmb504R 5'-ACTTGTGCTTGGATCCTTTCTCTTC-3' (*Bam*HI) for PCR. The resulting plasmid was digested with *Eco*RI and *Not*I, filled with Klenow polymerase and religated to obtain plasmid pPmbHisC. The nucleotide sequences of the cloned DNA fragments were confirmed by the dideoxy chain termination method (Sanger *et al.*, 1977).

### **Heterologous expression of the genes encoding the *P. modestum* subunits a and b in *E. coli***

*E. coli* C43(DE3) (Miroux & Walker, 1996) was transformed with plasmids pPmaHisN or pPmbHisC, respectively, and the cells were grown in 2×TY (16 g/l tryptone, 10 g/l yeast extract, 5 g/l NaCl, pH 7.5) supplemented with 200 mg/l ampicillin to optical densities (600 nm) between 0.4 and 0.6. Subsequently 0.7 mM IPTG was added and the cultures were incubated for another 3 h at 37 °C. The cells were harvested, washed once with 10 mM Tris pH 8.0 and frozen at -20 °C. The formation of inclusion bodies was not tested.

### **Isolation of membranes and solubilisation**

5-10 g cells (wet weight) were suspended in 30 ml 10 mM Tris/HCl pH 8.0, containing 1 mM K<sub>2</sub>-EDTA and 0.1 mM DFP and disrupted in a French pressure cell at 11,000 psi (7.6×10<sup>7</sup> Pa). Two different types of membrane fractions were collected

during centrifugation as described (Arechaga *et al.*, 2000). The first fraction was obtained by low-speed centrifugation at  $2,500 \times g$  (lowspin-pellet). The second membrane fraction was isolated by high-speed centrifugation at  $200,000 \times g$  of the  $2,500 \times g$  supernatant (highspin-pellet). Both pellets were washed once with 30 ml 10 mM Tris/HCl pH 8.0, containing 1 mM K<sub>2</sub>-EDTA and 0.1 mM DFP. The membrane pellets were resuspended separately in 50 mM potassium phosphate buffer, pH 8.0, containing 20 % glycerol and 5 mM MgCl<sub>2</sub>, and solubilised with 1 % N-lauroyl-sarcosine while gently stirring for 30 min at 25 °C. Unsolubilised material was removed by ultracentrifugation (1 h,  $200,000 \times g$ ).

#### **Purification of subunit a from *E. coli* C43(DE3)/pPmaHisN**

Solubilised proteins were loaded onto 1 ml bed volume His-bind resin (Novagen) loaded with Ni<sup>2+</sup> and equilibrated with binding buffer (5 mM imidazole, 500 mM NaCl, 20 mM potassium phosphate buffer pH 8.0) in a polypropylene column (5 mm diameter). The column was washed with 20 ml binding buffer containing 0.1 % Triton X-100 followed by 20 ml wash buffer (120 mM imidazole, 500 mM NaCl, 20 mM potassium phosphate buffer pH 6.0, 0.1 % Triton X-100). Subunit a was eluted in eight 1 ml fractions with elution buffer (400 mM imidazole, 500 mM NaCl, 20 mM potassium phosphate buffer pH 7.0, 0.1 % Triton X-100). Fractions two to four containing 90 % of the protein were pooled and concentrated by centrifugation at 4 °C and  $5000 \times g$  through a Centricon-YM10 filter unit (Millipore, Bedford (US)) to a final volume of 1 ml. The protein solution was stored in liquid nitrogen. The purification procedure was monitored by SDS-PAGE (Schägger & Jagow, 1987) and protein concentrations were determined using the BCA protein assay (Pierce).

#### **Purification of subunit b from *E. coli* C43(DE3)/pPmbHisC**

Solubilised proteins were purified *via* Ni<sup>2+</sup> chelate affinity chromatography (1.5 ml bed volume) essentially as described above. Chromatography was performed with 9 ml binding buffer containing 0.1 % dodecyl maltoside instead of 0.1 % Triton X-100, followed by 9 ml wash buffer (60 mM imidazole, 500 mM NaCl, 20 mM potassium phosphate buffer pH 6.0, 0.1 % dodecyl maltoside). The protein was eluted with  $6 \times 1.5$  ml elution buffer (400 mM imidazole, 500 mM NaCl, 20 mM

potassium phosphate buffer pH 9.0, 0.1 % dodecyl maltoside), and the fractions containing subunit b were stored in liquid nitrogen.

### **Purification of monomeric subunit c from PEF42(DE3)/pT7c and of c<sub>11</sub> from *P. modestum* and *I. tartaricus***

Monomeric subunit c was synthesised and purified by extraction with organic solvents as described (Matthey *et al.*, 1997; Matthey *et al.*, 1999). Prior to utilisation 0.1 volume of 10 % sodium cholate was added to 70  $\mu$ l (70  $\mu$ g) of the protein solution in chloroform/methanol (2:1) and the solvent was evaporated under a stream of argon. The pellet was dried in a vacuum centrifuge and resuspended in 70  $\mu$ l 5 mM potassium phosphate buffer, pH 8.0, containing 5 mM MgCl<sub>2</sub>. The c<sub>11</sub> oligomers were purified as described recently (Meier *et al.*, 2002).

### **Preparation of liposomes containing F<sub>0</sub>**

80 mg phosphatidylcholine (Sigma type II-S from soybean) were resuspended in 1 ml buffer containing 15 mM Tricine/NaOH, pH 8.0, 7.5 mM DTT, 0.2 mM K<sub>2</sub>-EDTA, 1.6 % sodium cholate and 0.8 % sodium deoxycholate by shaking the suspension vigorously for 3 min. The suspension was sonicated to clarity in a water bath sonicator for 5 min.

The reconstitution was performed in accordance with the procedure used for *E. coli* F<sub>0</sub> (Dmitriev *et al.*, 1995). 25  $\mu$ g of subunit a, 29  $\mu$ g of subunit b and 70  $\mu$ g of subunit c were mixed. The volume was adjusted to 250  $\mu$ l with 10 mM Tris/HCl, pH 8.0, 150 mM NaCl, 10 % glycerol, 1 % sodium cholate and the sample was sonicated in a Branson bath sonicator for 20 min at 25 °C. Following incubation on ice for 2-3 h 250  $\mu$ l of the above phosphatidylcholine suspension was added and the sample sonicated for 5 min. The solution was dialysed overnight against 1000 volumes of 5 mM Bistris-propane/HCl, pH 7.4, 2.5 mM MgCl<sub>2</sub>, 0.2 mM K<sub>2</sub>-EDTA, 0.2 mM DTT. The dialysed proteoliposomes were diluted into an equal volume of 5 mM Bistris-propane/HCl pH 7.4 and sonicated four times for 5 s in a water bath. The sonicated proteoliposomes were frozen in liquid nitrogen for 15 min and thawed at 25 °C. After thawing 750  $\mu$ l 5 mM Bistris-propane/HCl/1 mM MgCl<sub>2</sub>, pH 7.4, were added and the sample was centrifuged at 200'000  $\times$  g for 1 h. The pellet was resuspended in 5 mM Bistris-propane/HCl/1 mM MgCl<sub>2</sub>, pH 7.4, to a final

volume of 100  $\mu$ l, sonicated as described above and frozen in liquid nitrogen. During this reconstitution procedure the non-dialysable detergents (TX-100 and dodecyl maltoside) were diluted out to concentrations lower than the critical micellar concentration. Prior to usage the samples were thawed and sonicated four times for 5 s in a water bath type sonicator.

### **Reconstitution of the ATPase enzyme complex from reconstituted F<sub>0</sub> liposomes and F<sub>1</sub>**

F<sub>1</sub>-ATPase was purified as described (Kluge & Dimroth, 1992). F<sub>1</sub> from DK8/pHEP100 (Kaim & Dimroth, 1994) was used for <sup>22</sup>Na<sup>+</sup> transport studies and F<sub>1</sub> from DK8/pHEPHisL5C (a derivative of pHEP100 with N-terminal His<sub>10</sub>-tag at subunit  $\beta$ , Yvonne Appoldt, unpublished result) was utilised for ATP hydrolysis experiments. This F<sub>1</sub> moiety contains the  $\alpha$ ,  $\beta$ ,  $\gamma$  and  $\epsilon$  subunits from *E. coli* and the  $\delta$  subunit from *P. modestum*. Proteoliposomes containing 20 mg phospholipids and 124  $\mu$ g F<sub>0</sub> (0.8 nmoles) were incubated with an equimolar amount of F<sub>1</sub> at 4 °C for 1 h or overnight, respectively. The membrane-bound enzyme complex was separated from excess F<sub>1</sub>-ATPase by centrifugation (1 h, 200,000  $\times$  g) and resuspension of the pellet in 5 mM Bistris-propane/HCl, pH 7.4, 1 mM MgCl<sub>2</sub> to a final volume of 100  $\mu$ l. The preparation of F<sub>1</sub>F<sub>0</sub> liposomes harbouring a His<sub>10</sub>-tag at the  $\beta$  subunit served for a convenient purification of F<sub>1</sub>F<sub>0</sub>-ATPase after solubilisation of the proteoliposomes.

### **Transport experiments**

*$\Delta\Psi$ -driven <sup>22</sup>Na<sup>+</sup>-uptake into proteoliposomes.* The incubation mixture contained in 1 ml at 25 °C: 2 mM Tricine/KOH buffer, pH 7.4, 5 mM MgCl<sub>2</sub>, 200 mM choline chloride, 2 mM <sup>22</sup>NaCl (0.36  $\mu$ Ci), and 50  $\mu$ l F<sub>0</sub> proteoliposomes (10 mg of lipid) loaded with 200 mM KCl. After equilibrating the mixture for 5 min, a membrane potential of -77 mV was established by the addition of 5  $\mu$ M valinomycin. Samples (140  $\mu$ l) were taken at various times and passed over 1 ml columns of Dowex 50, K<sup>+</sup>, to adsorb the external <sup>22</sup>Na<sup>+</sup> (Dimroth, 1982). The resin was washed with 0.6 ml of 2 mM Tricine/KOH pH 7.4, containing 5 mM MgCl<sub>2</sub> and 200 mM sucrose. The radioactivity detected in the wash fraction reflects the <sup>22</sup>Na<sup>+</sup> entrapped in the proteoliposomes and was determined by  $\gamma$ -counting.



*<sup>22</sup>Na<sup>+</sup><sub>out</sub>/<sup>22</sup>Na<sup>+</sup><sub>in</sub>-exchange.* 50 µl of Na<sup>+</sup>-loaded (100 mM NaCl) F<sub>0</sub> proteoliposomes (10 mg of lipid) were diluted into 1 ml 2 mM Tricine/KOH buffer, pH 7.4 containing 5 mM MgCl<sub>2</sub>, 100 mM choline chloride and 0.47 µCi <sup>22</sup>NaCl (5 mM NaCl). <sup>22</sup>Na<sup>+</sup> uptake was determined after separation of external from internal <sup>22</sup>Na<sup>+</sup> by Dowex 50, K<sup>+</sup>. The columns were washed with 0.6 ml 2 mM Tricine/KOH buffer, pH 7.4 containing 5 mM MgCl<sub>2</sub> and 100 mM sucrose.

*ATP-driven <sup>22</sup>Na<sup>+</sup>-uptake.* The incubation mixture contained the following components in 0.7 ml at 25 °C: 50 mM potassium phosphate buffer, pH 7.0, 5 mM MgCl<sub>2</sub>, 2 mM <sup>22</sup>NaCl (0.11 µCi) and 50 µl F<sub>1</sub>F<sub>0</sub> proteoliposomes (10 mg phospholipid). In addition, the assay was supplemented with 20 units of pyruvate kinase and 6 mM phosphoenolpyruvate providing an ATP regenerating system. Sodium transport was initiated after 5 min by adding 1.25 mM ATP (potassium salt). Samples (90 µl) were taken at various time points and external <sup>22</sup>Na<sup>+</sup> was separated from that entrapped within the liposomes by passage over a small column of Dowex 50, K<sup>+</sup>, as described (Dimroth, 1982). The resin was washed with 600 µl 5 mM potassium phosphate buffer, pH 7.0, 5 mM MgCl<sub>2</sub>, 100 mM K<sub>2</sub>SO<sub>4</sub> and the radioactivity was determined by γ-counting.

### **Determination of ATPase activity**

ATP hydrolysing activity was determined spectrophotometrically in a coupled assay measuring the oxidation of NADH at 340 nm (Laubinger & Dimroth, 1988). As the F<sub>1</sub>F<sub>0</sub> proteoliposomes were too opaque, the ATPase was solubilised in a buffer containing 5 mM Bistris-propane pH 7.4 and 1 % sodium cholate from the liposomes (40 mg phospholipid) in a total volume of 1 ml for 30 min at 25 °C while gently stirring. Unsolubilised material was removed by ultracentrifugation (1 h, 200'000 x g). Excess detergent and Na<sup>+</sup> were removed by binding the solubilised enzyme complex on 500 µl Ni-NTA (QIAGEN) equilibrated with 5 mM Bistris-propane pH 7.4. After washing the column with 10 volumes of equilibration buffer, the protein was eluted with 1 ml 5 mM Bistris-propane pH 7.4, containing 20 % glycerol and 40 mM imidazole. Subsequently, the protein was precipitated by 15 % PEG6000 and 50 mM MgCl<sub>2</sub> for 30 min at 4 °C and harvested by centrifugation. The pellet was resuspended in 50µl 5 mM Bistris-propane pH 7.4, containing 1 mM MgCl<sub>2</sub> and 20 % glycerol and

assayed immediately. 50µl protein solution represented the amount of ATPase reconstituted in 40 mg lipid (0.8 nmoles F<sub>1</sub>F<sub>0</sub>).

## 2.4 Results and Discussion

### Expression and purification of subunits a and b from *P. modestum*

*P. modestum* subunits a and b were individually synthesised by expression of plasmids pPmaHisN or pPmbHisC, respectively, in *E. coli* C43(DE3) (Miroux & Walker, 1996) and purified as His-tag fusion proteins. Plasmid pPmaHisN encodes subunit a with an N-terminal His<sub>10</sub>-tag and pPmbHisC codes for subunit b with a His<sub>6</sub>-extension at the C-terminal end. To confirm the synthesis of both polypeptides, cell extracts were subjected to SDS-PAGE. Subunit b was subsequently identified by N-terminal sequencing and subunit a was identified by immuno-blotting with an antibody directed against subunit a (Figure 1). Maximal yield of subunit b was achieved 3 h after induction with 0.7 mM IPTG at 37 °C. The amount of subunit a synthesised by the recombinant *E. coli* cells increased during a period of 6 h after induction, but subunit a of higher purity was obtained from cells harvested 3 h after induction. Both proteins were efficiently solubilised with 1 % N-lauroyl-sarcosine, while with 1 % Triton X-100 or 1 % dodecyl maltoside, only about 10 % of the recombinant proteins were extracted.

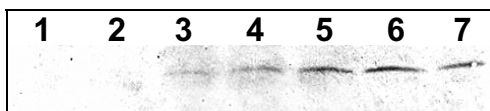


**Figure 1: Immunoblot of whole cell lysates of *E. coli* C43(DE3)/pPmaHisN synthesising subunit a from *P. modestum*.** Lane 1: before induction, lane 2, 3, 4, 5, 6 and 7: 1 h, 2.5 h, 3.5 h, 4.5 h, 5.5 h and 6.5 h after induction with 0.7 mM IPTG. The Western blot was developed using an antibody directed against subunit a.

Initial attempts to purify subunit a with a His<sub>6</sub>-tag at the C-terminus were not satisfactory. Subunit a was obtained in higher yield and better purity with a His<sub>10</sub>-tag fused to the N-terminus. The best results were obtained with *E. coli* C43(DE3) (Miroux & Walker, 1996) as the host strain by the purification protocol outlined in Materials and Methods (Figure 2; lane 1). The two bands of lower molecular weight

in lane 1 originate from impurities that could not be removed during the purification procedure.

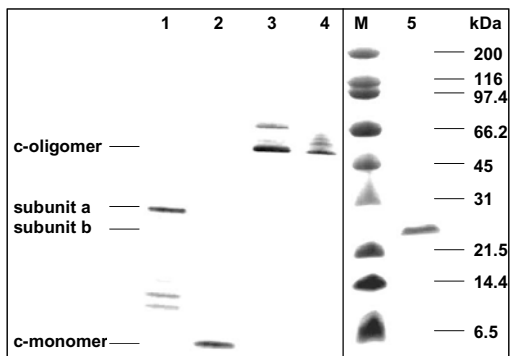


**Figure 2: Purity of individual F<sub>o</sub> subunits estimated by SDS-PAGE.** Subunits a, b, or c of the ATP synthase from *P. modestum* were individually synthesised in *E. coli*, purified and analysed by SDS-PAGE (12 % acrylamide) (Schägger & Jagow, 1987). Lane 1: subunit a with N-terminal His<sub>10</sub>-tag (33.6 kDa); lane 2: monomeric subunit c (8.7 kDa); lane 5: subunit b with C-terminal His<sub>6</sub>-tag (20 kDa); lane M: protein standard (sizes are given in kDa). Oligomeric c<sub>11</sub> of *P. modestum* (lane 3; 95.7 kDa) or *I. tartaricus* (lane 4; 96.7 kDa) was also applied. The left part of the gel was stained with silver and the right part was stained with Coomassie brilliant blue.

Ni<sup>2+</sup> affinity chromatography of subunit b resulted in 95 % pure protein as estimated from Coomassie-stained SDS-PAGE (Figure 2; lane 5). An alkaline pH of the elution buffer and the choice of dodecyl maltoside as detergent turned out to be crucial for the stability of the protein. With 0.1 % Triton X-100 in the buffer or during storage at neutral pH, subunit b was rapidly inactivated losing its potential for reconstitution into a functional F<sub>o</sub> complex.

### Reconstitution of functional F<sub>o</sub> from its purified subunits

To determine the functional integrity of purified subunits a and b, attempts were made to re-assemble the F<sub>o</sub> complex from these two subunits and the c subunit. As the latter had been isolated by extraction with chloroform/methanol (Matthey *et al.*, 1997), subunit c was first transferred into an aqueous buffer containing 1 % sodium cholate. Subunits a and b were then added in a ratio a:b:c = 1:2:10 and the mixture

was incubated for 2-3 h at 0 °C. Adding phospholipids followed by freezing/thawing and sonication completed the reconstitution of F<sub>0</sub> into proteoliposomes.

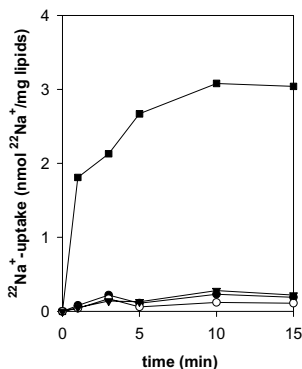


**Figure 3:**  $^{22}\text{Na}^+_{\text{in}}/\text{Na}^+_{\text{out}}$ -exchange by mixtures of purified subunits a, b, and c from *P. modestum* reconstituted into proteoliposomes. Proteoliposomes were reconstituted with subunits a, b, and c (■), a and b (●), b and c (◻), or a and c (▼) and then loaded with 100 mM NaCl. Exchange was initiated by diluting 50  $\mu\text{l}$  proteoliposomes (10 mg lipids) into 1 ml 2 mM Tricine/KOH, pH 7.4, containing 5 mM  $\text{MgCl}_2$ , 100 mM choline chloride and 0.47  $\mu\text{Ci}$   $^{22}\text{NaCl}$  (5 mM). Samples were taken at the times indicated, passed over Dowex 50,  $\text{K}^+$  to adsorb external  $^{22}\text{Na}^+$ , and the  $^{22}\text{Na}^+$  entrapped inside the proteoliposomes was subsequently determined by  $\gamma$ -counting.

The activity of the reconstituted F<sub>0</sub> was determined by  $^{22}\text{Na}^+_{\text{out}}/\text{Na}^+_{\text{in}}$  exchange and  $\Delta\Psi$ -driven  $^{22}\text{Na}^+$  uptake measurements. The results of Figure 3 show efficient  $^{22}\text{Na}^+_{\text{out}}/\text{Na}^+_{\text{in}}$  exchange activity with proteoliposomes containing the reconstituted F<sub>0</sub> moiety. It is also shown that combinations of only two of the F<sub>0</sub> subunits resulted in catalytically inactive specimens. This is in agreement with reconstitution experiments performed with the a, b, and c subunits of the *E. coli* ATP synthase (Schneider & Altendorf, 1985). Proteoliposomes with F<sub>0</sub> reconstituted from a, b, and c subunits of the *P. modestum* ATP synthase also catalysed  $^{22}\text{Na}^+$  uptake after applying a diffusion potential of -77 mV by adding valinomycin to KCl-loaded liposomes (Figure 4A). This transport was completely inhibited after incubation with DCCD, which modifies the essential glutamate 65 residue of subunit c (Kluge & Dimroth, 1993a; Kluge & Dimroth, 1993b).

The F<sub>0</sub> liposomes were further characterised after reconstitution of the F<sub>1</sub>F<sub>0</sub> holoenzyme. For convenience we reconstituted a hybrid holoenzyme with purified F<sub>1</sub> from *E. coli* DK8/pHEP100 (Kaim & Dimroth, 1994). This F<sub>1</sub>-ATPase is composed of subunits  $\alpha_3\beta_3\gamma$  and  $\epsilon$  from *E. coli* and subunit  $\delta$  from *P. modestum*. The use of this chimera was crucial for the stability of the holoenzyme.

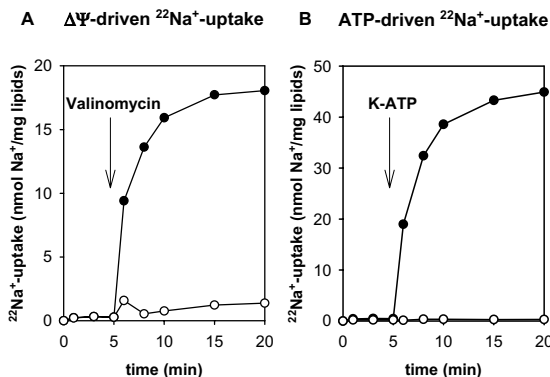


**Figure 4: Kinetics of  $^{22}\text{Na}^+$  transport in reconstituted proteoliposomes.** **A** Uptake of  $^{22}\text{Na}^+$  into proteoliposomes reconstituted with purified subunits a, b, and c from *P. modestum*. The reconstituted proteoliposomes were loaded with 200 mM KCl by overnight incubation. Subsequently, 50  $\mu\text{l}$  of these proteoliposomes were diluted into 1 ml buffer containing 2 mM Tricine/KOH, pH 7.4, 5 mM  $\text{MgCl}_2$ , 200 mM choline chloride and 2 mM  $^{22}\text{NaCl}$  (0.36  $\mu\text{Ci}$ ). At the arrow, 5  $\mu\text{M}$  valinomycin was added to generate a  $\text{K}^+$  diffusion potential. Uptake of  $^{22}\text{Na}^+$  was subsequently determined with samples taken at the times indicated (●).  $^{22}\text{Na}^+$  uptake after incubation of the F<sub>0</sub> liposomes with 50  $\mu\text{M}$  DCCD for 20 min (○). **B** ATP-driven  $^{22}\text{Na}^+$  transport into proteoliposomes reconstituted as in A after incubation with F<sub>1</sub> from *E. coli* DK8/pHEP100 (containing subunits  $\alpha$ ,  $\beta$ ,  $\gamma$ ,  $\epsilon$  from *E. coli* and subunit  $\delta$  from *P. modestum*) to assemble the F<sub>1</sub>F<sub>0</sub> complex. The reaction was initiated with 1.25 mM K-ATP (arrow), samples were taken at the times indicated and analysed for  $^{22}\text{Na}^+$  uptake (●).  $^{22}\text{Na}^+$  uptake after incubation with 50  $\mu\text{M}$  DCCD for 20 min (○).

In earlier studies poor stability and coupling of *in vitro* reconstituted hybrids of *P. modestum* F<sub>0</sub> and *E. coli* F<sub>1</sub> were demonstrated (Laubinger *et al.*, 1990). Further studies with *in vivo* expressed *P. modestum*/*E. coli* ATPase hybrids demonstrated that an identical origin of subunits b and  $\delta$  seems to be an important prerequisite for a fully functional ATP synthase (Kaim & Dimroth, 1994; Gerike *et al.*, 1995). As shown in Figure 4B the hybrid F<sub>1</sub>F<sub>0</sub> was an efficient ATP-driven  $\text{Na}^+$  pump and  $\text{Na}^+$  transport

was completely inhibited by DCCD. Hence, the re-assembled F<sub>0</sub> moiety retains the capacity to properly interact with F<sub>1</sub> to an F<sub>1</sub>F<sub>0</sub> complex that is competent in energy coupling. These results also indicate that the C-terminal His<sub>6</sub>-tag of subunit b does not interfere with the correct binding to the  $\alpha$  and/or  $\delta$  subunits. The result of Figure 5A shows that ATP hydrolysis activity of the solubilised, re-assembled hybrid F<sub>1</sub>F<sub>0</sub> was low without Na<sup>+</sup> addition and increased up to 8-fold at saturating Na<sup>+</sup> concentrations. The results of Figure 5B show that the ATPase activity is rapidly lost by incubation with DCCD so that only 15 % of the initial activity was retained after 15 min. These results are very similar to wild-type F<sub>1</sub>F<sub>0</sub> from *P. modestum* (Kluge & Dimroth, 1993b), demonstrating the functionality of the enzyme complex assembled *in vitro*. Measuring ATP synthesis supported this conclusion. When  $\Delta\Psi$  of ~210 mV (inside positive) was applied by a potassium diffusion potential, ATP synthesis started immediately with a rate of about 240 fmol/sec-mg lipids (not shown).

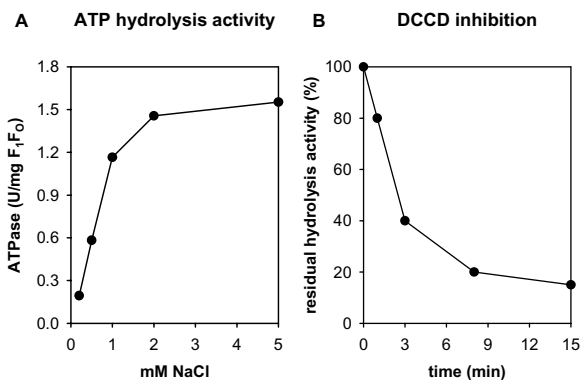


**Figure 5: ATP hydrolysis activities of reconstituted F<sub>0</sub>F<sub>1</sub> liposomes.** **A** Sodium activation profile of solubilised F<sub>1</sub>F<sub>0</sub>-ATPase re-assembled from a, b, and c subunits of *P. modestum* and the F<sub>1</sub> complex of *E. coli* DK8/pHEP100 at pH 8.0. **B** Time course of inhibition of solubilised F<sub>1</sub>F<sub>0</sub>-ATPase by DCCD. The F<sub>1</sub>F<sub>0</sub>-ATPase was incubated with 50  $\mu$ M DCCD at 25 °C and residual ATPase activities were determined at the indicated times by diluting samples into the ATPase assay mixture.

As details of the assembly of F<sub>0</sub> are not known, we investigated whether this requires the presence of the three different subunits in their monomeric state or whether preformed c<sub>11</sub> is competent for reconstitution as well. The c-oligomers of *P. modestum* or *I. tartaricus* are exceptionally stable, and even boiling with sodium

dodecyl sulfate (SDS) is not sufficient to dissociate the complexes into monomers. These undecameric c-rings were isolated from *P. modestum* or *I. tartaricus* (Meier *et al.*, 2002) and incubated with purified subunits a and b from *P. modestum* synthesised in *E. coli*. After incorporation of the reformed F<sub>0</sub> specimens into proteoliposomes,  $\Delta\Psi$ -driven Na<sup>+</sup> uptake was determined. The results of Figure 6 show similar transport kinetics for F<sub>0</sub> reconstituted with c<sub>1</sub> or c<sub>11</sub> from either *P. modestum* or *I. tartaricus*. Hence, preformed c<sub>11</sub> can be assembled *in vitro* together with subunits a and b into functional F<sub>0</sub> moieties, and subunits c from *I. tartaricus* assemble properly to functional F<sub>0</sub> complexes together with the a and b subunits from *P. modestum*. This interchangeability of the two different c subunits is probably due to very similar structures since both proteins are identical except for four conservative amino acid exchanges. Earlier attempts to form F<sub>0</sub> hybrids from combinations of *P. modestum* and *E. coli* subunits failed, however, probably because structural deviations between these heterologous proteins prevent their proper interactions in the chimeras (Gerike & Dimroth, 1994).

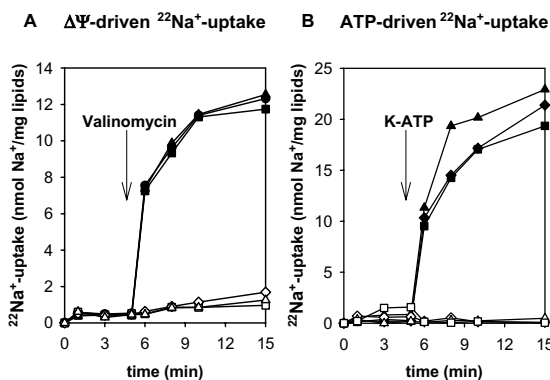


**Figure 6:** <sup>22</sup>Na<sup>+</sup> transport activities of reconstituted proteoliposomes. **A** <sup>22</sup>Na<sup>+</sup> uptake into proteoliposomes reconstituted with the a and b subunits from *P. modestum* plus monomeric subunit c from *P. modestum* (◆); plus c<sub>11</sub> from *P. modestum* (▲); plus c<sub>11</sub> from *I. tartaricus* (■). To induce a K<sup>+</sup> diffusion potential, the liposomes were loaded with KCl, diluted, and supplied with valinomycin (arrow). **B** The F<sub>0</sub> liposomes of A were complemented with the F<sub>1</sub> moiety of *E. coli* DK8/pHEP100 and ATP-driven <sup>22</sup>Na<sup>+</sup> uptake was determined. Control experiments were performed after incubation of the proteoliposomes with 50  $\mu$ M DCCD (open symbols).

The results of Figure 6A also show efficient inhibition of the  $\Delta\Psi$ -driven Na<sup>+</sup> uptake of all reconstituted F<sub>0</sub> liposomes by DCCD. Like F<sub>0</sub> complexes formed from *P. modestum* subunits only, those containing c<sub>11</sub> of *I. tartaricus* and subunits a and b from *P. modestum* could be functionally assembled to F<sub>1</sub>F<sub>0</sub> chimeras with F<sub>1</sub> of *E. coli*. These F<sub>1</sub>F<sub>0</sub> ATP synthases with subunits derived from three different bacteria were almost as effective in ATP-driven Na<sup>+</sup> pumping than those with homologous *P. modestum* F<sub>0</sub> subunits (Figure 6B). The uptake of Na<sup>+</sup> into the reconstituted proteoliposomes was abolished completely after incubation with DCCD, indicating that this transport is due to the active ATP-driven Na<sup>+</sup> pumping. The variance among the transport rates observed in Figure 4 and Figure 6 depends on both, the yield of active F<sub>0</sub> obtained during the reconstitution and the quality of subunits a, b, and c obtained during purification.

In summary, these results establish the conditions for the synthesis and the purification of individual F<sub>0</sub> subunits of the Na<sup>+</sup>-translocating ATP synthase of *P. modestum* and their reconstitution into functional complexes. These methods will undoubtedly be of great value for future investigations of the F<sub>0</sub> mechanism.

### Acknowledgements

We would like to thank Thomas Meier for providing us with purified c-oligomers from *P. modestum* and *I. tartaricus*. This work was supported by a grant from the ETH research commission.

## 2.5 References

- ABRAHAMS, J. P., LESLIE, A. G., LUTTER, R. & WALKER, J. E. (1994). Structure at 2.8 Å resolution of F<sub>1</sub>-ATPase from bovine heart mitochondria. *Nature* 370, 621-628.
- ARECHAGA, I., MIROUX, B., KARRASCH, S., HUIJBREGTS, R., DE KRUIFF, B., RUNSWICK, M. J. & WALKER, J. E. (2000). Characterisation of new intracellular membranes in *Escherichia coli* accompanying large scale over-production of the b subunit of F<sub>1</sub>F<sub>0</sub> ATP synthase. *FEBS Lett.* 482(3), 215-219.
- CAPALDI, R. A., SCHULENBERG, B., MURRAY, J. & AGGELER, R. (2000). Cross-linking and electron microscopy studies of the structure and functioning of the *Escherichia coli* ATP synthase. *J. Exp. Biol.* 203 Pt 1, 29-33.
- DIMROTH, P. (1982). The generation of an electrochemical gradient of sodium ions upon decarboxylation of oxaloacetate by the membrane-bound and Na<sup>+</sup>-activated oxaloacetate decarboxylase from *Klebsiella aerogenes*. *Eur. J. Biochem.* 121(2), 443-449.
- DIMROTH, P. (2000). Operation of the F<sub>0</sub> motor of the ATP synthase. *Biochim. Biophys. Acta* 1458(2-3), 374-386.



- DMITRIEV, O. Y., ALTENDORF, K. & FILLINGAME, R. H. (1995). Reconstitution of the F<sub>o</sub> complex of *Escherichia coli* ATP synthase from isolated subunits. Varying the number of essential carboxylates by co-incorporation of wild-type and mutant subunit c after purification in organic solvent. *Eur. J. Biochem.* 233(2), 478-483.
- DUNN, S. D. & CHANDLER, J. (1998). Characterization of a b<sub>2</sub>δ complex from *Escherichia coli* ATP synthase. *J. Biol. Chem.* 273(15), 8646-8651.
- DUNN, S. D., MCLACHLIN, D. T. & REVINGTON, M. (2000). The second stalk of *Escherichia coli* ATP synthase. *Biochim. Biophys. Acta* 1458(2-3), 356-363.
- GERIKE, U. & DIMROTH, P. (1994). Expression of subunits a and c of the sodium-dependent ATPase of *Propionigenium modestum* in *Escherichia coli*. *Arch. Microbiol.* 161(6), 495-500.
- GERIKE, U., KAIM, G. & DIMROTH, P. (1995). In vivo synthesis of ATPase complexes of *Propionigenium modestum* and *Escherichia coli* and analysis of their function. *Eur. J. Biochem.* 232(2), 496-602.
- KAIM, G. (2001). The Na<sup>+</sup>-translocating F<sub>1</sub>F<sub>o</sub> ATP synthase of *Propionigenium modestum*: mechanochemical insights into the F<sub>o</sub> motor that drives ATP synthesis. *Biochim. Biophys. Acta* 1505(1), 94-107.
- KAIM, G. & DIMROTH, P. (1994). Construction, expression and characterization of a plasmid-encoded Na<sup>+</sup>-specific ATPase hybrid consisting of *Propionigenium modestum* F<sub>o</sub>-ATPase and *Escherichia coli* F<sub>1</sub>-ATPase. *Eur. J. Biochem.* 222(2), 615-623.
- KAIM, G. & DIMROTH, P. (1998a). ATP synthesis by the F<sub>1</sub>F<sub>o</sub> ATP synthase of *Escherichia coli* is obligatorily dependent on the electric potential. *FEBS Lett.* 434(1-2), 57-60.
- KAIM, G. & DIMROTH, P. (1998b). Voltage-generated torque drives the motor of the ATP synthase. *EMBO J.* 17(20), 5887-5895.
- KAIM, G. & DIMROTH, P. (1999). ATP synthesis by F-type ATP synthases is obligatorily dependent on the transmembrane voltage. *EMBO J.* 18(15), 4118-4127.
- KLUGE, C. & DIMROTH, P. (1992). Studies on Na<sup>+</sup> and H<sup>+</sup> translocation through the F<sub>o</sub> part of the Na<sup>+</sup>-translocating F<sub>1</sub>F<sub>o</sub>-ATPase from *Propionigenium modestum*: Discovery of a membrane potential dependent step. *Biochemistry* 31, 12665-12672.
- KLUGE, C. & DIMROTH, P. (1993a). Kinetics of inactivation of the F<sub>1</sub>F<sub>o</sub>-ATPase of *Propionigenium modestum* by dicyclohexylcarbodiimide in relationship to H<sup>+</sup> and Na<sup>+</sup> concentration: Probing the binding site for the coupling ions. *Biochemistry* 32(39), 10378-10386.
- KLUGE, C. & DIMROTH, P. (1993b). Specific protection by Na<sup>+</sup> or Li<sup>+</sup> of the F<sub>1</sub>F<sub>o</sub>-ATPase of *Propionigenium modestum* from the reaction with dicyclohexylcarbodiimide. *J. Biol. Chem.* 268(20), 14557-14560.
- LAUBINGER, W., DECKERS-HEBESTREIT, G., ALTENDORF, K. & DIMROTH, P. (1990). A hybrid adenosinetriphosphatase composed of F<sub>1</sub> of *Escherichia coli* and F<sub>o</sub> of *Propionigenium modestum* is a functional sodium ion pump. *Biochemistry* 29(23), 5458-5463.
- LAUBINGER, W. & DIMROTH, P. (1988). Characterization of the ATP synthase of *Propionigenium modestum* as a primary sodium pump. *Biochemistry* 27(19), 7531-7537.
- MATTHEY, U., KAIM, G., BRAUN, D., WÜTHRICH, K. & DIMROTH, P. (1999). NMR studies of subunit c of the ATP synthase from *Propionigenium modestum* in dodecylsulfate micelles. *Eur. J. Biochem.* 261(2), 459-467.
- MATTHEY, U., KAIM, G. & DIMROTH, P. (1997). Subunit c from the sodium-ion-translocating F<sub>1</sub>F<sub>o</sub>-ATPase of *Propionigenium modestum*. Production, purification and properties of the protein in dodecylsulfate solution. *Eur. J. Biochem.* 247(3), 820-825.
- MCLACHLIN, D. T., BESTARD, J. A. & DUNN, S. D. (1998). The b and δ subunits of the *Escherichia coli* ATP synthase interact *via* residues in their C-terminal regions. *J. Biol. Chem.* 273(24), 15162-15168.
- MEIER, T., MATTHEY, U., HENZEN, F., DIMROTH, P. & MULLER, D. J. (2002). The central plug in the reconstituted undecameric c cylinder of a bacterial ATP synthase consists of phospholipids. *FEBS Lett.* 505(3), 353-356.

- MIROUX, B. & WALKER, J. E. (1996). Over-production of proteins in *Escherichia coli*: mutant hosts that allow synthesis of some membrane proteins and globular proteins at high levels. *J. Mol. Biol.* 260(3), 289-298.
- OGILVIE, I., AGGELER, R. & CAPALDI, R. A. (1997). Cross-linking of the delta subunit to one of the three alpha subunits has no effect on functioning, as expected if delta is a part of the stator that links the F<sub>1</sub> and F<sub>0</sub> parts of the *Escherichia coli* ATP synthase. *J. Biol. Chem.* 272(26), 16652-16656.
- RODGERS, A. J., WILKENS, S., AGGELER, R., MORRIS, M. B., HOWITT, S. M. & CAPALDI, R. A. (1997). The subunit delta-subunit b domain of the *Escherichia coli* F<sub>1</sub>F<sub>0</sub>-ATPase. The b subunits interact with F<sub>1</sub> as a dimer and through the δ subunit. *J. Biol. Chem.* 272(49), 31058-31064.
- SANGER, F., NICKLEN, S. & COULSON, A. R. (1977). DNA sequencing with chain-terminating inhibitors. *Proc. Natl. Acad. Sci. USA* 74(12), 5463-5467.
- SCHÄGGER, H. & JAGOW, G. (1987). Tricine-sodium dodecyl sulfate-polyacrylamide gel electrophoresis for the separation of proteins in the range from 1 to 100 kDa. *Anal. Biochem.* 166, 368-379.
- SCHNEIDER, E. & ALTENDORF, K. (1985). All three subunits are required for the reconstitution of an active proton channel (F<sub>0</sub>) of *Escherichia coli* ATP synthase (F<sub>1</sub>F<sub>0</sub>). *EMBO J.* 4(2), 515-518.
- SEELERT, H., POETSCH, A., DENCHER, N. A., ENGEL, A., STAHLBERG, H. & MÜLLER, D. J. (2000). Proton-powered turbine of a plant motor. *Nature* 405, 418-419.
- STAHLBERG, H., MÜLLER, D. J., SUDA, K., FOTIADIS, D., ENGEL, A., MEIER, T., MATTHEY, U. & DIMROTH, P. (2001). Bacterial Na<sup>+</sup>-ATP synthase has an undecameric rotor. *EMBO reports* 2(3), 229-233.
- STOCK, D., LESLIE, A. G. & WALKER, J. E. (1999). Molecular architecture of the rotary motor in ATP synthase. *Science* 286, 1700-1705.
- WEBER, J. & SENIOR, A. E. (1997). Catalytic mechanism of F<sub>1</sub>-ATPase. *Biochim. Biophys. Acta* 1319, 19-58.
- WILKENS, S. & CAPALDI, R. A. (1998). ATP synthase's second stalk comes into focus. *Nature* 393, 29.
- YOSHIDA, M., MUNEYUKI, E. & HISABORI, T. (2001). ATP synthase - a marvellous rotary engine of the cell. *Nat. Rev. Mol. Cell Biol.* 2(9), 669-677.

## CHAPTER 3

### **Molecular mechanism of the ATP synthase's $F_0$ motor probed by mutational analyses of subunit a**

Franziska Wehrle, Georg Kaim and Peter Dimroth

Institut für Mikrobiologie, Eidgenössische Technische Hochschule  
CH-8092 Zürich, Switzerland

*Journal of Molecular Biology* (2002), 322(2):369-381

### 3.1 Abstract

The most prominent residue of subunit a of the  $F_1F_0$  ATP synthase is an universally conserved arginine (aR227 in *Propionigenium modestum*), which was reported to permit no substitution with retention of ATP synthesis or  $H^+$ -coupled ATP hydrolysis activity. We show here that ATP synthases with R227K or R227H mutations in the *P. modestum* a subunit catalyse ATP-driven  $Na^+$  transport above or below pH 8.0, respectively. Reconstituted  $F_0$  with either mutation catalysed  $^{22}Na^+_{out}/Na^+_{in}$  exchange with similar pH profiles as found in ATP-driven  $Na^+$  transport. ATP synthase with an aR227A substitution catalysed  $Na^+$ -dependent ATP hydrolysis, which was completely inhibited by dicyclohexylcarbodiimide, but not coupled to  $Na^+$  transport. This suggests that in the mutant the dissociation of  $Na^+$  becomes more difficult and that the alkali ions remain therefore permanently bound to the c subunit sites. The reconstituted mutant enzyme was also able to synthesise ATP in the presence of a membrane potential, which stopped at elevated external  $Na^+$  concentrations. These observations reinforce the importance of aR227 to facilitate the dissociation of  $Na^+$  from approaching rotor sites. This task of aR227 was corroborated by other results with the aR227A mutant: (i) after reconstitution into liposomes,  $F_0$  with the aR227A mutation did not catalyse  $^{22}Na^+_{out}/Na^+_{in}$  exchange at high internal sodium concentrations, and (ii) at a constant  $\Delta pNa^+$ ,  $^{22}Na^+$  uptake was inhibited at elevated internal  $Na^+$  concentrations. Hence, in mutant aR227A, sodium ions can only dissociate from their rotor sites into a reservoir of low sodium ion concentration, whereas in the wild-type enzyme the positively charged aR227 allows the dissociation of  $Na^+$  even into compartments of high  $Na^+$  concentration.

*Abbreviations:* DCCD, *N,N'*-dicyclohexylcarbodiimide; CCCP, carbonyl cyanide *m*-chlorophenylhydrazone; IPTG, isopropyl-2-D-thio-galacto-pyranoside; PCR, polymerase chain reaction; Tris, tris-(hydroxymethyl)-aminomethane; Bistris-propane, 1,3-bis-[tris-(hydroxymethyl)-methylamino]-propane; Tricine, N-(tris-(hydroxymethyl)-methyl)-glycine; MES, 4-morpholinoethanesulfonic acid; MOPS, 4-morpholinopropanesulfonic acid; PEG, polyethylene glycol; NTA, nitrilotriacetic acid;  $\Delta\Psi$ , transmembrane electrical potential;  $\Delta pNa^+$ , transmembrane  $Na^+$  concentration gradient

### 3.2 Introduction

Every living cell depends on a continuous supply of ATP, the majority of which is synthesised by the  $F_1F_0$  ATP synthase at the expense of an electrochemical gradient of  $H^+$  or  $Na^+$  ions. Detailed knowledge on structure and function is available for the water-soluble  $F_1$  headpiece with the subunit composition  $\alpha_3\beta_3\gamma\delta\epsilon$ . Alternating  $\alpha$  and  $\beta$  subunits form a cylinder surrounding subunit  $\gamma$ . Part of the  $\gamma$  subunit protrudes from the bottom of the cylinder and forms the central stalk together with the  $\epsilon$  subunit. At its foot the stalk is connected with the oligomeric c-ring of the membrane-intrinsic  $F_0$  moiety (Abrahams *et al.*, 1994; Stock *et al.*, 1999; Gibbons *et al.*, 2000). The other  $F_0$  subunits of bacterial ATP synthases are a and  $b_2$ , which are connected laterally to the c-ring (Birkenhäger *et al.*, 1995; Singh *et al.*, 1996; Takeyasu *et al.*, 1996; Jiang & Fillingame, 1998). The major part of the two b subunits is  $\alpha$ -helical, making up the peripheral stalk together with subunit  $\delta$  connecting subunit a to subunit  $\alpha$  (McLachlin *et al.*, 1998; Wilkens & Capaldi, 1998). Interestingly, the number of c subunits within the ring varies among species, being 10, 11, or 14 for the ATP synthases from yeast mitochondria, from the bacterium *Ilyobacter tartaricus* or from spinach chloroplasts, respectively (Stock *et al.*, 1999; Seelert *et al.*, 2000; Stahlberg *et al.*, 2001).

The ATP synthase is the smallest known molecular motor. Evidence indicates that ATP hydrolysis elicits the rotation of the rotor subunits  $\gamma$ ,  $\epsilon$  and  $c_{10-14}$  against the stator subunits  $\alpha_3\beta_3\delta ab_2$  (Noji *et al.*, 1997; Sambongi *et al.*, 1999; Pänke *et al.*, 2000; Tsunoda *et al.*, 2001). Most current models for ATP synthesis imply that the flux of  $Na^+$  or  $H^+$  across  $F_0$  induces the rotation of the rotor versus the stator. This rotation promotes conformational changes in the  $\beta$  subunits, which are instrumental for releasing tightly-bound ATP from the catalytic sites. Recent work by cross-linking studies with the  $Na^+$ -translocating ATP synthase of *I. tartaricus* has shown that the  $Na^+$  binding sites of  $c_{11}$  are located in the centre of the membrane (von Ballmoos *et al.*, 2002). This is also the anticipated location of the  $H^+$  binding sites in the ATP synthase of *Escherichia coli* (Dmitriev *et al.*, 1999). Models for ion translocation by the *E. coli* enzyme postulate two half channels in subunit a, which connect the c subunit sites with the two reservoirs separated by the membrane (Junge *et al.*, 1997; Elston *et al.*, 1998; Rastogi & Girvin, 1999). On the other hand, a large body of evidence indicates that most of the  $Na^+$ -binding sites of  $c_{11}$  from *Propionigenium modestum* or *I. tartaricus* are directly accessible from the aqueous phase without the

help of subunit a (Kluge & Dimroth, 1993; Kaim & Dimroth, 1998c; Kaim *et al.*, 1998; Kaim & Dimroth, 1999). In the crystal structure of  $c_{11}$  from *I. tartaricus*, cavities are apparent between an inner ring of helices and each two helices of an outer ring that could serve as access channels from the cytoplasmic surface (manuscript in preparation). The role of the a subunit is then to make a channel connection from the c subunit site contacting it to the periplasmic surface of the membrane. Evidence for an ion-selective a subunit channel is available: in a triple mutant of subunit a, the channel lost the ability to conduct  $\text{Na}^+$  with retention of its  $\text{Li}^+$ - or  $\text{H}^+$ -conducting activities (Kaim & Dimroth, 1998b).

An important feature for the ATP synthesis mechanism is the necessity of a membrane potential (Kaim *et al.*, 1998; Kaim & Dimroth, 1999). A number of mechanisms for torque generation by  $F_0$  have been proposed (Junge *et al.*, 1997; Elston *et al.*, 1998; Dimroth *et al.*, 1999; Dmitriev *et al.*, 1999), but the only one that takes the essential role of the membrane potential into account is described in Dimroth *et al.* (1999). Extensive mutational studies have been conducted with subunit a of *E. coli*. It was concluded that the universally conserved residue aR210 (aR227 in *P. modestum*) is the only one tolerating no exchange (Valiyaveetil & Fillingame, 1997 and references therein). This arginine was proposed in some models to present a positive stator charge interacting electrostatically with the negatively charged rotor sites of the c-ring in the torque-generating mechanism (Elston *et al.*, 1998; Dimroth *et al.*, 1999). The role of arginine 227 of subunit a in the  $F_0$  mechanism has now been probed with mutants of this residue in the ATP synthase from *P. modestum*. We observed that a positive charge at position 227 of the a subunit is essential for the efficient dissociation of  $\text{Na}^+$  ions bound to nearby rotor sites.

### 3.3 Materials and Methods

#### Bacterial strains and plasmids

Plasmids pPmaHisN, containing the *atpB* gene encoding subunit a, and pPmbHisC harbouring the *atpF* gene encoding subunit b of the *P. modestum* ATPase, were previously constructed (Wehrle *et al.*, 2002). For routine cloning procedures *E. coli* DH5 $\alpha$  (Sambrook *et al.*, 1989) and for overexpression studies *E. coli* PEF42(DE3) (Matthey *et al.*, 1997) were used. All *E. coli* strains were

cultivated in Luria-Bertani (LB) medium (Sambrook *et al.*, 1989) supplemented with 200  $\mu\text{g/ml}$  ampicillin.

### **Preparation of subunits a, b, and c of the ATP synthase from *P. modestum***

Recombinant subunits a and b were overexpressed in *E. coli* C43(DE3) (Miroux & Walker, 1996) as His-tag fusion proteins and purified by  $\text{Ni}^{2+}$  chelate affinity chromatography as described previously (Miroux & Walker, 1996; Wehrle *et al.*, 2002). Monomeric subunit c was expressed in *E. coli* PEF42(DE3) and purified by extraction with organic solvents as described (Matthey *et al.*, 1997; Matthey *et al.*, 1999). Immediately prior to usage, 1 % sodium cholate was added to 70  $\mu\text{g}$  (70  $\mu\text{l}$ ) of protein in chloroform/methanol (2:1) and the organic solvent evaporated under a stream of argon. The pellet was dried in a vacuum centrifuge and resuspended in 70  $\mu\text{l}$  5 mM potassium phosphate buffer, pH 8.0, containing 5 mM  $\text{MgCl}_2$ .

### **Construction of mutants aR227A, aR227K and aR227H**

The mutant *atpB* genes were constructed by site-directed mutagenesis applying the PCR overlap extension method (Horton *et al.*, 1990). A 5' oligonucleotide harbouring a *NdeI* site, a 3' oligonucleotide containing a *BamHI* site, and the 5' and 3' mutagenic primers (Table 1) containing the desired mutations were used in this approach. The plasmid pPmaHisN served as template. After digestion with *NdeI* and *BamHI* the PCR fragments were purified with the NucleoTrap Kit (Macherey Nagel) and ligated into vector pET16b (Novagen). DNA sequencing was performed according to the dideoxy chain termination method (Sanger *et al.*, 1977) using the ABI PRISM 310 genetic analyzer from Applied Biosystems (Foster City, USA).

### **Cloning of pMA762(RA)**

The four point mutations R227A, K220R, V264R, and I278N were introduced into the gene for *P. modestum* subunit a by PCR with specific oligonucleotides (Table 1) using a modification of the above method. Three subfragments were synthesised first with the following oligonucleotide pairs using pPmaHisN as template: Pma1V/Mpa220R, Mpa220V/Mpa264-278R and Mpa264-278V/Pma889R. The three resulting DNA fragments were isolated from 1 % agarose gels with NucleoTrap (Macherey Nagel) and served as template for the second PCR step with

oligonucleotides Pma1V and Pma889R. Cloning and sequencing was done as described above.

**Table 1: Oligonucleotides used for PCR.** The mutated bases are underlined, and the corresponding newly introduced restriction sites are shown in italics.

oligonucleotide	sequence (5'-3')	mutation	restriction site
Pma1V	TAAATGGAGACATATGAAAAAATGG	none	<i>NdeI</i>
Pma889R	TGTTTAAACTGGATCCAACCTAATCTTC	none	<i>BamHI</i>
Mpa227A-V	CGAATATTTCAATAGCGCTTTTGGTACATG	aR227A	<i>Eco47III</i>
Mpa227A-R	CATGTACCAAAAAGCGCTATTGAAATATTCG	aR227A	<i>Eco47III</i>
Mpa227K-V	CGAACATTCAATCAAACTTTGGTAAACATG	aR227K	<i>-SspI</i>
Mpa227K-R	CATGTTACCAAAAAGTTTGATTGAAATGTTTCG	aR227K	<i>-SspI</i>
Mpa227H-V	CAAAACCAACGAACATTTCAATCCACCTTTTGG	aR227H	<i>-SspI</i>
Mpa227H-R	CAAAAAGGTGGATTGAAATGTTTCGTTGGTTTTG	aR227H	<i>-SspI</i>
Mpa220R-V	GGGAGAATTCGAAAGACCAACGAAC	aK220R	<i>EcoRI</i>
Mpa220R-R	GTTCGTTGGTCTTGC GAATTCCTCC	aK220R	<i>EcoR</i>
Mpa264/278-V	TTCAGTGGAGAGGTACAAGCTTCGTATTCATC TGCTGACAATGGTTTATAATCAAGGATC	aV264E/I278N	<i>HindIII</i>
Mpa264/278-R	GATCCTTGATTATAAACCATTTGTCAGCAGATGA ATACGAAGCTTTGTACCTCTCCACTGAA	aV264E/I278N	<i>HindIII</i>

### Expression and purification of mutant a subunits

Strain PEF42(DE3) was transformed with a plasmid encoding a mutant a subunit and incubated overnight in Luria-Bertani (LB) medium supplemented with 200 µg/ml ampicillin at 37 °C. Expression cultures were then inoculated with 2 % of the overnight culture and incubated at 37 °C until an OD<sub>600</sub> of 0.6 was reached. Protein expression was induced with 1 mM IPTG and cells were grown at 37 °C for another 3 h. The cells were collected by centrifugation, washed once with 10 mM Tris/HCl pH 8.0 and stored at -20 °C. Thawed cells were resuspended in 50 mM potassium phosphate buffer, pH 8.0, containing 20 % glycerol, 5 mM MgCl<sub>2</sub>, 0.1 mM diisopropylfluorophosphate and a trace amount of DNaseI. Cells were broken in a French pressure cell at 11,000 psi (7.6×10<sup>7</sup> Pa) and cell debris was removed by centrifugation at 12,000 × g for 30 min. Membranes were collected by centrifugation of the supernatant for 1 h at 200,000 × g. After resuspending the pellet in 50 mM potassium phosphate buffer, pH 8.0, containing 20 % glycerol and 5 mM MgCl<sub>2</sub>, the membrane proteins were solubilised with 1 % N-lauroyl-sarcosine while gently stirring for 30 min at 25 °C. The mutant a subunits were further purified as described for the wild-type protein (Wehrle *et al.*, 2002).



### Reconstitution of $F_0$ liposomes containing a mutant a subunit

The mutant a subunit was mixed with wild-type subunits b and c from *P. modestum* in a 1:2:10 molar ratio and the mixture kept on ice for 2-3 h. Phospholipids were then added and  $F_0$  liposomes were reconstituted as described (Wehrle *et al.*, 2002).

### Reconstitution of $F_1F_0$ liposomes

For studies on the  $F_1F_0$  holoenzyme, the  $F_0$  liposomes were incubated with purified  $F_1$  as described elsewhere (Kluge *et al.*, 1992; Wehrle *et al.*, 2002).  $F_1$  from DK8/pHEP100 (Kaim & Dimroth, 1994) was used for  $^{22}\text{Na}^+$  transport studies and  $F_1$  from DK8/pHEPHisL5C (pHEP100 with N-terminal His<sub>10</sub>-tag at subunit  $\beta$ , Yvonne Appoldt, unpublished results) was utilised for ATP hydrolysis experiments.

### $^{22}\text{Na}^+$ transport experiments

$^{22}\text{Na}^+_{\text{out}}/\text{Na}^+_{\text{in}}$ -exchange.  $^{22}\text{Na}^+_{\text{out}}/\text{Na}^+_{\text{in}}$ -exchange was measured in an assay containing the following at 25 °C in 1 ml: 2 mM Tricine/KOH, pH 7.4, 5 mM  $\text{MgCl}_2$ , 100 mM choline chloride, 3 mM  $^{22}\text{NaCl}$  (0.47  $\mu\text{Ci}$ ) and 30  $\mu\text{l}$  of  $\text{Na}^+$  loaded (100 mM)  $F_0$  proteoliposomes (8.6 mg phospholipids).  $^{22}\text{Na}^+$  uptake was determined at the indicated time points after separation of internal and external  $^{22}\text{Na}^+$  by passage over a small column of Dowex 50,  $\text{K}^+$  as described (Dimroth, 1982). The resin was washed with 0.6 ml of 2 mM Tricine/KOH, pH 7.4, containing 5 mM  $\text{MgCl}_2$  and 100 mM sucrose. The radioactivity of  $^{22}\text{Na}^+$  eluted from the columns reflects  $^{22}\text{Na}^+$  entrapped in the proteoliposomes and was determined by  $\gamma$ -counting. The pH dependence of the exchange activity was measured in the above assay buffer with the following modification: 2 mM Tricine/KOH, pH 7.4, was replaced by 20 mM each of MES, MOPS and Tricine between pH 5.5 and 6.5, and by 20 mM each of MOPS, Tricine and glycine between pH 6.5 and 9.5. The pH was adjusted with KOH or HCl, respectively. 20  $\mu\text{l}$  of  $\text{Na}^+$ -loaded (100 mM) reconstituted  $F_0$  liposomes (4 mg of phospholipids) were added to 500  $\mu\text{l}$  assay mixture containing 20 mM of the respective buffer at the pH indicated, 5 mM  $\text{MgCl}_2$ , 100 mM choline chloride, and 3.8 mM  $^{22}\text{NaCl}$  (0.24  $\mu\text{Ci}$ ). The exchange rate was determined as described above after 60 s and 90 s with 200  $\mu\text{l}$  samples.

*$\Delta\Psi$ -driven  $^{22}\text{Na}^+$  uptake.*  $\Delta\Psi$ -driven  $^{22}\text{Na}^+$  uptake was determined in an incubation mixture containing in 1 ml at 25 °C: 2 mM Tricine/KOH, pH 7.4, 5 mM  $\text{MgCl}_2$ , 200 mM choline chloride, 2 mM  $^{22}\text{NaCl}$  (0.36  $\mu\text{Ci}$ ), and 50  $\mu\text{l}$   $F_0$  liposomes (10 mg phospholipids) loaded with 200 mM KCl. After 5 min a membrane potential of -77 mV was established by adding 5  $\mu\text{M}$  valinomycin. At the indicated time points  $^{22}\text{Na}^+$  uptake was determined as described above.

*ATP-driven  $^{22}\text{Na}^+$  uptake.* ATP-driven  $^{22}\text{Na}^+$  uptake into  $F_1F_0$  liposomes was measured with incubation mixtures containing the following components in 0.7 ml at 25 °C: 50 mM potassium phosphate buffer, pH 7.0, or 20 mM Tricine, pH 8.9, 5 mM  $\text{MgCl}_2$ , 2 mM  $^{22}\text{NaCl}$  (0.11  $\mu\text{Ci}$ ), 20 units pyruvate kinase, 6 mM phosphoenolpyruvate and 50  $\mu\text{l}$  liposomes with reconstituted  $F_1F_0$ -ATPase (10 mg phospholipids). Sodium transport was initiated after 5 min by the addition of 1.25 mM ATP (potassium salt). Samples (90  $\mu\text{l}$ ) were taken at the indicated time points and the radioactivity of the internal  $^{22}\text{Na}^+$  was determined as described above. The pH dependence of ATP-driven  $^{22}\text{Na}^+$  uptake was determined with the modified buffer mixture as described for the  $^{22}\text{Na}^+_{\text{out}}/\text{Na}^+_{\text{in}}$  exchange. The assay contained the following components in 500  $\mu\text{l}$ : 20 mM of the appropriate buffer at the indicated pH, 5 mM  $\text{MgCl}_2$ , 2 mM  $^{22}\text{NaCl}$  (0.24  $\mu\text{Ci}$ ), 20 units pyruvate kinase, 6 mM phosphoenolpyruvate and 20  $\mu\text{l}$   $F_1F_0$  proteoliposomes (4 mg phospholipids). After incubating the assay for 2 min at 25 °C  $^{22}\text{Na}^+$  uptake was started by the addition of 1.25 mM ATP (potassium salt). Samples (160  $\mu\text{l}$ ) were taken after 30 s and 60 s, and  $^{22}\text{Na}^+$  uptake was determined as described (Dimroth, 1982).

*$\Delta p\text{Na}^+$ -driven  $^{22}\text{Na}^+$  uptake.* 30  $\mu\text{l}$   $F_0$  liposomes (8.6 mg lipid; 10  $\mu\text{M}$   $\text{Na}^+$ ) were loaded overnight with 50 mM KCl and added to 1 ml 2 mM Tricine/KOH buffer, pH 7.4, containing 5 mM  $\text{MgCl}_2$ , 100 mM choline chloride, 50 mM KCl, 5  $\mu\text{M}$  valinomycin and 100  $\mu\text{M}$   $^{22}\text{NaCl}$  (0.47  $\mu\text{Ci}$ ), establishing a  $\Delta p\text{Na}^+$  of -59 mV. The mixture was incubated at 25 °C, and at various time points 160  $\mu\text{l}$  samples were taken and passed over Dowex 50,  $\text{K}^+$  columns to remove external  $^{22}\text{Na}^+$ . The radioactivity entrapped in the proteoliposomes was determined by  $\gamma$ -counting.  $\Delta p\text{Na}^+$ -driven  $^{22}\text{Na}^+$  uptake was also determined at higher internal  $\text{Na}^+$  concentrations (up to 2.5 mM) keeping the  $\Delta p\text{Na}^+$  at -59 mV. For this purpose, 30  $\mu\text{l}$  proteoliposomes (5 mg lipid) were loaded overnight with 50 mM KCl and NaCl of the desired concentration and

diluted into 500  $\mu$ l assay mixture containing 2 mM Tricine/KOH buffer, pH 7.4, 50 mM KCl, 5 mM  $MgCl_2$ , 100 mM choline chloride, 5  $\mu$ M valinomycin and  $^{22}NaCl$  of 10-fold higher concentration than in the proteoliposomes with a specific activity of 500 cpm/nmol. Samples were taken after various times and  $^{22}Na^+$  uptake into the proteoliposomes was determined as described above.

### **Determination of ATPase reconstituted into proteoliposomes**

The turbidity of the proteoliposomes prevented the direct spectrophotometric measurement of the reconstituted ATPase. Therefore, the enzyme was extracted from the liposomes (40 mg phospholipids) with 1 % sodium cholate in a total volume of 1 ml 5 mM Bistris-propane, pH 7.4 (30 min, 25 °C) and unsolubilised material was removed by ultracentrifugation (1 h, 200'000 x g). The solubilised proteins were subsequently adsorbed to 500  $\mu$ l Ni-NTA (Qiagen) and equilibrated with equilibration buffer (5 mM Bistris-propane, pH 7.4). The column was washed with 10 volumes equilibration buffer, and the enzyme was eluted with 1 ml equilibration buffer containing 20 % glycerol and 40 mM imidazole. The protein was precipitated with 15 % PEG6000 in presence of 50 mM  $MgCl_2$ , and the precipitate resuspended in 50  $\mu$ l equilibration buffer containing 1 mM  $MgCl_2$  and 20 % glycerol. ATPase activity was measured by NADH oxidation at 340 nm as described (Laubinger & Dimroth, 1988).

### **ATP synthesis**

$F_1F_0$  liposomes were reconstituted in 5 mM Bistris-propane, pH 7.4, 1 mM  $MgCl_2$  as described (Wehrle *et al.*, 2002). The proteoliposomes were loaded with 10 mM NaCl by overnight incubation at 4 °C. 5  $\mu$ l proteoliposomes (1 mg phospholipids) were diluted into 345  $\mu$ l assay buffer (pH 7.5) containing 5 mM potassium phosphate, 2 mM Tricine/KOH, 200 mM KCl, 0.5 mM  $MgCl_2$  and 0.25 mM ADP. ATP synthesis was started by adding 2.9  $\mu$ M valinomycin, which induces a potassium diffusion potential of approximately 210 mV. Samples (45  $\mu$ l) were taken at different incubation periods and added to 405  $\mu$ l of assay buffer containing 10  $\mu$ M CCCP and 1 mM azide to stop the reaction. The ATP content was subsequently determined by the luciferin/luciferase reaction using the CLSII assay (Roche). Light emission was detected with a luminometer (Biolumat LB 9500 C, Berthold).

## Analytical methods

Protein concentration was determined by the BCA (bicinchonic acid) protein assay (enhanced protocol) as described by the manufacturer (Pierce) with bovine serum albumin as standard. The concentration of  $\text{Na}^+$  was determined by atomic absorption spectroscopy.

## 3.4 Results

### **The universally conserved arginine of subunit a of the ATP synthase from *P. modestum* can be exchanged by lysine or histidine with retention of function**

The most prominent residue of subunit a of the ATP synthase is the conserved arginine in the penultimate transmembrane helix (R210 in *E. coli*). Numerous reports have appeared in the literature that replacement of this arginine by any other amino acid leads to the complete loss of function (Lightowers *et al.*, 1987; Cain & Simoni, 1989; Howitt & Cox, 1992; Valiyaveetil & Fillingame, 1997). Not even the most conservative aR210K mutant showed any ATP synthesis or proton translocation activity (Cain & Simoni, 1989; Eya *et al.*, 1991; Howitt & Cox, 1992). On the other hand, functional models were proposed for the  $F_0$  motor, in which the role of aR210 was to provide a positive stator charge (Elston *et al.*, 1998; Dimroth *et al.*, 1999). Such a role cannot easily be reconciled with the complete loss of function in the aR210K mutant. We have therefore mutated the corresponding aR227 residue of the ATP synthase from *P. modestum* to lysine and analysed the sodium ion pumping activity. For this purpose, the  $F_0$  complex was first reconstituted into proteoliposomes from the purified a, b and c subunits of *P. modestum* synthesised by *E. coli*. The  $F_1F_0$  holoenzyme was then completed by adding an  $F_1$  hybrid containing subunit  $\delta$  from *P. modestum* and subunits  $\alpha$ ,  $\beta$ ,  $\gamma$ , and  $\epsilon$  from *E. coli*. The results of Figure 1 show the kinetics of  $\text{Na}^+$  uptake into the proteoliposomes. At pH 7.0, the reconstituted enzyme with the wild-type a subunit showed substantial ATP-driven  $^{22}\text{Na}^+$  pumping activity, whereas that with the aR227K mutation was completely inactive. These results are thus in complete harmony with the data reported for the *E. coli* ATP synthase (Cain & Simoni, 1989; Eya *et al.*, 1991; Howitt & Cox, 1992). Surprisingly, however, the mutant ATP synthase became an active  $\text{Na}^+$  pump at pH 8.9, where the activity was approximately 50 % that of the wild-type enzyme at pH 7.0.

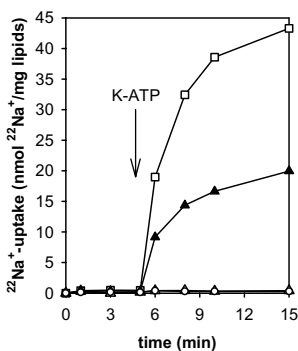


**Figure 1: Kinetics of ATP-driven  $^{22}\text{Na}^+$  uptake into  $F_1F_0$  liposomes containing mutants aR227K (▲), aR227A (○) or wild-type subunit a (□).** Assay mixtures contained in 0.7 ml at 25 °C: 50 mM potassium phosphate buffer, pH 7.0 (open symbols), or 20 mM Tricine, pH 8.9 (filled symbols), 5 mM  $\text{MgCl}_2$ , 2 mM  $^{22}\text{NaCl}$  (0.11  $\mu\text{Ci}$ ), 20 units pyruvate kinase, 6 mM phosphoenolpyruvate and 50  $\mu\text{l}$  of the reconstituted proteoliposomes (10 mg phospholipids).  $^{22}\text{Na}^+$  uptake was initiated by the addition of 1.25 mM potassium-ATP ( $\downarrow$ ). For details see Materials and methods.

From these results it became obvious that the ATP synthase with the aR227K mutation was a catalytically active  $\text{Na}^+$  pump, but only in the alkaline pH range. This observation was further analysed by measuring ATP-driven  $^{22}\text{Na}^+$  transport into the reconstituted proteoliposomes between pH 5.5 and 9.5. The results of Figure 2A show that the wild-type enzyme has a pH optimum of 8.0 and exhibits considerable activities in the pH range between 6.0 and 9.0. In contrast, the ATP synthase with the aR227K mutation has its optimum at pH 8.5, but is completely inactive at pH 7.5 and below.

These results prompted us to investigate an ATP synthase mutant, in which aR227 was replaced by histidine. Like arginine or lysine, histidine can carry a positive charge, albeit at more acidic pH values. ATP synthase with the aR227H mutation showed similar ATP-driven  $\text{Na}^+$  transport activities as the wild-type enzyme between pH 6.0 and 7.5 with the optimum at pH 7.0. On increasing the pH further into the alkaline region, the activity of the mutant ATP synthase dropped rapidly to reach undetectable levels at pH 8.5, close to the pH optimum for the wild-type enzyme.

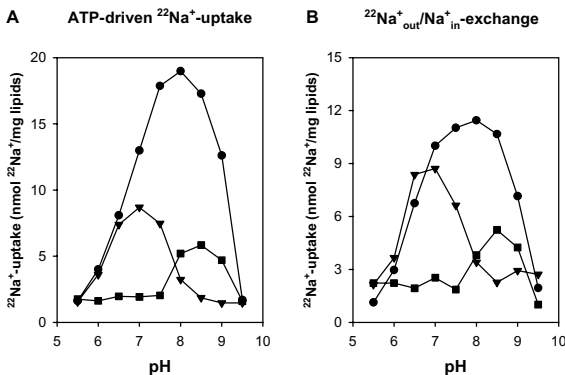


**Figure 2: pH dependence of  $^{22}\text{Na}^+$  uptake into  $F_1F_0$  liposomes (A) or  $F_0$  liposomes (B) containing wild-type subunit a (●), the aR227H mutant (▼) or the R227K mutant (■).** **A** Assay mixtures for ATP-driven  $^{22}\text{Na}^+$  uptake contained in 500  $\mu\text{l}$  at 25  $^\circ\text{C}$ : 20 mM MES/MOPS/Tricine or 20 mM MOPS/Tricine/glycine buffer of the pH indicated, 5 mM  $\text{MgCl}_2$ , 2 mM  $^{22}\text{NaCl}$  (0.24  $\mu\text{Ci}$ ), 20  $\mu\text{l}$   $F_1F_0$  liposomes (4 mg phospholipids), 20 U of pyruvate kinase and 6 mM phosphoenolpyruvate.  $^{22}\text{Na}^+$  uptake was initiated by adding 1.25 mM potassium-ATP and after 1 min internal  $^{22}\text{Na}^+$  was determined by  $\gamma$ -counting. **B**  $F_0$  liposomes (20  $\mu\text{l}$ , 4 mg phospholipids) loaded with 100 mM NaCl by overnight incubation were diluted into 500  $\mu\text{l}$  assay mixture containing 20 mM buffer of the pH indicated, 5 mM  $\text{MgCl}_2$ , 100 mM choline chlorid and 0.24  $\mu\text{Ci}$  carrier-free  $^{22}\text{NaCl}$  to yield an external  $^{22}\text{NaCl}$  concentration of 3.8 mM. The amount of  $^{22}\text{Na}^+$  taken up into the proteoliposomes by  $^{22}\text{Na}^+_{\text{out}}/\text{Na}^+_{\text{in}}$  exchange was determined after 1 min incubation at 25  $^\circ\text{C}$  as described under Materials and methods.

The results of Figure 2B show the pH-dependence of  $^{22}\text{Na}^+_{\text{out}}/\text{Na}^+_{\text{in}}$  exchange by reconstituted  $F_0$  liposomes. The pH profiles for the wild-type ATP synthase and the two aR227 mutants were very similar to those measured for ATP-driven  $^{22}\text{Na}^+$  uptake. The wild-type enzyme exhibits a broad pH optimum with similar activities between pH 7.0 and 8.5 and measurable activities over the pH range from 6.0 to 9.0. The aR227K mutant showed activity in the alkaline pH range (>8) with the optimum at pH 8.5 and the aR227H mutant had its optimum between pH 6.5 and 7.0 and became inactive above pH 8.0. In conclusion, we show here that the restrictions to mutate arginine 227 of subunit a are not as serious as has been thought before. ATP synthases with aR227K or aR227H mutations are catalytically active  $\text{Na}^+$  pumps, but only within a rather narrow pH range, whereas the wild-type enzyme is active at pH values ranging from 6.0-9.0.

### Biochemical characterization of the aR227A mutant

We also investigated the aR227A mutant with the more distinct substitution of a positive by a neutral amino acid residue. Proteoliposomes containing the ATP synthase with the aR227A mutation did not show any ATP-driven  $\text{Na}^+$  translocation at pH 7.0 (Figure 1). At pH 7.4, we also analysed the activity of the aR227A mutant in  $\psi$ -driven  $\text{Na}^+$  uptake and  $^{22}\text{Na}^+_{\text{out}}/\text{Na}^+_{\text{in}}$  exchange modes. The results of Figure 3A show rapid uptake of  $^{22}\text{Na}^+$  into the  $F_0$  liposomes containing either the wild-type or the mutant a subunit in response to a valinomycin-induced potassium diffusion potential. While the wild-type  $F_0$  required approximately 15 min to approach saturation, this seemed to be accomplished in less than 3 min in case of the mutant  $F_0$ . Accordingly, the initial rate of  $^{22}\text{Na}^+$  uptake was about 1.3 times faster for the mutant than for the wild-type. This result could indicate that the membrane potential attracts an empty, negatively charged rotor site more rapidly in the mutant without the electrostatic interference by the positively charged arginine 227 residue. In both cases,  $^{22}\text{Na}^+$  uptake was abolished after incubation of the  $F_0$  liposomes with DCCD, indicating that the  $\psi$ -driven  $\text{Na}^+$  transport mechanism in wild-type and mutant enzyme is probably the same.

To measure ion exchange between internal unlabelled and external radioactively labelled  $\text{Na}^+$  ions,  $F_0$  liposomes were loaded with 100 mM NaCl and diluted 33-fold into buffer containing  $^{22}\text{NaCl}$  at a final concentration of 3 mM (Figure 3B). Under these conditions, wild-type  $F_0$  liposomes catalysed rapid  $^{22}\text{Na}^+$  accumulation in the interior compartment. No  $^{22}\text{Na}^+$  uptake was found, however, at an internal  $\text{Na}^+$  concentration of 10  $\mu\text{M}$  and an external  $^{22}\text{Na}^+$  concentration of 100  $\mu\text{M}$  creating a  $\Delta\text{pNa}^+$  of about -60 mV. Remarkably different results were obtained with  $F_0$  liposomes containing the aR227A mutation. While  $^{22}\text{Na}^+$  uptake by  $^{22}\text{Na}^+_{\text{out}}/\text{Na}^+_{\text{in}}$  exchange was not detectable, significant  $\Delta\text{pNa}^+$ -driven  $^{22}\text{Na}^+$  accumulation was observed. Hence, the aR227A mutation results in a switch from  $^{22}\text{Na}^+_{\text{out}}/\text{Na}^+_{\text{in}}$  exchange to  $\Delta\text{pNa}^+$ -driven  $^{22}\text{Na}^+$  uptake.

These results and others described below probably indicate that the aR227A mutant can translocate  $\text{Na}^+$  only into a compartment with low  $\text{Na}^+$  concentration. To investigate this hypothesis, we measured  $^{22}\text{Na}^+$  transport into the mutant  $F_0$  liposomes at varying internal  $\text{Na}^+$  concentrations and at a constant  $\Delta\text{pNa}^+$  of -59 mV. The results of Figure 4 show, that on increasing the internal  $\text{Na}^+$  concentration from 10  $\mu\text{M}$  to

2.5 mM, the initial  $^{22}\text{Na}^+$  transport rate decreased about 5-fold with half maximal inhibition at about 0.5 mM NaCl. This value compares well with the  $\text{Na}^+$  concentration required for half maximal activation of ATP hydrolysis by the wild-type enzyme and therefore probably reflects the dissociation constant for  $\text{Na}^+$  from the c subunit sites.

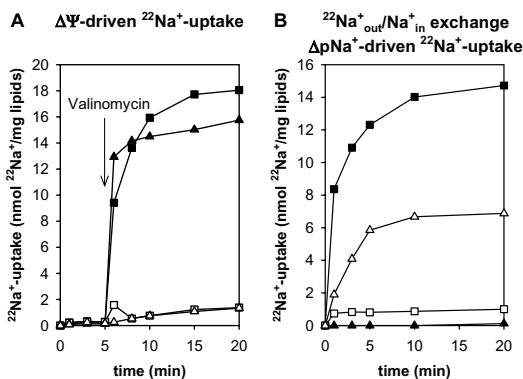


**Figure 3: Kinetics of  $^{22}\text{Na}^+$  uptake into  $F_0$  liposomes containing wild-type subunit a (■, □), or the aR227A mutant (▲, △).** **A**  $^{22}\text{Na}^+$  uptake driven by a  $\text{K}^+$ /valinomycin diffusion potential of  $-77$  mV. The  $F_0$  liposomes (10 mg phospholipids in  $50\ \mu\text{l}$  5 mM Bistris-propane, pH 7.4, 1 mM  $\text{MgCl}_2$ ) were loaded with 200 mM KCl by overnight incubation at  $4\ ^\circ\text{C}$  and then diluted 20-fold into assay buffer (2 mM Tricine/KOH, pH 7.4, 5 mM  $\text{MgCl}_2$ , 200 mM choline chloride, 2 mM  $^{22}\text{NaCl}$  (0.36  $\mu\text{Ci}$ )).  $^{22}\text{Na}^+$  uptake was initiated by adding 5  $\mu\text{M}$  valinomycin ( $\downarrow$ ) and samples were taken at the times indicated.  $^{22}\text{Na}^+$  uptake was determined by  $\gamma$ -counting after removal of the external  $^{22}\text{Na}^+$  by ion exchange chromatography.  $F_0$  liposomes (■, ▲);  $F_0$  liposomes incubated for 20 min with 50  $\mu\text{M}$  DCCD (□, △). **B**  $^{22}\text{Na}^+_{\text{out}}/\text{Na}^+_{\text{in}}$  exchange or  $\Delta p\text{Na}^+$ -driven uptake. For exchange measurements  $F_0$  liposomes from wild-type (■) and mutant aR227A (▲) were loaded with 100 mM NaCl by overnight incubation at  $4\ ^\circ\text{C}$ .  $^{22}\text{Na}^+$  uptake was initiated by diluting 30  $\mu\text{l}$  of these  $F_0$  liposomes (8.6 mg phospholipids) into 1 ml buffer containing 2 mM Tricine/KOH, pH 7.4, 5 mM  $\text{MgCl}_2$ , 100 mM choline chloride and 3 mM  $^{22}\text{NaCl}$  (0.47  $\mu\text{Ci}$ ). Uptake of  $^{22}\text{Na}^+$  was determined with samples taken at the indicated time points.  $\Delta p\text{Na}^+$ -driven uptake was started by diluting 30  $\mu\text{l}$  of  $F_0$  liposomes from wild-type (□) or mutant aR227A (△) (8.6 mg phospholipids, 10  $\mu\text{M}$  internal  $\text{Na}^+$ ) loaded with 50 mM KCl into 1 ml buffer containing 2 mM Tricine/KOH, pH 7.4, 5 mM  $\text{MgCl}_2$ , 50 mM KCl, 5  $\mu\text{M}$  valinomycin, 100 mM choline chloride and 100  $\mu\text{M}$   $^{22}\text{NaCl}$  (0.47  $\mu\text{Ci}$ ), which established a  $\Delta p\text{Na}^+$  of  $-59$  mV. Uptake of  $^{22}\text{Na}^+$  was subsequently determined as described above.



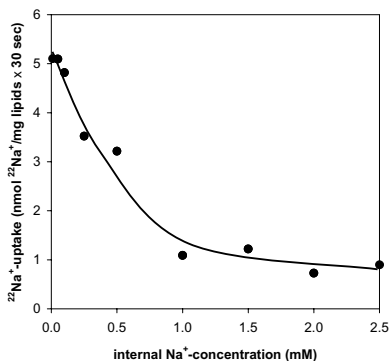


**Figure 4: Effect of internal NaCl on  $^{22}\text{Na}^+$  uptake driven by  $\Delta\mu\text{Na}^+$  in reconstituted  $F_0$  liposomes from mutant aR227A.** 30  $\mu\text{l}$  proteoliposomes (5 mg phospholipids) were loaded overnight with 50 mM KCl and the indicated sodium concentrations and diluted into 500  $\mu\text{l}$  assay buffer (2 mM Tricine/KOH, pH 7.4, 5 mM  $\text{MgCl}_2$ , 100 mM choline chloride, 50 mM KCl, 5  $\mu\text{M}$  valinomycin and  $^{22}\text{NaCl}$  at a 10-fold higher concentration than in the interior volume of the proteoliposomes with a specific activity of 500 cpm/nmol).  $^{22}\text{Na}^+$  uptake started immediately after diluting the samples into the assay buffer and was determined with aliquots taken after 30 s by  $\gamma$ -counting.

### **$F_1F_0$ ATP synthase with the aR227A mutation catalyses $\text{Na}^+$ -dependent ATP hydrolysis uncoupled from $\text{Na}^+$ pumping**

Previous work with the  $F_1F_0$  ATP synthase of *P. modestum* has established that ATP hydrolysis is  $\text{Na}^+$ -dependent and coupled to  $\text{Na}^+$  transport across the membrane (Laubinger & Dimroth, 1987; Laubinger & Dimroth, 1988). As shown above,  $F_1F_0$  liposomes with the aR227A mutation were unable to perform ATP-driven  $\text{Na}^+$  transport across the membrane (Figure 1). Therefore, the mutation might block ATP hydrolysis or ATP hydrolysis might become uncoupled from  $\text{Na}^+$  translocation. The results of Figure 5A show that the mutant enzyme has retained the capacity to hydrolyse ATP. Like in the wild-type ATP synthase, ATP hydrolysis by the mutant is  $\text{Na}^+$ -dependent and both enzymes show similar  $\text{Na}^+$  activation profiles. Furthermore, ATP hydrolysis by both enzymes was inhibited by DCCD with similar kinetics (Figure 5B). These results suggest that in the aR227A mutant the mechanical coupling between ATP hydrolysis and c-ring rotation is indistinguishable from the wild-type enzyme. Unlike to the wild-type enzyme, however, this c-ring rotation by the mutant is not associated with  $\text{Na}^+$  translocation across the membrane (Figure 1).

A reasonable explanation for these data is an obligatory binding of  $\text{Na}^+$  to the c subunit sites to overcome constraints in the ATP-driven rotation of the  $c_{11}$  ring versus subunit a, as already noticed for the wild-type enzyme (Laubinger & Dimroth, 1989; Dimroth *et al.*, 1999). While the positively charged aR227 promotes the dissociation of  $\text{Na}^+$  from a nearby rotor site and its release through the a subunit channel, the electroneutral aA227 residue has no positive effect on the dissociation of  $\text{Na}^+$  from the rotor sites.

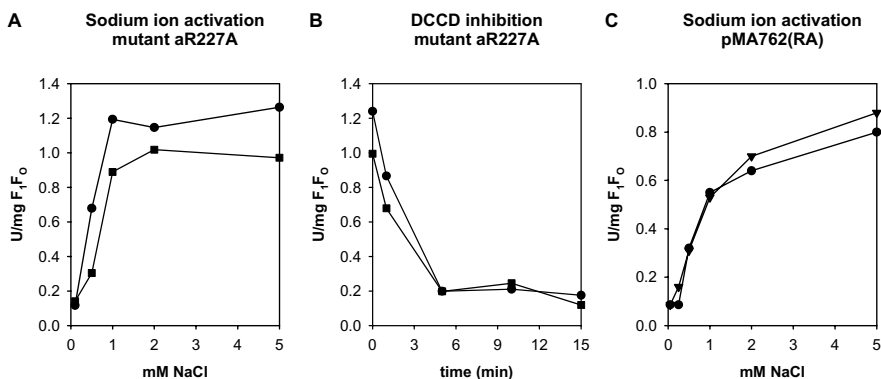


**Figure 5: Sodium ion activation profiles of  $F_1F_0$ -ATPase containing mutant aR227A (■) or mutant pMA762(RA) (▼) at pH 8.0.** **A** ATPase activities were determined with 34  $\mu\text{g}$   $F_1F_0$ -ATPase harbouring mutant aR227A. The assay mixture contained in 1 ml: 50 mM potassium phosphate buffer, pH 8.0, 100 mM  $\text{K}_2\text{SO}_4$ , 5 mM  $\text{MgCl}_2$ , 3 mM phosphoenolpyruvate, 0.25 mM NADH (potassium salt) 10 units pyruvate-kinase, 15 units lactate-dehydrogenase, 2.5 mM ATP (potassium salt) and NaCl in the indicated concentrations. ATP hydrolysis was measured as described under Materials and methods. As a control, re-assembled wild-type ATPase was measured identically (●). **B** Kinetics of ATPase inhibition by DCCD. Re-assembled  $F_1F_0$ -ATPase from mutant aR227A (■) and wild-type (●) were incubated at 25 °C with 20  $\mu\text{M}$  DCCD in a buffer containing 5 mM Bistris-propane, pH 7.4, 20 % glycerol and 1 mM  $\text{MgCl}_2$ . At the indicated time points samples of 5  $\mu\text{l}$  (34  $\mu\text{g}$  ATPase) were diluted into 0.98 ml assay buffer containing 5 mM NaCl to stop the reaction and used immediately for measuring ATPase activities. **C** Sodium activation profile of  $F_1F_0$ -ATPase from mutant pMA762(RA) harbouring mutations R227A, K220R, V264R and I278N on subunit a. The ATP hydrolysis activity was determined as described above with 41  $\mu\text{g}$   $F_1F_0$ -ATPase. After incubation of the proteoliposomes with 50  $\mu\text{M}$  DCCD, ATP hydrolysis from both wild-type and mutant was inhibited to about 10 % of the initial activity (not shown). Re-assembled wild-type ATPase activity was determined similarly (●).

If this interpretation was valid, the  $\text{Na}^+$ -stimulated ATP hydrolysis activity of the aR227A mutant should not be affected by the aK220R, V264E, I278N background, by which the subunit a channel becomes impermeable for  $\text{Na}^+$  ions (Kaim & Dimroth, 1998b). The results of Figure 5C show that this was indeed the case. Blocking only the a subunit  $\text{Na}^+$  channel with the K220R, V264E, I278N triple mutation, however, results in severe inhibition of ATP hydrolysis by  $\text{Na}^+$  ions (Kaim & Dimroth, 1998b). These results, therefore, support the idea that an important role of aR227 is to promote dissociation of the coupling  $\text{Na}^+$  ions from the rotor sites approaching this positively charged residue.

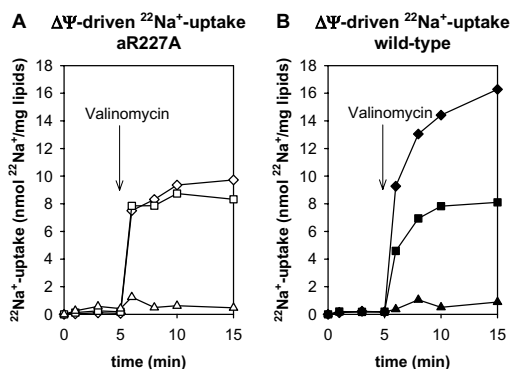


**Figure 6:**  $\Delta\Psi$ -driven  $^{22}\text{Na}^+$  uptake into  $F_0$  liposomes containing the aR227A mutation. **A**  $\Delta\Psi$ -driven  $^{22}\text{Na}^+$  transport into  $F_0$  liposomes from mutant aR227A ( $\diamond$ ) was determined in an assay mixture containing in 1 ml: 2 mM Tricine/KOH, pH 7.4, 5 mM  $\text{MgCl}_2$ , 200 mM choline chloride, 2 mM  $^{22}\text{NaCl}$  (0.36  $\mu\text{Ci}$ ) and 50  $\mu\text{l}$   $F_0$  liposomes (10 mg phospholipids) loaded with 200 mM KCl. By the addition of 5  $\mu\text{M}$  valinomycin ( $\downarrow$ ) a membrane potential of  $-77$  mV was established and  $^{22}\text{Na}^+$  transport was initiated. At the indicated time points  $^{22}\text{Na}^+$  transport was determined after separating internal and external  $^{22}\text{Na}^+$ .  $^{22}\text{Na}^+$  transport after reconstitution of  $F_1F_0$  liposomes by  $F_1$  addition to the outside ( $\square$ ). The measurements were performed under otherwise the conditions used for  $^{22}\text{Na}^+$  uptake into  $F_0$  liposomes. As a control  $F_1F_0$  liposomes were treated with 50  $\mu\text{M}$  DCCD for 20 min ( $\triangle$ ) and measured as described above. **B** A control experiment was performed in parallel under identical conditions for wild-type  $F_0$ -liposomes ( $\blacklozenge$ ), wild-type  $F_0$ -liposomes after  $F_1$  addition to the outside ( $\blacksquare$ ) and wild-type  $F_0$ -liposomes with  $F_1$  addition to the outside after modification with 50  $\mu\text{M}$  DCCD ( $\blacktriangle$ ).

Taking these data into account we reasoned that  $\Delta\Psi$ -driven  $^{22}\text{Na}^+$  uptake into  $F_0$ -liposomes with the aR227A mutation may depend on the orientation of the enzyme

within the membrane. Rotor sites exposed to the outer reservoir containing 2 mM  $^{22}\text{NaCl}$  should be permanently occupied with the alkali ion and should therefore not contribute to  $^{22}\text{Na}^+$  uptake. Rotor sites exposed to the inner reservoir with only low contaminating  $\text{Na}^+$  concentrations will, however, be empty most of the time.  $F_0$  molecules in this orientation can deliver  $^{22}\text{Na}^+$  from the outside through the a subunit channel onto an empty rotor site and from there to the inner reservoir after the rotor has turned. This hypothesis was analysed by measuring  $\Delta\Psi$ -driven  $^{22}\text{Na}^+$  transport into reconstituted  $F_0$  liposomes before and after incubation with the  $F_1$  moiety. The idea was to block specifically  $\text{Na}^+$  transport by  $F_0$  with outward oriented rotor sites. The results of Figure 6B show that  $\Delta\Psi$ -driven  $^{22}\text{Na}^+$  transport into wild-type  $F_0$  was approximately halved after  $F_1$  addition, as expected if  $F_0$  is oriented equally to both sides of the membrane and is active in either orientation. In contrast,  $\Delta\Psi$ -driven  $^{22}\text{Na}^+$  uptake by  $F_0$  with the aR227A mutation was not significantly affected by the incubation with  $F_1$ , in accord with the supposition that the  $F_0$  specimens with the rotor sites exposed outwards are not functional under our conditions (Figure 6A). Sodium ion transport by wild-type or mutant  $F_0$  was abolished by DCCD, indicating that it is catalysed by the usual mechanism which involves the rotation of the  $c_{11}$ -ring versus subunit a.

### **ATP synthesis by reconstituted $F_1F_0$ with the aR227A mutation**

We investigated whether ATP synthase with the aR227A mutation was able to synthesise ATP. For this purpose, the reconstituted proteoliposomes were loaded with 10 mM NaCl and diluted 70-fold into ATP synthesis buffer to reduce the external  $\text{Na}^+$  concentration to 0.14 mM. Simultaneously, a potassium diffusion potential of about 210 mV was applied. The results of Figure 7A show an increase of the amount of ATP synthesised by the mutant with time during a period of about 15 s. It is also shown that ATP synthesis by the wild-type enzyme was not significantly different from that of the mutant under these conditions. The results of Figure 7B show, that at an external  $\text{Na}^+$  concentration of 10 mM under otherwise identical conditions, ATP synthesis by the wild-type  $F_1F_0$  is not affected, while ATP synthesis by the mutant is hardly detectable. In ATP synthesis, the flux of  $\text{Na}^+$  ions is from the inner reservoir through the a subunit channel onto an empty rotor site and from there into the outer reservoir after the rotor has turned. In the mutant, dissociation of  $\text{Na}^+$  into the outside

reservoir is only possible at low external  $\text{Na}^+$  concentrations. This dissociation is essential to generate torque to drive ATP synthesis because the membrane potential will attract only empty sites with the negatively charged cE65 residue. In the wild-type enzyme, however, the aR227 residue assures dissociation of  $\text{Na}^+$  from the rotor sites even at elevated external  $\text{Na}^+$  concentrations, and ATP synthesis is therefore not inhibited under these conditions.

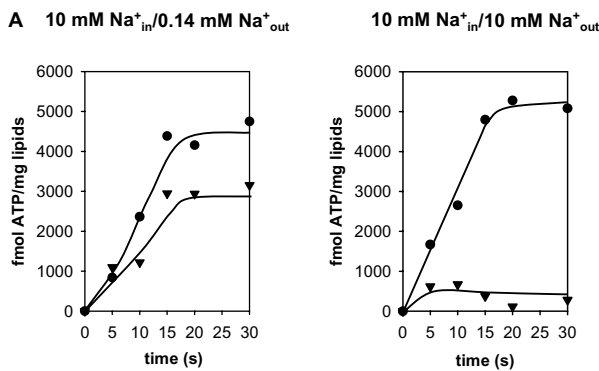


**Figure 7:** ATP synthesis by  $F_1F_0$  liposomes containing wild-type subunit a (●) or subunit a with the aR227A mutation (▼) in the presence of low (0.14 mM) or high (10 mM) external NaCl concentration. **A** ATP synthesis in the presence of low external sodium concentration. 5  $\mu\text{l}$   $F_1F_0$  liposomes (1 mg phospholipids) from mutant aR227A were loaded with 10 mM NaCl by overnight incubation and diluted 70-fold into buffer containing at pH 7.5: 5 mM potassium phosphate, 2 mM Tricine, 200 mM KCl, 0.5 mM  $\text{MgCl}_2$  and 0.25 mM ADP, yielding an external sodium concentration of 0.14 mM. By the addition of 2.9  $\mu\text{M}$  valinomycin a  $\text{K}^+$  diffusion potential of 210 mV was established and the ATP synthesis rate was determined by the luciferin/luciferase reaction at the indicated time points as described under Materials and methods. **B** ATP synthesis at high external sodium concentration. Proteoliposomes were prepared as described above and diluted into assay mixture (see above) containing 10 mM NaCl. The ATP synthesis rate was measured as described above. In control experiments wild-type proteoliposomes were measured at both external sodium concentrations as described for mutant aR227A.

### 3.5 Discussion

For a detailed understanding of the operation of the  $F_0$  motor, structure information is required, and this has to be complemented by biochemical knowledge. In this context, the discovery of the obligatory role of the membrane potential (Kaim

& Dimroth, 1998a; Dimroth *et al.*, 1999; Kaim & Dimroth, 1999) in the torque-generating mechanism leading to ATP synthesis is highly significant and of central importance in a recently proposed functional model for  $F_0$  from the  $\text{Na}^+$ -coupled ATP synthase of *P. modestum* (Kaim & Dimroth, 1998a; Dimroth *et al.*, 1999; Kaim & Dimroth, 1999). The model predicts that in ATP synthesis direction empty, negatively charged rotor sites are attracted electrostatically by the universally conserved positive stator charge (aR227 in *P. modestum*). The rotor site can escape the potential well by thermal fluctuations, and the membrane potential biases the diffusion towards the a subunit half channel that is open to the p-side of the membrane. The site quickly picks up a  $\text{Na}^+$  ion from the channel, which prevents it from being attracted backwards by the stator charge. This charge rather attracts the next empty rotor site and unidirectional rotation continues. Simultaneously, the  $\text{Na}^+$ -boarded rotor site moves through a hydrophobic area of subunit a, which would not be feasible energetically for an empty, negatively charged site. After exiting the stator, the bound  $\text{Na}^+$  dissociates and diffuses through its adjacent rotor channel to the n-side of the membrane.

The profound role of aR210 of the *E. coli* ATP synthase (equivalent to aR227 in *P. modestum*) was established by extensive mutational studies (Lightowers *et al.*, 1987; Cain & Simoni, 1989; Eya *et al.*, 1991; Howitt & Cox, 1992; Hatch *et al.*, 1995; Valiyaveetil & Fillingame, 1997). It was concluded that any substitution of aR210 results in the complete loss of ATP synthesis or  $\text{H}^+$ -coupled ATP hydrolysis activity. The loss of function markedly of the aR210K mutant could not easily be reconciled, however, with the role of aR210 as a positive stator charge (Elston *et al.*, 1998; Dimroth *et al.*, 1999).

We have now studied mutants of aR227 in the  $\text{Na}^+$ -translocating ATP synthase of *P. modestum* and found much to our surprise that the changes we introduced at this position were not as detrimental for the function of the enzyme as thought before. In all the aR227 mutants investigated we found distinct ATP synthesis or coupled ATP hydrolysis activities, albeit at restricted conditions of pH and  $\text{Na}^+$  concentrations. Following the stator charge concept, we first replaced aR227 by lysine or histidine because these can also be positively charged. The aR227K mutant was unable to catalyse ATP-driven  $\text{Na}^+$  transport at pH 7.0, consistent with the results published for the *E. coli* enzyme (Cain & Simoni, 1989; Eya *et al.*, 1991). Distinct activities were found, however, at pH 8.0-9.0, where no data are available for the *E. coli* ATP synthase. Inhibition of this activity by DCCD indicates that mutant and wild-type

enzyme have the same coupling mechanism. Furthermore, the pH profile of this reaction and that of  $^{22}\text{Na}^+_{\text{out}}/\text{Na}^+_{\text{in}}$  exchange catalysed by the  $F_0$  mutant was the same. This indicates that the degree of protonation of lysine at position a227 is critical for either  $\text{Na}^+$ -translocation activity. It may at first glance appear surprising that the activity of the lysine mutant requires elevated pH values because protonation and thus charging of the lysine is certainly more favourable at lower pH values. A comparison of the charge distribution in arginine or lysine may provide a plausible explanation. In lysine, the positive charge is localised on the  $\epsilon$ -ammonium group, whereas in arginine the charge is delocalised over the entire guanidinium group. A localised positive charge generates a very strong electrostatic interaction with the negatively charged glutamate 65 of the rotor, which is likely to impede the rotor's diffusion out of the potential well and hence lead to functional impairment. On raising the pH to 8.0-9.0, however, the  $\epsilon$ -ammonium group of the stator lysine is expected to be deprotonated part of the time, which facilitates the diffusion of the rotor and provides catalytic power to the mutant.

The importance of a positive charge at residue a227 was corroborated by results with the aR227H mutant. The ATP synthase with this mutation catalysed ATP-driven  $\text{Na}^+$  translocation with a pH optimum of 7.0, about 1 pH unit lower than that of the wild-type enzyme. The lower pH optimum probably reflects the lower pK of histidine compared to arginine. Please note that the charge of a protonated histidine is delocalised and therefore probably not preventing the rotor's diffusion out of the potential well.

For the *E. coli* ATP synthase an aR210A mutation was reported to be completely inactive in catalysing ATP synthesis or  $\text{H}^+$ -coupled ATP hydrolysis, but  $F_0$  with the a subunit mutation catalysed passive proton transport across the membrane (Valiyaveetil & Fillingame, 1997). Our results with the aR227A mutation in the *P. modestum* ATP synthase correspond with the conclusions from the *E. coli* enzyme only partially. The mutant enzyme catalysed  $\text{Na}^+$ -dependent ATP hydrolysis that was sensitive to inhibition by DCCD but not coupled to  $\text{Na}^+$  transport. These data indicate proper mechanical interaction between the  $F_1$  and  $F_0$  parts in the mutant enzyme but an improper dissociation of  $\text{Na}^+$  ions from the rotor sites. The aR227 residue of the wild-type enzyme but not the aA227 residue of the mutant apparently facilitates the dissociation of  $\text{Na}^+$  from an approaching rotor site. In the wild-type enzyme, the free

$\text{Na}^+$  ion diffuses through the a subunit channel to the p-side of the membrane, thereby completing its transport. In the mutant, however, the  $\text{Na}^+$  does not dissociate from the rotor sites and  $\text{Na}^+$  translocation is not catalysed. This interpretation is consistent with the lack of any  $^{22}\text{Na}^+_{\text{out}}/\text{Na}^+_{\text{in}}$  exchange activity by the mutant  $F_0$  moiety because under our conditions ( $[^{22}\text{Na}^+_{\text{out}}] = 3 \text{ mM}$ ;  $[\text{Na}^+_{\text{in}}] = 100 \text{ mM}$ ) the rotor sites exposed to either side of the membrane will probably be permanently occupied with the alkali ion, which obviously prevents its transport across the membrane.

Unlike to wild-type  $F_0$ , that with the aR227A mutation catalysed  $\Delta\text{pNa}^+$ -driven  $^{22}\text{Na}^+$  uptake. The putative mechanism for this activity is as follows: rotor sites in contact with the reservoir of low  $\text{Na}^+$  concentration are empty. They can diffuse to the a subunit channel along aA227 without electrostatic constraints and pick up a  $\text{Na}^+$  ion from the channel, which is in contact with the reservoir of high  $\text{Na}^+$  concentration. After diffusion of the occupied site through the hydrophobic part of subunit a, the  $\text{Na}^+$  dissociates into the reservoir of low  $\text{Na}^+$  concentration. In accord with the unidirectional rotational mechanism, the  $\Delta\text{pNa}^+$ -driven  $\text{Na}^+$  transport was completely inhibited by DCCD. Interestingly, the transport was about 50 % inhibited by 0.5 mM  $\text{Na}^+$  on the inside. This concentration correlates well with the  $K_m$  for  $\text{Na}^+$  in activating ATP hydrolysis by  $F_1F_0$ , as one would expect if the binding of  $\text{Na}^+$  to the rotor sites is in equilibrium with the  $\text{Na}^+$  concentration in the outside reservoir.

According to this model, the  $F_0$  liposomes with the aR227A mutation should catalyse  $\Delta\Psi$ -driven  $\text{Na}^+$  uptake only at low internal  $\text{Na}^+$  concentrations. The  $F_0$  liposomes are oriented approximately equally to either side of the membrane. We reasoned that  $F_0$  liposomes having their sites exposed to the outside reservoir with 2 mM  $\text{Na}^+$  are always occupied with the alkali ion and therefore not contributing to the transport.  $F_1$  addition specifically inhibits  $\text{Na}^+$  transport by  $F_0$  molecules with this orientation. Accordingly, this treatment did not affect the  $\Delta\Psi$ -driven  $\text{Na}^+$  uptake by the mutant  $F_0$  liposomes. With wild-type  $F_0$ , however, the transport was reduced to about 50 %, indicating catalytic activity for wild-type  $F_0$  in either orientation. These results confirm our conclusion that in the aR227A mutant  $\text{Na}^+$  only dissociates from the rotor sites into a reservoir of low  $\text{Na}^+$  concentration. In the wild-type, the positively charged arginine 227 facilitates the dissociation of  $\text{Na}^+$  from any nearby rotor site and thus allows transport of the alkali ion also into reservoirs of high  $\text{Na}^+$  concentration.



These results prompted us to hypothesise that reconstituted proteoliposomes containing the  $F_1F_0$  ATP synthase with the aR227A mutation were able to synthesise ATP at a low external  $\text{Na}^+$  concentration. ATP synthesis by the mutant enzyme was indeed found after applying a membrane potential to proteoliposomes containing 10 mM NaCl on the inside and 0.14 mM NaCl on the outside. We anticipate that empty rotor sites exposed to the external surface are attracted by the membrane potential and rotate towards the a subunit channel where they pick up a  $\text{Na}^+$  delivered from the internal reservoir. After exiting the interface with the a subunit by further rotation, the  $\text{Na}^+$  ion dissociates into the outside reservoir. As expected, increasing the external  $\text{Na}^+$  concentration to 10 mM abolished ATP synthesis by the mutant, but was without effect on this activity by the wild type enzyme.

In summary, our results give a detailed picture on the role of aR227 in the catalytic mechanism of the ATP synthase's  $F_0$  motor. A positive charge at this position is of essence to facilitate the dissociation of  $\text{Na}^+$  ions bound to rotor sites approaching this residue from either side. The charge has to be delocalised to avoid locking the rotor in an immobile position by too strong electrostatic interactions with the negatively charged rotor sites. Our data do not support previous suggestions that the conserved arginine of subunit a plays a role in proton translocation (Valiyaveetil & Fillingame, 1997) and they disprove the view that any change of the arginine by another residue is detrimental for coupled ATP hydrolysis or synthesis activity of the enzyme.

Strictly, these conclusions are derived from experiments performed with the  $\text{Na}^+$ -translocating ATP synthase from *P. modestum* and aR210 of the *E. coli* enzyme might have another function. However, the universal conservation of this residue and the phylogenetic relationship of both enzymes as documented by the formation of functional hybrids (Kaim & Dimroth, 1993; Kaim & Dimroth, 1994) make such a conclusion rather doubtful. We hypothesise therefore that aR210 of the *E. coli* ATP synthase plays a profound role in the dissociation of  $\text{H}^+$  from approaching rotor sites. It may be more difficult to verify this conclusion for a  $\text{H}^+$ -translocating ATP synthase because, unlike  $\text{Na}^+$  concentrations,  $\text{H}^+$  concentrations can only be varied within a narrow range without denaturation of the enzyme. Therefore, these results provide another example for the advantages of a  $\text{Na}^+$ -translocating enzyme to probe the ion translocation mechanism experimentally.

### 3.6 References

- ABRAHAMS, J. P., LESLIE, A. G., LUTTER, R. & WALKER, J. E. (1994). Structure at 2.8 Å resolution of  $F_1$ -ATPase from bovine heart mitochondria. *Nature* 370, 621-628.
- BIRKENHÄGER, R., HOPPERT, M., DECKERS-HEBESTREIT, G., MAYER, F. & ALTENDORF, K. (1995). The  $F_0$  complex of the *Escherichia coli* ATP synthase. Investigation by electron spectroscopic imaging and immunoelectron microscopy. *Eur. J. Biochem.* 230(1), 58-67.
- CAIN, B. D. & SIMONI, R. D. (1989). Proton translocation by the  $F_1F_0$ -ATPase of *Escherichia coli*. Mutagenic analysis of the a subunit. *J. Biol. Chem.* 264(6), 3292-3300.
- DIMROTH, P. (1982). The generation of an electrochemical gradient of sodium ions upon decarboxylation of oxaloacetate by the membrane-bound and  $Na^+$ -activated oxaloacetate decarboxylase from *Klebsiella aerogenes*. *Eur. J. Biochem.* 121(2), 443-449.
- DIMROTH, P., WANG, H., GRABE, M. & OSTER, G. (1999). Energy transduction in the sodium  $F$ -ATPase of *Propionigenium modestum*. *Proc. Natl. Acad. Sci. USA* 96(9), 4924-4929.
- DMITRIEV, O. Y., JONES, P. C. & FILLINGAME, R. H. (1999). Structure of the subunit c oligomer in the  $F_1F_0$  ATP synthase: model derived from solution structure of the monomer and cross-linking in the native enzyme. *Proc. Natl. Acad. Sci. USA* 96(14), 7785-7790.
- ELSTON, T., WANG, H. & OSTER, G. (1998). Energy transduction in ATP synthase. *Nature* 391, 510-513.
- EYA, S., MAEDA, M. & FUTAI, M. (1991). Role of the carboxyl terminal region of  $H^+$ -ATPase ( $F_0F_1$ ) a subunit from *Escherichia coli*. *Arch. Biochem. Biophys.* 284(1), 71-77.
- GIBBONS, C., MONTGOMERY, M. G., LESLIE, A. G. & WALKER, J. E. (2000). The structure of the central stalk in bovine  $F_1$ -ATPase at 2.4 Å resolution. *Nat. Struct. Biol.* 7(11), 1055-1061.
- HATCH, L. P., COX, G. B. & HOWITT, S. M. (1995). The essential arginine residue at position 210 in the a subunit of the *Escherichia coli* ATP synthase can be transferred to position 252 with partial retention of activity. *J. Biol. Chem.* 270(49), 29407-29412.
- HORTON, R. M., CAI, Z. L., HO, S. N. & PEASE, L. R. (1990). Gene splicing by overlap extension: tailor-made genes using the polymerase chain reaction. *Biotechniques* 8(5), 528-535.
- HOWITT, S. M. & COX, G. B. (1992). Second-site revertants of an arginine-210 to lysine mutation in the a subunit of the  $F_0F_1$ -ATPase from *Escherichia coli*: implications for structure. *Proc. Natl. Acad. Sci. USA* 89(20), 9799-9803.
- JIANG, W. & FILLINGAME, R. H. (1998). Interacting helical faces of subunits a and c in the  $F_1F_0$  ATP synthase of *Escherichia coli* defined by disulfide cross-linking. *Proc. Natl. Acad. Sci. USA* 95(12), 6607-6612.
- JUNGE, W., LILL, H. & ENGELBRECHT, S. (1997). ATP synthase: An electrochemical transducer with rotatory mechanics. *Trends Biochem. Sci.* 22(11), 420-423.
- KAIM, G. & DIMROTH, P. (1993). Formation of a functionally active sodium-translocating hybrid  $F_1F_0$ -ATPase in *Escherichia coli* by homologous recombination. *Eur. J. Biochem.* 218(3), 937-944.
- KAIM, G. & DIMROTH, P. (1994). Construction, expression and characterization of a plasmid-encoded  $Na^+$ -specific ATPase hybrid consisting of *Propionigenium modestum*  $F_0$ -ATPase and *Escherichia coli*  $F_1$ -ATPase. *Eur. J. Biochem.* 222(2), 615-623.
- KAIM, G. & DIMROTH, P. (1998a). ATP synthesis by the  $F_1F_0$  ATP synthase of *Escherichia coli* is obligatorily dependent on the electric potential. *FEBS Lett.* 434(1-2), 57-60.
- KAIM, G. & DIMROTH, P. (1998b). A triple mutation in the a subunit of the *Escherichia coli*/*Propionigenium modestum*  $F_1F_0$ -ATPase hybrid causes a switch from  $Na^+$  stimulation to  $Na^+$  inhibition. *Biochemistry* 37(13), 4626-4634.
- KAIM, G. & DIMROTH, P. (1998c). Voltage-generated torque drives the motor of the ATP synthase. *EMBO J.* 17(20), 5887-5895.

- KAIM, G. & DIMROTH, P. (1999). ATP synthesis by F-type ATP synthases is obligatorily dependent on the transmembrane voltage. *EMBO J.* 18(15), 4118-4127.
- KAIM, G., MATTHEY, U. & DIMROTH, P. (1998). Mode of interaction of the single a subunit with the multimeric c subunits during the translocation of the coupling ions by  $F_1F_0$ -ATPases. *EMBO J.* 17(3), 688-695.
- KLUGE, C. & DIMROTH, P. (1993). Kinetics of inactivation of the  $F_1F_0$ -ATPase of *Propionigenium modestum* by dicyclohexylcarbodiimide in relationship to  $H^+$  and  $Na^+$  concentration: Probing the binding site for the coupling ions. *Biochemistry* 32(39), 10378-10386.
- KLUGE, C., LAUBINGER, W. & DIMROTH, P. (1992). The  $Na^+$ -translocating ATPase of *Propionigenium modestum*. *Biochem. Soc. Trans.* 20(3), 572-577.
- LAUBINGER, W. & DIMROTH, P. (1987). Characterization of the  $Na^+$ -stimulated ATPase of *Propionigenium modestum* as an enzyme of the  $F_1F_0$  type. *Eur. J. Biochem.* 168(168), 475-480.
- LAUBINGER, W. & DIMROTH, P. (1988). Characterization of the ATP synthase of *Propionigenium modestum* as a primary sodium pump. *Biochemistry* 27(19), 7531-7537.
- LAUBINGER, W. & DIMROTH, P. (1989). The sodium ion translocating adenosinetriphosphatase of *Propionigenium modestum* pumps protons at low sodium ion concentrations. *Biochemistry* 28(18), 7194-7198.
- LIGHTOWLERS, R. N., HOWITT, S. M., HATCH, L., GIBSON, F. & COX, G. B. (1987). The proton pore in *Escherichia coli*  $F_0F_1$ -ATPase: A requirement of arginine at position 210 of the a-subunit. *Biochim. Biophys. Acta* 894(3), 399-406.
- MATTHEY, U., KAIM, G., BRAUN, D., WÜTHRICH, K. & DIMROTH, P. (1999). NMR studies of subunit c of the ATP synthase from *Propionigenium modestum* in dodecylsulfate micelles. *Eur. J. Biochem.* 261(2), 459-467.
- MATTHEY, U., KAIM, G. & DIMROTH, P. (1997). Subunit c from the sodium-ion-translocating  $F_1F_0$ -ATPase of *Propionigenium modestum*. Production, purification and properties of the protein in dodecylsulfate solution. *Eur. J. Biochem.* 247(3), 820-825.
- MCLACHLIN, D. T., BESTARD, J. A. & DUNN, S. D. (1998). The b and  $\delta$  subunits of the *Escherichia coli* ATP synthase interact *via* residues in their C-terminal regions. *J. Biol. Chem.* 273(24), 15162-15168.
- MIROUX, B. & WALKER, J. E. (1996). Over-production of proteins in *Escherichia coli*: mutant hosts that allow synthesis of some membrane proteins and globular proteins at high levels. *J. Mol. Biol.* 260(3), 289-298.
- NOJI, H., YASUDA, R., YOSHIDA, M. & KINOSHITA, K. (1997). Direct observation of the rotation of  $F_1$ -ATPase. *Nature* 386, 299-302.
- PÄNKE, O., GUMBIOWSKI, K., JUNGE, W. & ENGELBRECHT, S. (2000). F-ATPase: specific observation of the rotating c subunit oligomer of  $EF_0EF_1$ . *FEBS Lett.* 472(1), 34-38.
- RASTOGI, V. K. & GIRVIN, M. E. (1999). Structural changes linked to proton translocation by subunit c of the ATP synthase. *Nature* 402, 263-268.
- SAMBONGI, Y., IKO, Y., TANABE, M., OMOTE, H., IWAMOTO-KIHARA, A., UEDA, I., YANAGIDA, T., WADA, Y. & FUTAI, M. (1999). Mechanical rotation of the c subunit oligomer in ATP synthase  $F_1F_0$ : direct observation. *Science* 286(5445), 1722-1724.
- SAMBROOK, J., FRITSCH, E. F. & MANIATIS, T. (1989). *Molecular cloning. A laboratory manual.* Cold Spring Harbor Laboratory Press, Cold Spring Harbor, NY.
- SANGER, F., NICKLEN, S. & COULSON, A. R. (1977). DNA sequencing with chain-terminating inhibitors. *Proc. Natl. Acad. Sci. USA* 74(12), 5463-5467.
- SEELERT, H., POETSCH, A., DENCHER, N. A., ENGEL, A., STAHLBERG, H. & MÜLLER, D. J. (2000). Proton-powered turbine of a plant motor. *Nature* 405, 418-419.
- SINGH, S., TURINA, P., BUSTAMANTE, C. J., KELLER, D. J. & CAPALDI, R. (1996). Topographical structure of membrane-bound *Escherichia coli*  $F_1F_0$  ATP synthase in aqueous buffer. *FEBS Lett.* 397(1), 30-34.

- STAHLBERG, H., MÜLLER, D. J., SUDA, K., FOTIADIS, D., ENGEL, A., MEIER, T., MATTHEY, U. & DIMROTH, P. (2001). Bacterial  $\text{Na}^+$ -ATP synthase has an undecameric rotor. *EMBO reports* 2(3), 229-233.
- STOCK, D., LESLIE, A. G. & WALKER, J. E. (1999). Molecular architecture of the rotary motor in ATP synthase. *Science* 286, 1700-1705.
- TAKEYASU, K., OMOTE, H., NETTIKADAN, S., TOKUMASU, F., IWAMOTU-KIHARA, A. & FUTAI, M. (1996). Molecular imaging of *Escherichia coli*  $F_1F_0$ -ATPase in reconstituted membranes using atomic force microscopy. *FEBS Lett.* 392(2), 110-113.
- TSUNODA, S. P., AGGELER, R., YOSHIDA, M. & CAPALDI, R. (2001). Rotation of the c subunit oligomer in fully functional  $F_1F_0$  ATP synthase. *Proc. Natl. Acad. Sci. USA* 98(3), 898-902.
- VALIYAVEETIL, F. I. & FILLINGAME, R. H. (1997). On the role of Arg-210 and Glu-219 of subunit a in proton translocation by the *Escherichia coli*  $F_0F_1$ -ATP synthase. *J. Biol. Chem.* 272(51), 32635-32641.
- VON BALLMOOS, C., APPOLDT, Y., BRUNNER, J., GRANIER, T., VASELLA, A. & DIMROTH, P. (2002). Membrane topography of the coupling ion binding site in  $\text{Na}^+$ -translocating  $F_1F_0$  ATP synthase. *J. Biol. Chem.* 277(5), 3504-3510.
- WEHRLE, F., APPOLDT, Y., KAIM, G. & DIMROTH, P. (2002). Reconstitution of  $F_0$  of the ATP synthase of *Propionigenium modestum* from its heterologously expressed and purified subunits. *Eur. J. Biochem.* 269(10), 2567-2573.
- WILKENS, S. & CAPALDI, R. A. (1998). ATP synthase's second stalk comes into focus. *Nature* 393, 29.

## CHAPTER 4

### **Mutational analysis of Asp259 of subunit a from *Propionigenium modestum* F<sub>1</sub>F<sub>0</sub> ATP synthase**

Franziska Wehrle, Georg Kaim and Peter Dimroth

Institut für Mikrobiologie, Eidgenössische Technische Hochschule  
CH-8092 Zürich, Switzerland

## 4.1 Abstract

Functionally important residues of subunit a of the ATPase of *Escherichia coli* are E219 and H245, which are interchangeable. At equivalent positions of subunit a of the Na<sup>+</sup>-translocating ATP synthase from *Propionigenium modestum* M236 and D259 are found, respectively. We have mutated aD259 to glutamate, glycine or lysine and characterised the catalytic properties of these mutants. Mutant F<sub>o</sub> liposomes catalysed <sup>22</sup>Na<sup>+</sup><sub>out</sub>/Na<sup>+</sup><sub>in</sub> exchange or ΔΨ-driven <sup>22</sup>Na<sup>+</sup> uptake, and mutant F<sub>1</sub>F<sub>o</sub> liposomes catalysed ATP-driven <sup>22</sup>Na<sup>+</sup> transport or ATP synthesis when a membrane potential was applied. The rates decreased in the order wild-type>aD259E>aD259G>aD259K mutant and the mutations affected ATP synthesis more severely than Na<sup>+</sup> transport in either exchange or uptake mode.

*Abbreviations:* DCCD, *N,N'*-dicyclohexylcarbodiimide; CCCP, carbonyl cyanide *m*-chlorophenylhydrazone; PCR, polymerase chain reaction; Tris, tris-(hydroxymethyl)-aminomethane; Bistris-propane, 1,3-bis-[tris-(hydroxymethyl)-methylamino]-propane; Tricine, N-[tris-(hydroxymethyl)-methyl]-glycine; DTT, 1,4-dithio-DL-threitol; ΔΨ, transmembrane electrical potential.

## 4.2 Introduction

Structurally similar F<sub>1</sub>F<sub>o</sub> ATP synthases are present in mitochondria, chloroplasts or eubacteria, where they catalyse ATP formation with the energy stored in a transmembrane electrochemical gradient of protons or Na<sup>+</sup> ions. The enzyme is composed of an extrinsic membrane domain, F<sub>1</sub>, which harbours the catalytic sites for ATP synthesis. The subunit composition of F<sub>1</sub> is α<sub>3</sub>β<sub>3</sub>γδε (Weber & Senior, 1997; Yoshida *et al.*, 2001). Alternating α and β subunits form a cylinder around a central α-helical structure of the γ subunit (Abrahams *et al.*, 1994; Stock *et al.*, 1999; Groth & Pohl, 2001). Rotation of the γ subunit with respect to the α<sub>3</sub>β<sub>3</sub> subcomplex has been directly observed (Noji *et al.*, 1997). There is strong evidence to support a mechanism in which the central stalk of the soluble F<sub>1</sub> domain, together with the oligomeric c-ring

in the membrane domain, rotates as an assembly coupling ion movement with ATP synthesis or hydrolysis (Sambongi *et al.*, 1999; Pänke *et al.*, 2000).

The  $F_0$  membrane domain of eubacteria consists of three different subunits in the stoichiometry  $ab_2c_n$  (for review see Deckers-Hebestreit *et al.*, 2000). The number of  $c$  subunits forming the ring varies among species, being 10 for yeast mitochondria (Stock *et al.*, 1999), 14 for spinach chloroplasts (Seelert *et al.*, 2000) and 11 for the  $Na^+$ -translocating  $F_1F_0$  ATP synthase from *Ilyobacter tartaricus* (Stahlberg *et al.*, 2001). Each monomeric unit folds as a helical hairpin. The N-terminal helices form a tightly packed inner ring and the C-terminal helices form a more loosely packed outer ring (Vonck *et al.*, 2002; Stock *et al.*, 1999). Cavities between neighbouring outer helices and the inner ring were suggested to act as  $Na^+$  access channels to the binding sites, which are located in the middle of the membrane (von Ballmoos *et al.*, 2002; Vonck *et al.*, 2002). The single  $a$  subunit and the two  $b$  subunits are supposed to contact the  $c$ -ring laterally (Birkenhäger *et al.*, 1995; Singh *et al.*, 1996; Takeyasu *et al.*, 1996; Jiang & Fillingame, 1998). At the subunit  $a/c$  interface  $Na^+$  ions are thought to dissociate from the  $c$  subunit site into a channel of subunit  $a$  that connects it with the opposite surface of the membrane.

So far, mutational analyses of subunit  $a$  from *E. coli* have identified R210, E219 and H245 as important residues for ion translocation (Cain & Simoni, 1986; Lightowlers *et al.*, 1987; Cain & Simoni, 1988; Lightowlers *et al.*, 1988; Cain & Simoni, 1989). Recent studies with the ATP synthase of *P. modestum* have shown that the equivalent of aR210 is of essence for the dissociation of  $Na^+$  from occupied rotor sites approaching this residue (Wehrle *et al.*, 2002). *P. modestum* has a methionine (aM236) and an aspartate (aD259) at positions corresponding to aE219 and aH245 of *E. coli*, respectively. These residues can be interchanged without significant effect on activity, whereas in single mutants the activity is severely affected (Cain & Simoni, 1988).

We report here on mutants of D259 of the *P. modestum*  $a$  subunit. Coupled activities were retained at reduced levels after substituting aD259 by glutamate, glycine or lysine, and the effect of the mutations appeared to be more pronounced in ATP synthesis than in  $Na^+$ -coupled ATP hydrolysis direction.

## 4.3 Materials and Methods

### Bacterial strains and growth conditions

*E. coli* DH5 $\alpha$  (Bethesda Research Laboratories) was used as host for all cloning purposes and *E. coli* PEF42(DE3) (Matthey *et al.*, 1999) served as host for overproduction of mutant a subunits. All strains were grown at 37 °C in Luria-Bertani (LB) medium supplemented with 200  $\mu$ g/ml ampicillin.

### Purification of subunits a, b, and c from *P. modestum* ATP synthase

Recombinant subunits a and b were synthesised by expression of plasmids pPmaHisN and pPmbHisC, respectively in *E. coli* C43(DE3) (Miroux & Walker, 1996) as described (Wehrle *et al.*, 2002). Monomeric subunit c was overexpressed from plasmid pT7c and purified by extraction with organic solvents as described (Matthey *et al.*, 1997; Matthey *et al.*, 1999). Prior to usage, 7  $\mu$ l of 10 % sodium cholate were added to 70  $\mu$ l (70  $\mu$ g) of the protein in chloroform/methanol (2:1) and the solvent was evaporated under a stream of argon. The pellet was dried in a vacuum centrifuge and resuspended in 70  $\mu$ l 5 mM potassium phosphate buffer, pH 8.0, containing 5 mM MgCl<sub>2</sub>.

### Site directed mutagenesis of the *P. modestum* subunit a

Primers used for constructing mutants at position aD259 are listed in Table 1 and were custom synthesised by Microsynth (Balgach, Switzerland). Site directed mutants were obtained by two PCR steps as described (Horton *et al.*, 1990). The 5' and 3' subfragments were obtained using Pma1V (*Nde*I) and the 3' mutagenic primers, or Pma889R (*Bam*HI) and 5' the mutagenic primers, respectively. Plasmid pPmaHisN (Wehrle *et al.*, 2002) was used as template. The mutated PCR subfragments were purified with NucleoTrap (Macherey Nagel) and served as templates for the subsequent PCR reaction with primers Pma1V and Pmb889R. The polymerase chain reaction was performed with *Pfu* polymerase (Stratagene) in glass capillaries on an Air Thermocycler 1605 (Idaho Technology). The resulting 902 bp fragments were purified with the NucleoTrap Kit, digested with *Nde*I and *Bam*HI and purified using QIAquick PCR purification columns (Qiagen). The DNA fragments were cloned into vector pET16b (Novagen) resulting in plasmids pET16(DE) harbouring mutation aD259E, pET16(DG) containing mutation aD259G and pET16(DK) comprising



mutation aD259K, respectively. The nucleotide sequences of the cloned DNA fragments were confirmed according to the dideoxy-nucleotide chain termination method (Sanger *et al.*, 1977) using a *Taq* Dye-Dideoxy Terminator Sequencing Kit on an ABI PRISM 310 genetic analyzer from Applied Biosystems (Foster City, USA).

**Table 1: Oligonucleotides used for PCR.** The mutated bases are underlined, and the corresponding newly introduced restriction sites are shown in bold.

oligonucleotide	sequence (5'-3')	restriction site	mutation
Pma 1V	TAAATGGAGACATATGAAAAAAAAATGG	<i>Nde</i> I	none
Pma 889R	TGTTTAAAAC <b>TGGAT</b> CCAAC <b>T</b> AATCTTC	<i>Bam</i> HI	none
Mpa 259E-V	CACCTGTACTTT <b>TCGAA</b> CTTTTCAGTGGAG	<i>Nsp</i> V	aD259E
Mpa 259E-R	CTCCACTGAAAAG <b>TTTCG</b> AAAAGTACAGGTG	<i>Nsp</i> V	aD259E
Mpa 259G-V	CTT <b>CACCTGTATTTTCGGT</b> CTTTTCAGTGG	<i>-Taq</i> I	aD259G
Mpa 259G-R	CCACTGAAAAG <b>CCGAAATAC</b> AGGTGAAG	<i>-Taq</i> I	aD259G
Mpa 259K-V	CTT <b>CACCTGTATTTTCAA</b> CTTTTCAGTGG	<i>-Taq</i> I	aD259K
Mpa 259K-R	CCACTGAAAAG <b>TTTCAAATAC</b> AGGTGAAG	<i>-Taq</i> I	aD259K

### Heterologous expression of mutant *P. modestum* a subunits in *E. coli*

*E. coli* PEF42(DE3) (Matthey *et al.*, 1997) was transformed with plasmids pET16(DE), pET16(DG) or pET16(DK). Expression cultures were inoculated with 2 % of an overnight culture and grown to optical densities (600 nm) of 0.6. Then isopropyl-2-D-thio-galactopyranoside (IPTG) was added to a final concentration of 1 mM, and the cultures were incubated for another 3 h at 37 °C before harvest. Cells were washed once with 10 mM Tris, pH 8.0 and stored at -20 °C.

### Purification of the mutant a subunits

2-3 g of washed cells (wet weight) were thawed and resuspended in 5 ml 50 mM potassium phosphate buffer, pH 8.0, containing 20 % glycerol, 5 mM MgCl<sub>2</sub>, 0.1 mM diisopropylfluorophosphate and a trace amount of DNaseI. The cells were disrupted at 4 °C by two passages through a French pressure cell at 11,000 psi (76 MPa) and centrifuged at 12'000 × g to remove cell debris. The supernatant was centrifuged for 1 h at 200'000 × g, the membrane pellet was resuspended in 1 ml of 50 mM potassium phosphate buffer, pH 8.0, containing 20 % glycerol and 5 mM MgCl<sub>2</sub>, and the membrane proteins were solubilised with 1 % N-lauroyl-sarcosine while gently stirring for 30 min at 25 °C. Unsolubilised material was removed by ultracentrifugation (1 h, 200,000 × g). The mutant a subunits were further purified as described for the wild-type protein (Wehrle *et al.*, 2002).

### **Reconstitution of F<sub>0</sub> liposomes from isolated subunits a, b, and c**

Phosphatidylcholine (Sigma type II-S from soybean) was resuspended at 80 mg/ml in a buffer containing 15 mM Tricine/NaOH, pH 8.0, 7.5 mM DTT, 0.2 mM K<sub>2</sub>-EDTA, 1.6 % sodium cholate and 0.8 % sodium deoxycholate by shaking the mixture vigorously for 3 min. The suspension was then sonicated in a water bath to clarity (5 min).

The reconstitution was performed essentially as described for *E. coli* F<sub>0</sub> (Dmitriev *et al.*, 1995). 25 µg of subunit a, 29 µg of subunit b and 70 µg of subunit c were combined and the volume was adjusted to 250 µl with 10 mM Tris/HCl, pH 8.0, 150 mM NaCl, 10 % glycerol and 1 % sodium cholate. After sonicating the sample in a Branson bath sonicator for 20 min at 25 °C the mixture was incubated on ice for 2-3 h. 250 µl of the preformed liposomes were added to the protein mixture giving a protein/lipid ratio of 1:160 and the sample was sonicated for 5 min. The solution was dialysed overnight at 4 °C against 1000 volumes of 5 mM Bistris-propane/HCl, pH 7.4, 2.5 mM MgCl<sub>2</sub>, 0.2 mM K<sub>2</sub>-EDTA, 0.2 mM DTT to form the proteoliposomes. After addition of 0.5 ml 5 mM Bistris-propane/HCl pH 7.4 the proteoliposomes were sonicated four times for 5 s in a water bath. The mixture was frozen in liquid nitrogen, kept there for 15 min, and thawed at 25 °C. After addition of 750 µl 5 mM Bistris-propane/HCl, pH 7.4, 1 mM MgCl<sub>2</sub> the proteoliposomes were collected by centrifugation (200'000 × g, 1 h). The pellet was resuspended in 5 mM Bistris-propane/HCl, pH 7.4, 1 mM MgCl<sub>2</sub>, adjusted to a final volume of 100 µl, sonicated as described above and used immediately or stored in liquid nitrogen. Prior to usage, the samples were thawed and sonicated four times for 5 s in a water bath type sonicator.

### **Reconstitution of the ATPase enzyme complex from reconstituted F<sub>0</sub> liposomes and purified F<sub>1</sub>**

F<sub>1</sub>-ATPase from DK8/pHEP100 (Kaim & Dimroth, 1994) was purified as described (Laubinger *et al.*, 1990). This strain harbours a hybrid F<sub>1</sub> moiety consisting of α, β, γ and ε subunits from *E. coli* and the δ subunit from *P. modestum*. 20 mg phospholipids reconstituted with 124 µg F<sub>0</sub> (0.8 nmoles) were incubated overnight at 4 °C with an equimolar amount of F<sub>1</sub> and membrane bound enzyme complexes were collected by centrifugation (1 h, 200,000 × g). F<sub>1</sub>F<sub>0</sub> proteoliposomes were

resuspended in 5 mM Bistris-propane/HCl, pH 7.4, 1 mM MgCl<sub>2</sub>, and adjusted to a final volume of 100 µl.

### Sodium transport experiments

*ΔΨ-driven <sup>22</sup>Na<sup>+</sup> uptake into F<sub>0</sub> proteoliposomes.* 50 µl F<sub>0</sub> proteoliposomes (10 mg of phospholipids) were loaded with 200 mM KCl by overnight incubation at 4 °C and diluted 1:20 into assay buffer containing at 25 °C: 2 mM Tricine/KOH buffer, pH 7.4, 5 mM MgCl<sub>2</sub>, 200 mM choline chloride and 2 mM <sup>22</sup>NaCl (0.36 µCi). A membrane potential of -77 mV was established by the addition of 5 µM valinomycin after equilibrating the mixture for 5 min. The rate of <sup>22</sup>Na<sup>+</sup> uptake was determined by passage of samples (140 µl) over 1 ml columns of Dowex 50, K<sup>+</sup>, to adsorb the external <sup>22</sup>Na<sup>+</sup> (Dimroth, 1982). The resin was washed with 0.6 ml of 2 mM Tricine/KOH pH 7.4, containing 5 mM MgCl<sub>2</sub> and 200 mM sucrose. The radioactivity eluted from the columns represents the <sup>22</sup>Na<sup>+</sup> in the lumen of the proteoliposomes and was determined by γ-counting.

*<sup>22</sup>Na<sup>+</sup><sub>out</sub>/<sup>22</sup>Na<sup>+</sup><sub>in</sub>-exchange.* 50 µl F<sub>0</sub> proteoliposomes (10 mg of phospholipids) were incubated overnight with 100 mM NaCl at 4 °C and subsequently diluted into 1 ml 2 mM Tricine/KOH buffer, pH 7.4 containing 5 mM MgCl<sub>2</sub>, 100 mM choline chloride and 5 mM <sup>22</sup>NaCl (0.47 µCi). <sup>22</sup>Na<sup>+</sup> uptake was determined after separation of external from internal <sup>22</sup>Na<sup>+</sup> by Dowex 50, K<sup>+</sup> columns as described above. The columns were washed with 0.6 ml 2 mM Tricine/KOH buffer, pH 7.4 containing 5 mM MgCl<sub>2</sub> and 100 mM sucrose.

*ATP-driven <sup>22</sup>Na<sup>+</sup> uptake into F<sub>1</sub>F<sub>0</sub> proteoliposomes.* Na<sup>+</sup> transport into F<sub>1</sub>F<sub>0</sub> liposomes was determined in assay buffer, which was supplemented with 20 units of pyruvate kinase and 6 mM phosphoenolpyruvate to provide an ATP regenerating system. The assay buffer contained the following components in 0.7 ml at 25 °C: 50 mM potassium phosphate buffer, pH 7.0, 5 mM MgCl<sub>2</sub>, 2 mM <sup>22</sup>NaCl (0.11 µCi) and 50 µl F<sub>1</sub>F<sub>0</sub> proteoliposomes (10 mg phospholipids). After equilibrating the system for 5 min, sodium transport was initiated by adding 1.25 mM ATP (potassium salt). Samples of 90 µl were taken at the indicated time points and external <sup>22</sup>Na<sup>+</sup> was separated from that entrapped within the liposomes by passage over a small column of Dowex 50, K<sup>+</sup>, as described (Dimroth, 1982). The resin was washed with 0.6 ml

2 mM Tricine/KOH buffer, pH 7.4 containing 5 mM MgCl<sub>2</sub> and 100 mM sucrose and the radioactivity was determined by  $\gamma$ -counting.

### Determination of ATP synthesis

F<sub>1</sub>F<sub>0</sub> liposomes were reconstituted as described above and loaded with 10 mM NaCl by overnight incubation at 4 °C. 5  $\mu$ l F<sub>1</sub>F<sub>0</sub> liposomes (1 mg phospholipids; 50  $\mu$ M internal K<sup>+</sup>) were diluted 70-fold into assay buffer containing at pH 7.5: 2 mM Tricine, 5 mM potassium phosphate, 200 mM KCl, 0.5 mM MgCl<sub>2</sub> and 0.25 mM ADP. ATP synthesis was started at 25 °C by induction of a KCl/valinomycin diffusion potential of  $\sim$ 210 mV (inside positive). At the indicated time points aliquots of 45  $\mu$ l were taken and diluted 1:10 into assay buffer supplemented with 10  $\mu$ M CCCP and 1 mM azide to stop the reaction. The ATP concentration was subsequently determined by the luciferin/luciferase reaction by the CLSII assay from Roche (Switzerland) as described by the manufacturer. Light emission was recorded with a luminometer (Biolumat LB 9500 C, Berthold).

## 4.4 Results and Discussion

Charged residues within the hydrophobic domains of a membrane protein are usually of functional significance. Such a residue is aspartate 259 of subunit a of the Na<sup>+</sup>-translocating ATP synthase from *P. modestum*. This residue is located within the C-terminal transmembrane helix probably close to the centre of the membrane. To probe the importance of this aspartate residue for the function of the enzyme it was mutated to glutamate, glycine or lysine. The mutant a subunits are synthesised in *E. coli* and reconstituted together with the b and c subunits into proteoliposomes. With these F<sub>0</sub> liposomes we measured the <sup>22</sup>Na<sup>+</sup><sub>out</sub>/Na<sup>+</sup><sub>in</sub> exchange and  $\Delta\Psi$ -driven <sup>22</sup>Na<sup>+</sup> uptake activities. The results of Figure 1 indicate only a marginal effect on the exchange activity if aspartate 259 of subunit a is replaced by glutamate, while the initial transport activities decrease to approximately 60 % of the wild-type activity in the aD259G or aD259K mutants. In the  $\Delta\Psi$ -driven <sup>22</sup>Na<sup>+</sup> uptake mode all three mutants were active and the activities of the mutants were reduced to similar degrees as observed in the exchange mode. These results indicate that an acidic residue at position 259 of the a subunit is advantageous for these Na<sup>+</sup> transport activities, but is not essential.

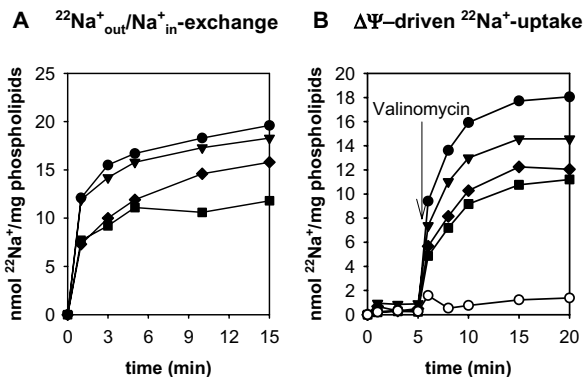


**Figure 1: Kinetics of  $^{22}\text{Na}^+$  transport into  $F_0$  liposomes harbouring mutants aD259E (▼), aD259K (◆) and aD259G (■) or wild-type subunit a (●○).** **A**  $^{22}\text{Na}^+_{\text{out}}/\text{Na}^+_{\text{in}}$  exchange activity. 50  $\mu\text{l}$  of reconstituted  $F_0$  liposomes (10 mg phospholipids) in 5 mM Bistris-propane/HCl, pH 7.4, 1 mM  $\text{MgCl}_2$ , 100 mM NaCl were diluted 1:20 into assay buffer (2 mM Tricine/KOH, pH 7.4, 5 mM  $\text{MgCl}_2$ , 100 mM choline chloride) containing 5 mM  $^{22}\text{Na}^+$  (0.47  $\mu\text{Ci}$ ).  $^{22}\text{Na}^+$  uptake was determined with samples taken after different incubation periods. **B**  $\Delta\Psi$ -dependent uptake of  $^{22}\text{Na}^+$  into reconstituted  $F_0$  liposomes. A  $\Delta\Psi$  of -77 mV was generated by a  $\text{K}^+$  diffusion potential by diluting 50  $\mu\text{l}$   $F_0$  liposomes (10 mg phospholipids) loaded with 200 mM KCl into 1 ml assay buffer (2 mM Tricine/KOH, pH 7.4, 5 mM  $\text{MgCl}_2$ , 200 mM choline chloride, 2 mM  $^{22}\text{Na}^+$  (0.36  $\mu\text{Ci}$ )) and addition of 5  $\mu\text{M}$  valinomycin (↓). At the indicated time points  $^{22}\text{Na}^+$  uptake was subsequently determined. Control experiments were performed after incubation of the  $F_0$  liposomes with 50  $\mu\text{M}$  DCCD (○). Similarly  $^{22}\text{Na}^+$  uptake was inhibited after incubating mutant  $F_0$  liposomes with DCCD (not shown).

Similar conclusions can be drawn from ATP-driven  $^{22}\text{Na}^+$  uptake experiments into  $F_1F_0$  liposomes (Figure 2). Again, the aD259E mutant was almost as active as the wild-type enzyme, while the aD259K and aD259G mutants showed reduced activities. As expected for functionally coupled enzyme specimens, the  $\text{Na}^+$  transport by all mutant enzymes was completely inhibited by DCCD.

The results of Figure 3 show the effect of the aD259 mutants on ATP synthesis. The aD259E mutant showed approximately 90 % of the wild-type activity, that with the aD259G mutant retained 78 % of wild-type activity and that with the aD259K mutation 28 % of wild-type activity.

The more severe effect of the lysine substitution on the ATP synthesis than on  $\text{Na}^+$  translocation activities is remarkable. A positive charge at position 259 of the a subunit may interfere more severely with  $\text{Na}^+$  translocation through the a subunit

half-channel onto an empty rotor site as required for ATP synthesis than in the opposite direction during ATP hydrolysis.

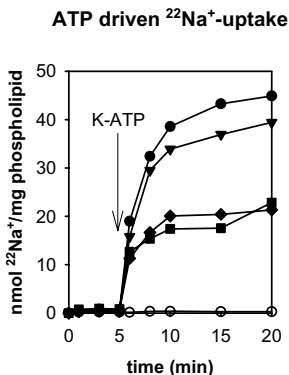


**Figure 2: Kinetics of ATP-driven  $^{22}\text{Na}^+$  uptake into proteoliposomes containing  $\text{F}_1\text{F}_0$ -ATPase from wild-type (●) or mutants ad259E (▼), ad259K (◆) and ad259G (■), respectively.** Assay mixtures contained in 0.7 ml at 25 °C: 50 mM potassium phosphate buffer, pH 7.0, 5 mM  $\text{MgCl}_2$ , 6 mM phosphoenolpyruvate, 20 units pyruvate kinase, 2 mM  $^{22}\text{NaCl}$  (0.11  $\mu\text{Ci}$ ) and 50  $\mu\text{l}$  of the reconstituted proteoliposomes (10 mg phospholipids).  $^{22}\text{Na}^+$  uptake was initiated by the addition of 1.25 mM ATP (potassium salt) as indicated by an arrow. After separating external  $^{22}\text{Na}^+$  by cation exchange chromatography, internal  $^{22}\text{Na}^+$  was determined by  $\gamma$ -counting. After incubation of the  $\text{F}_1\text{F}_0$  proteoliposomes with 50  $\mu\text{M}$  DCCD the enzyme did not catalyse  $^{22}\text{Na}^+$  uptake (○). The mutants showed similar uptake rates as the wild-type after modification with DCCD.

In *E. coli* the two most intensely studied residues on subunit a, apart from R210, are E219 and H245. Mutations of either site showed various degrees of impairment on proton translocation. It had been suggested previously, that aE219 was an essential component of the proton pathway through  $\text{F}_0$ . This was based on the replacement of aE219 by tyrosine, glutamine or leucine, resulting in ATPase enzymes that were not able to translocate protons, whereas the conservative replacement by an aspartate or a histidine was tolerated at this site (Lightowlers *et al.*, 1987; Cain & Simoni, 1988; Eya *et al.*, 1991). In a more recent study, however, aE219G and aE219K were found to be active indicating that aE219 was not an essential residue for a coupled enzyme, but might be involved in the proton translocation process (Valiyaveetil & Fillingame, 1997).

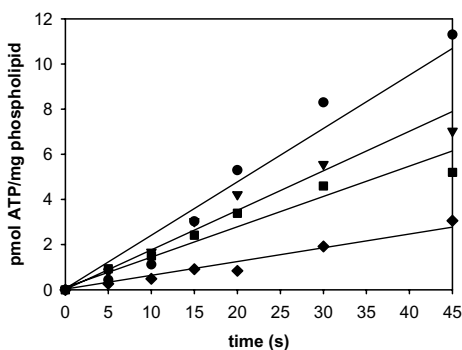


**Figure 3: ATP synthesis of proteoliposomes containing reconstituted  $F_1F_0$ -ATPase from wild-type (●), mutants aD259E (▼), aD259G (■) and aD259K (◆).**  $F_1F_0$  liposomes were reconstituted as described in Materials and Methods and loaded by overnight incubation with 10 mM NaCl. After dilution of 5  $\mu$ l  $F_1F_0$  liposomes (1 mg phospholipids) into 345  $\mu$ l assay buffer (2 mM Tricine/KOH, 5 mM potassium phosphate, 200 mM KCl, 0.5 mM  $MgCl_2$  and 0.25 mM ADP, pH 7.5) ATP synthesis was initiated by the addition of 2.9  $\mu$ M valinomycin. The ATP concentration was determined by the luciferin/luciferase assay after different incubation periods.

In the a subunits of mitochondrial ATPases the homologous sites to aE219 and aH245 of *E. coli* are interchanged (Cain & Simoni, 1988), and in *E. coli* subunit a the effect of mutations in aE219 could be suppressed by placing a glutamate instead of a histidine at position aH245 (Cain & Simoni, 1988). This interaction between aE219 and aH245 indicates that the two amino acid residues could be in proximity to each other. In *P. modestum*, the equivalent sites to aE219 and aH245 from *E. coli* are aM236 and aD259. Our data obtained by mutational analysis of aD259 support the requirement of a hydrophilic environment near residues aE219 and aH245. The findings that an acidic residue can be functionally replaced by a glycine or a lysine suggests that the presence of a carboxylate side chain at this position is not essential for ion translocation through  $F_0$ . Alternatively, this residue might contribute an ionisable group promoting the translocation of the coupling ions. However, from the amino acid substitutions only the glutamate or the lysine can be protonated/deprotonated. The unexpected ATP synthesis/hydrolysis activity of aD259G might be explained with the small side chain of the glycine, which allows a water molecule to occupy the space normally filled by the carboxylate side chain of the aspartate. This water molecule could likewise contribute the hydrophilic

environment required for ion translocation. These data are also in accordance with the study by Eya *et al.* (1991), reporting that the aE219H mutant showed low level of function, as the imidazole ring of a histidine can be protonated at physiological pH.

## 4.5 References

- ABRAHAMS, J. P., LESLIE, A. G., LUTTER, R. & WALKER, J. E. (1994). Structure at 2.8 Å resolution of F<sub>1</sub>-ATPase from bovine heart mitochondria. *Nature* 370, 621-628.
- BIRKENHÄGER, R., HOPPERT, M., DECKERS-HEBESTREIT, G., MAYER, F. & ALTENDORF, K. (1995). The F<sub>o</sub> complex of the *Escherichia coli* ATP synthase. Investigation by electron spectroscopic imaging and immunoelectron microscopy. *Eur. J. Biochem.* 230(1), 58-67.
- CAIN, B. D. & SIMONI, R. D. (1986). Impaired proton conductivity resulting from mutations in the a subunit of F<sub>1</sub>F<sub>o</sub>-ATPase in *Escherichia coli*. *J. Biol. Chem.* 261(22), 10043-10050.
- CAIN, B. D. & SIMONI, R. D. (1988). Interaction between Glu-219 and His-245 within the a subunit of F<sub>1</sub>F<sub>o</sub>-ATPase in *Escherichia coli*. *J. Biol. Chem.* 263(14), 6606-6612.
- CAIN, B. D. & SIMONI, R. D. (1989). Proton translocation by the F<sub>1</sub>F<sub>o</sub>-ATPase of *Escherichia coli*. Mutagenic analysis of the a subunit. *J. Biol. Chem.* 264(6), 3292-3300.
- DECKERS-HEBESTREIT, G., GREIE, J., STALZ, W. & ALTENDORF, K. (2000). The ATP synthase of *Escherichia coli*: structure and function of F<sub>o</sub> subunits. *Biochim. Biophys. Acta* 1458(2-3), 364-373.
- DIMROTH, P. (1982). The generation of an electrochemical gradient of sodium ions upon decarboxylation of oxaloacetate by the membrane-bound and Na<sup>+</sup>-activated oxaloacetate decarboxylase from *Klebsiella aerogenes*. *Eur. J. Biochem.* 121(2), 443-449.
- DMITRIEV, O. Y., ALTENDORF, K. & FILLINGAME, R. H. (1995). Reconstitution of the F<sub>o</sub> complex of *Escherichia coli* ATP synthase from isolated subunits. Varying the number of essential carboxylates by co-incorporation of wild-type and mutant subunit c after purification in organic solvent. *Eur. J. Biochem.* 233(2), 478-483.
- EYA, S., MAEDA, M. & FUTAI, M. (1991). Role of the carboxyl terminal region of H<sup>+</sup>-ATPase (F<sub>o</sub>F<sub>1</sub>) a subunit from *Escherichia coli*. *Arch. Biochem. Biophys.* 284(1), 71-77.
- GROTH, G. & POHL, E. (2001). The structure of the chloroplast F<sub>1</sub>-ATPase at 3.2 Å resolution. *J. Biol. Chem.* 276(2), 1345-1352.
- HORTON, R. M., CAI, Z. L., HO, S. N. & PEASE, L. R. (1990). Gene splicing by overlap extension: tailor-made genes using the polymerase chain reaction. *Biotechniques* 8(5), 528-535.
- JIANG, W. & FILLINGAME, R. H. (1998). Interacting helical faces of subunits a and c in the F<sub>1</sub>F<sub>o</sub> ATP synthase of *Escherichia coli* defined by disulfide cross-linking. *Proc. Natl. Acad. Sci. USA* 95(12), 6607-6612.
- KAIM, G. & DIMROTH, P. (1994). Construction, expression and characterization of a plasmid-encoded Na<sup>+</sup>-specific ATPase hybrid consisting of *Propionigenium modestum* F<sub>o</sub>-ATPase and *Escherichia coli* F<sub>1</sub>-ATPase. *Eur. J. Biochem.* 222(2), 615-623.
- LAUBINGER, W., DECKERS-HEBESTREIT, G., ALTENDORF, K. & DIMROTH, P. (1990). A hybrid adenosinetriphosphatase composed of F<sub>1</sub> of *Escherichia coli* and F<sub>o</sub> of *Propionigenium modestum* is a functional sodium ion pump. *Biochemistry* 29(23), 5458-5463.
- LIGHTOWLERS, R. N., HOWITT, S. M., HATCH, L., GIBSON, F. & COX, G. (1988). The proton pore in the *Escherichia coli* F<sub>o</sub>F<sub>1</sub>-ATPase: Substitution of glutamate by glutamine at position 219 of the alpha-subunit prevents F<sub>o</sub>-mediated proton permeability. *Biochim. Biophys. Acta* 933(2), 241-248.



- LIGHTOWLERS, R. N., HOWITT, S. M., HATCH, L., GIBSON, F. & COX, G. B. (1987). The proton pore in *Escherichia coli* F<sub>0</sub>F<sub>1</sub>-ATPase: A requirement of arginine at position 210 of the a-subunit. *Biochim. Biophys. Acta* 894(3), 399-406.
- MATTHEY, U., KAIM, G., BRAUN, D., WÜTHRICH, K. & DIMROTH, P. (1999). NMR studies of subunit c of the ATP synthase from *Propionigenium modestum* in dodecylsulfate micelles. *Eur. J. Biochem.* 261(2), 459-467.
- MATTHEY, U., KAIM, G. & DIMROTH, P. (1997). Subunit c from the sodium-ion-translocating F<sub>1</sub>F<sub>0</sub>-ATPase of *Propionigenium modestum*. Production, purification and properties of the protein in dodecylsulfate solution. *Eur. J. Biochem.* 247(3), 820-825.
- MIROUX, B. & WALKER, J. E. (1996). Over-production of proteins in *Escherichia coli*: mutant hosts that allow synthesis of some membrane proteins and globular proteins at high levels. *J. Mol. Biol.* 260(3), 289-298.
- NOJI, H., YASUDA, R., YOSHIDA, M. & KINOSITA, K. (1997). Direct observation of the rotation of F<sub>1</sub>-ATPase. *Nature* 386, 299-302.
- PÄNKE, O., GUMBIOWSKI, K., JUNGE, W. & ENGELBRECHT, S. (2000). F-ATPase: specific observation of the rotating c subunit oligomer of EF<sub>0</sub>EF<sub>1</sub>. *FEBS Lett.* 472(1), 34-38.
- SAMBONGI, Y., IKO, Y., TANABE, M., OMOTE, H., IWAMOTO-KIHARA, A., UEDA, I., YANAGIDA, T., WADA, Y. & FUTAI, M. (1999). Mechanical rotation of the c subunit oligomer in ATP synthase F<sub>1</sub>F<sub>0</sub>: direct observation. *Science* 286(5445), 1722-1724.
- SANGER, F., NICKLEN, S. & COULSON, A. R. (1977). DNA sequencing with chain-terminating inhibitors. *Proc. Natl. Acad. Sci. USA* 74(12), 5463-5467.
- SEELERT, H., POETSCH, A., DENCHER, N. A., ENGEL, A., STAHLBERG, H. & MÜLLER, D. J. (2000). Proton-powered turbine of a plant motor. *Nature* 405, 418-419.
- SINGH, S., TURINA, P., BUSTAMANTE, C. J., KELLER, D. J. & CAPALDI, R. (1996). Topographical structure of membrane-bound *Escherichia coli* F<sub>1</sub>F<sub>0</sub>ATP synthase in aqueous buffer. *FEBS Lett.* 397(1), 30-34.
- STAHLBERG, H., MÜLLER, D. J., SUDA, K., FOTIADIS, D., ENGEL, A., MEIER, T., MATTHEY, U. & DIMROTH, P. (2001). Bacterial Na<sup>+</sup>-ATP synthase has an undecameric rotor. *EMBO reports* 2(3), 229-233.
- STOCK, D., LESLIE, A. G. & WALKER, J. E. (1999). Molecular architecture of the rotary motor in ATP synthase. *Science* 286, 1700-1705.
- TAKEYASU, K., OMOTE, H., NETTIKADAN, S., TOKUMASU, F., IWAMOTU-KIHARA, A. & FUTAI, M. (1996). Molecular imaging of *Escherichia coli* F<sub>1</sub>F<sub>0</sub>-ATPase in reconstituted membranes using atomic force microscopy. *FEBS Lett.* 392(2), 110-113.
- VALIYAVEETIL, F. I. & FILLINGAME, R. H. (1997). On the role of Arg-210 and Glu-219 of subunit a in proton translocation by the *Escherichia coli* F<sub>0</sub>F<sub>1</sub>-ATP synthase. *J. Biol. Chem.* 272(51), 32635-32641.
- VON BALLMOOS, C., APPOLDT, Y., BRUNNER, J., GRANIER, T., VASELLA, A. & DIMROTH, P. (2002). Membrane topography of the coupling ion binding site in Na<sup>+</sup>-translocating F<sub>1</sub>F<sub>0</sub> ATP synthase. *J. Biol. Chem.* 277(5), 3504-3510.
- VONCK, J., KRUG VON NIDDA, T., MEIER, T., MATTHEY, U., MILLS, D. J., KÜHLBRANDT, W. & DIMROTH, P. (2002). Molecular architecture of the undecameric rotor of a bacterial Na<sup>+</sup>-ATP synthase. *J. Mol. Biol.* 321(2), 307-316.
- WEBER, J. & SENIOR, A. E. (1997). Catalytic mechanism of F<sub>1</sub>-ATPase. *Biochim. Biophys. Acta* 1319, 19-58.
- WEHRLE, F., APPOLDT, Y., KAIM, G. & DIMROTH, P. (2002). Reconstitution of F<sub>0</sub> of the ATP synthase of *Propionigenium modestum* from its heterologously expressed and purified subunits. *Eur. J. Biochem.* 269(10), 2567-2573.
- WEHRLE, F., KAIM, G. & DIMROTH, P. (2002). Molecular mechanism of the ATP synthase's F<sub>0</sub> motor probed by mutational analysis. *J. Mol. Biol.* 322(2), 369-381.

YOSHIDA, M., MUNYUKI, E. & HISABORI, T. (2001). ATP synthase - a marvellous rotary engine of the cell. *Nat. Rev. Mol. Cell Biol.* 2(9), 669-677.

## CHAPTER 5: GENERAL DISCUSSION

### 5.1 Rotary enzymes in biological membranes

Both, the bacterial flagellar motor and the F-type ATP synthase are membrane-bound macromolecular complexes coupling the movement of ions across the membrane to the revolution of the rotor part of the complex versus the stator part (Figure 1). Despite this similarity, the two devices are designed for different functions. The flagellar motor is responsible for the rotation of the flagellar filament in order to propel the cell, whereas the  $F_1F_0$  ATP synthase couples ion flux to ATP synthesis. Possible mechanisms for torque generation in both systems are discussed below. V-type ATPases are multisubunit complexes found in internal membranes of eukaryotic cells, the plasma membrane and the cytoplasmic membrane of bacteria. Although the overall structure of the V-type ATPase is similar to the F-type ATPase, this enzyme only operates in the ATP hydrolysis mode and therefore serves different objectives such as acidification of intracellular compartments, membrane energisation, and driving transport processes (Stevens & Forgac, 1997). The A-type ATPase is a further representative of ATP synthesising/hydrolysing enzymes and is found in archaea. It comprises a similar overall structure like F- and V-type ATPases and is able to synthesise or to hydrolyse ATP depending on the physiological conditions.

#### 5.1.1 Bacterial flagellar motor

Many species of bacteria move by means of reversibly rotating flagella, which share a common overall structure. A long helical filament, which is protruding from the outer membrane, is linked to a basal body *via* a flexible hook (Figure 1) (Macnab, 1996).

The basal body is anchored within the membrane and comprises five rings and a central rod connecting the basal body to the hook (Berg, 2000). The L ring (FlgH) is located in the outer (lipopolysaccharide) membrane and is linked by a cylindrical wall with the P ring (FlgI) in the peptidoglycan layer. The MS ring (FlfF) lies within the cytoplasmic membrane with FlfG bound to the cytoplasmic face of the M ring. The

innermost ring is termed C ring (FliM, FliN) and is also attached to the cytoplasmic face of the MS ring (Thomas *et al.*, 2001). It is presumed that the MS ring, the C ring and FliG are co-rotating together with the hook and the filament, whereas the P and L rings form a bearing for the rotating parts. However, the basal body does not work as a motor itself. Torque generating proteins are required for the function of the flagellar motor.

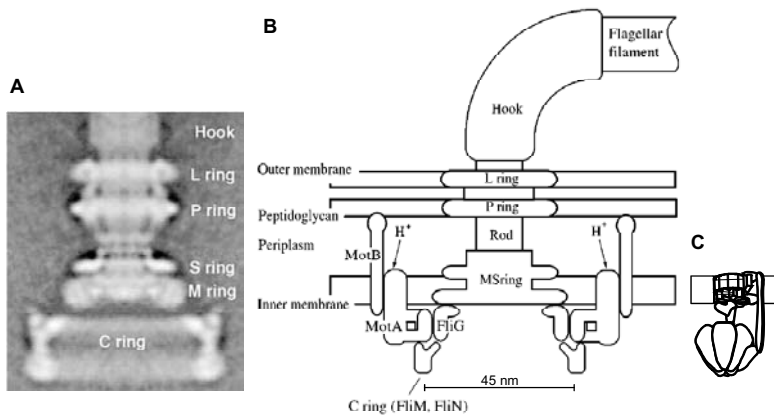


**Figure 1: A Electron micrograph of the basal body of a flagellum. B Structural model of a bacterial flagellum in a gram-negative membrane.** The basal body is composed of five rings, L, P, S, M, and C connected by a central rod. The P ring is located in the peptidoglycan layer and the L ring is in the outer membrane, the MS rings are embedded in the cytoplasmic membrane and the C ring is associated to the MS ring on the cytoplasmic side of the membrane. The Mot complexes are surrounding the MS ring and convert the proton motive force into rotary torque powering the flagellum. MotA and MotB form the torque generating unit together with FliG and are assumed to be the stator, whereas the rotor consists of FliG, the C ring and the MS ring, which is attached to the flagellar filament. **C Model of F<sub>1</sub>F<sub>0</sub>-ATPase** to show its relative to the bacterial flagellar motor.

MotA and MotB span the cytoplasmic membrane and are essential for motor rotation. The two components form a stator complex, which is able to translocate protons across the cytoplasmic membrane. It is suggested that several MotA/MotB complexes are arranged peripherally around the base of each flagellum. MotA is predicted to have four transmembrane helices with two short periplasmic loops and one large cytoplasmic loop (Dean *et al.*, 1984; Blair & Berg, 1991; Zhou *et al.*, 1995). MotB comprises a single N-terminal transmembrane segment and a large periplasmic

domain harbouring a peptidoglycan binding motif that could have an anchoring function of the stator elements (Stader *et al.*, 1986; Chun & Parkinson, 1988). Recent reports seem to indicate that the MotA/MotB complex consists of four copies of MotA and two copies of MotB (Sato & Homma, 2000).

In some bacteria the flagellar motors were found to be driven by an electrochemical  $\text{Na}^+$  potential (Hirota & Imae, 1983; Sugiyama *et al.*, 1985; Imae *et al.*, 1986; Imae & Atsumi, 1989). Two proteins were identified, which are essential for the  $\text{Na}^+$ -driven flagellar motor (Kojima *et al.*, 1999). PomA and PomB show homologies to the MotA/MotB complex and seem to function as the  $\text{Na}^+$  channel (Yorimitsu *et al.*, 1999). It is suggested that the force generating unit is composed of four copies of PomA and two copies of PomB (Sato & Homma, 2000). Sodium-dependent flagellar motors comprise two further proteins, MotX and MotY, which are essential for flagella rotation but not involved in ion translocation (Sato & Homma, 2000; Yorimitsu & Homma, 2001). No sequence similarities among MotA/MotB and MotX/MotY were found and the precise function of the two  $\text{Na}^+$  specific components is still uncertain. Taken together, these data suggest that the sodium-dependent flagellar motor is composed of four elements, PomA, PomB, MotX and MotY.

Three components, MotA, MotB and FliG are thought to be directly involved in torque generation of the  $\text{H}^+$ -driven flagellar motor. The stator elements MotA/MotB serve as force generating units and FliG serves as track element. Individual MotA/MotB complexes contribute independently to the generation of torque (Blair & Berg, 1988). In hypotheses about the mechanism of the flagellar motor, charged residues have been suggested to play key roles for the generation of torque. Mutational studies identified a number of important charged residues both in the rotor protein FliG and the stator protein MotA (Lloyd & Blair, 1997; Zhou *et al.*, 1997; Zhou *et al.*, 1998a). Single, charge-neutralising replacements had only mild effects on function, whereas double replacements or mutations that reverse charge caused more severe impairments. It is therefore assumed that essential electrostatic interactions occur between the rotor component FliG and the stator component MotA in order to propel the flagella. In addition, MotA harbours two important proline residues, which are assumed to be important for motor rotation, possibly by the regulation of conformational changes that couple proton translocation to rotor movement (Braun *et al.*, 1999). Furthermore, a highly conserved aspartate residue of MotB (Asp32 in

*E. coli*) has been found to be critical for the function of the flagellar motor (Zhou *et al.*, 1998b). Mutations of this carboxylate residue prevent motor rotation and proton translocation, and only the conservative replacement by a glutamate allowed marginal motility. It is suggested that Asp32 is directly involved in proton translocation.

The mechanism of coupling the transmembrane flux of protons to the rotation of a flagellum is not completely understood. Three models of the flagellar motor have been developed in recent years.

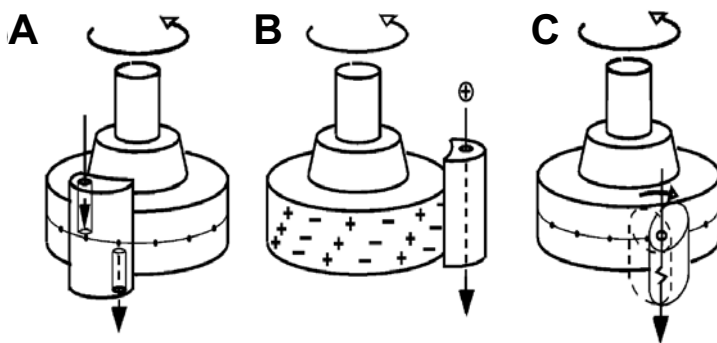


**Figure 2: Possible mechanisms for the flagellar motor.** **A** Two channel model. Ions access their binding sites on the rotor by a channel from the outside and are released by a second channel into the cytoplasm *via* turning the rotor. **B** Proton turbine model. The rotor carries tilted alternating rows of positive and negative charges. Protons pass through a channel in the stator (dashed line). Their interaction with the electric field generated by the rotor charges gives rise to torque. **C** Conformational change mechanism. The proton flux induces conformational changes in the MotA/MotB complex, which drive the rotation.

In a two-channel model (Figure 2A) protons bind from the periplasm to the rotor *via* a stator half channel, and are transferred by rotation of the rotor to a second half channel, which is connected to the cytoplasm. As long as the rotor is not protonated, it is not able to switch between the two half channels (Khan & Berg, 1983; Meister *et al.*, 1989). In this model, rotation and ion translocation are tightly coupled. The restrictions preventing uncoupled rotation are assumed to arise from electrostatic forces between the rotor and the stator charges. In Figure 2B a model is proposed, which suggests that the interaction between rotor and stator might be of electrostatic nature taking into account the high density of positive and negative rotor charges. The coupling is accomplished by tilted rows of positive and negative charges around the

rotor, which interact with the protons passing through the stator channel. The electrostatic interaction between a proton and the charges on the rotor is responsible for torque generation (Walz & Caplan, 2002). The most favoured model, so far, assumes that torque is generated by conformational changes in the MotA/MotB complex (Figure 2C). The binding of a proton to Asp32 of MotB causes a conformational change in the stator which alters the rotor/stator interface. This conformational change drives the rotor by electrostatic interaction between charged residues of MotA and FliG. To complete the cycle, the proton exits to the cytoplasm and the initial conformation is restored. Evidences sustaining these conformational changes were obtained by the susceptibility of wild-type and mutant MotA/MotB complexes to proteases (Kojima & Blair, 2001).

In contrast to the ATP synthases, the flagellar motor has to perform work in both directions of rotation at unidirectional ion flux. In the flagellum, FliG binds to FliM and FliN to form a switch complex that controls the direction of motor rotation upon CheY binding (Yamaguchi *et al.*, 1986). Switching between clockwise and counterclockwise rotation is believed to involve a conformational change in this complex, triggered by the binding of a phosphorylated CheY to FliM (Welch *et al.*, 1993).

### 5.1.2 V-type ATPases

V-type ATPases function as proton pumps that acidify various organelles and energise plasma membranes in eukaryotic cells and in bacteria (Wieczorek *et al.*, 1999; Nelson *et al.*, 2000). This acidification plays very important roles in many aspects of physiological functions, particularly membrane traffic processes (Forgac, 1989). Electron micrographs of V-type ATPases strongly resemble the organisation of F-ATPases. In both enzymes, a spherical headpiece is connected to a membrane intrinsic moiety *via* two stalks (Dschida & Bowman, 1992; Boekema *et al.*, 1997). V-type ATPases are multisubunit enzymes comprising a hydrophilic catalytic portion ( $V_1$ ) and a membrane-embedded portion ( $V_o$ ). Several subunits are related among F- and V-type ATPases, whereas five to six subunits share no obvious relationship in their amino acid sequence (Figure 3/Table 1). In both enzymes, energy transfer between ATP hydrolysis/synthesis and ion movement requires three catalytic sites in the catalytic moiety ( $V_1$  or  $F_1$ ) and a membrane-embedded portion that conducts the

ion flow ( $V_o$  or  $F_o$ ). Despite this structural similarity the two ATPases differ in many respects, particularly their function and regulation.

<i>Ms. mazei</i> Gö1 A <sub>1</sub> A <sub>0</sub>	<i>S. cerevisiae</i> V <sub>1</sub> V <sub>0</sub>	<i>E. coli</i> F <sub>1</sub> F <sub>0</sub>
A } B } C } D } E } F } A <sub>1</sub> subunits	Vma1p (A) } Vma2p (B) } V <sub>1</sub> subunits Vma6p (d) } Vma8p (D) } V <sub>0</sub> subunit Vma4p (E) } Vma7p (F) } Vma13p (H) } Vma5p (C) } V <sub>1</sub> subunits Vma10p (G) }	β } α } γ } δ } ε } F <sub>1</sub> subunits
H } G } structure? assembly?		b?
I } K } A <sub>0</sub> subunits	Vph1p/Stv1p (a) } Vma3p (c) } Vma11p (c') } Vma16p (c'') } V <sub>0</sub> subunits	a + b? } c } F <sub>0</sub> subunits

Table 1: Illustration of similar ATPase gene products of A-, V- and F-type ATPases.

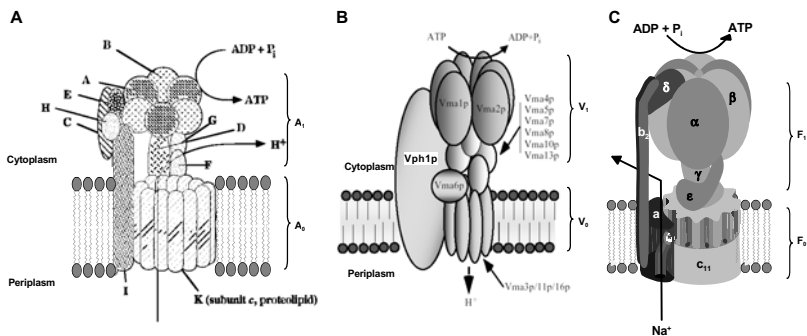


Figure 3: Comparison of the architecture of A-, V- and F-type ATPases. A A-type ATPase, B V-type ATPase and C F-type ATPase.

The peripheral V<sub>1</sub> domain, which is responsible for ATP hydrolysis, is composed of nine subunits (subunits A-H). The catalytic sites are located on the A subunit, whereas the nucleotide binding sites on subunit B are noncatalytic. The high  $\alpha$ -helical



content of subunits D and E suggests that one subunit might contribute to the central stalk, whereas subunits C, G, and H together with subunit d, are potential candidates to contribute to the peripheral stalk.

The  $V_o$  moiety contains five different subunits (a, d, c, c', and c''). Unlike the F-ATPases, the V-ATPases contain three different proteolipids (c, c', c''), which are similar to each other and show homologies to the c subunit from F-type ATPase (Mandel *et al.*, 1988; Hirata *et al.*, 1997). Subunits c as well as c' contain four putative transmembrane helices (TMH) with a critical acidic residue in TMH4, while subunit c'' harbours five transmembrane spans with an essential carboxyl group in TMH3 (Hirata *et al.*, 1997). The  $V_o$  domain comprises five to six copies of c/c' and a single copy of c'' (Arai *et al.*, 1988; Powell *et al.*, 2000). Figure 4 shows a putative arrangement of the three types of proteolipids in yeast V-type ATPase relative to subunit a. So far, there is no explanation for the requirement of different c subunits in  $V_1V_o$ -ATPases, but mutagenesis studies indicated that there must be at least one copy of each proteolipid subunit per V-ATPase complex (Hirata *et al.*, 1997) as cells lacking one of the genes for a proteolipid are defective in the assembly of V-ATPase. In addition it was demonstrated that non-functional mutants of one type of proteolipid produce an inactive but fully assembled complex. Immuno-blot analysis showed that Vma3p (c) is more abundant than the other two proteolipids, but, the actual stoichiometry of the assembly of the c-oligomer still needs to be determined (Hirata *et al.*, 1997). Thus, in contrast to the F-type c-oligomer, the c-ring of  $V_1V_o$ -ATPase is an asymmetric structure.

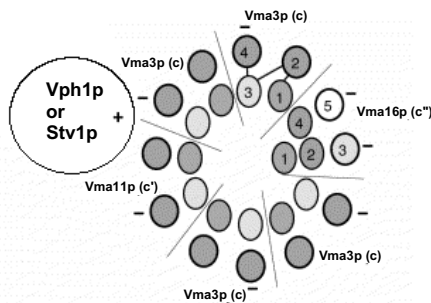


**Figure 4: Possible arrangements of the V-type ATPase c subunits in the membrane.** The various transmembrane segments are numbered and shaded in grey, the negatively charged residues within the transmembrane segments are marked. The 100 kDa subunit is associated laterally (Perzov *et al.*, 2001).

The a subunit (100 kDa) is a membrane protein harbouring a hydrophilic N-terminal domain and a hydrophobic, membrane-spanning C-terminal segment (Perin *et al.*, 1991; Manolson *et al.*, 1992; Manolson *et al.*, 1994). By the analysis of mutants of the yeast a subunit (Vph1p), several membrane-integral, charged residues were identified that were important for ion translocation (Leng *et al.*, 1996; Leng *et al.*, 1998). These data suggested that the role of the C-terminal part of V-type subunit a is homologous to the F-type subunit a (Figure 5), although no distinct sequence homology exists between the hydrophobic subunit a domain of the V-type ATPase and the F-type subunit a.

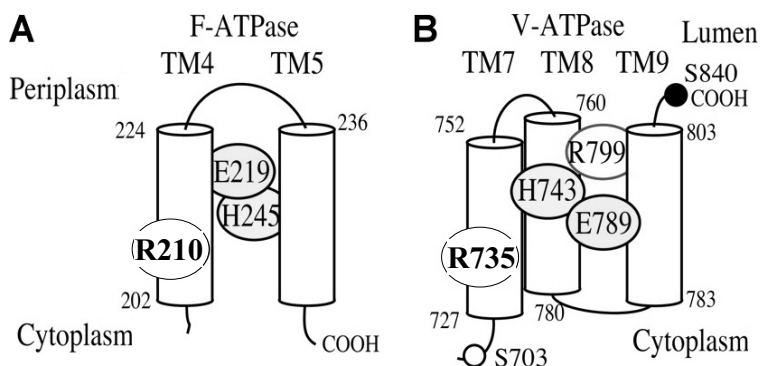


**Figure 5: Comparison of important residues on the C-terminal helices of subunit a from F<sub>1</sub>F<sub>o</sub>-ATPase and the yeast 100 kDa subunit from V<sub>1</sub>V<sub>o</sub>-ATPase.** The putative transmembrane helices are drawn as cylinders, with the bordering residue numbers indicated. **A** The two C-terminal helices of the *E. coli* subunit a are depicted. **B** Location of important residues in the C-terminal region of the yeast V-ATPase Vph1p subunit. The essential arginine residues are shaded in grey. Taken from (Kawasaki-Nishi *et al.*, 2001)

In all known a subunits from F-type ATPase there is a strictly conserved arginine residue. Mutagenesis studies showed that this residue is absolutely required for coupled ion translocation across the membrane (Cain & Simoni, 1989; Valiyaveetil & Fillingame, 1997). Although there is no obvious homology between the a subunits from F-type and V-type ATPases and different topologies were postulated for the two proteins (Jäger *et al.*, 1998; Long *et al.*, 1998; Leng *et al.*, 1999; Wada *et al.*, 1999), there are two conserved arginine residues in the C-terminal domain of the V-type subunit a. Among these, Arg735 (yeast V-type subunit a) was identified to be

essential for proton transport and even the conservative replacement with a lysine was only marginally active (Kawasaki-Nishi *et al.*, 2001). This phenotype is similar to the observations with the *E. coli* aArg210 (Cain & Simoni, 1989) and *P. modestum* aArg227 (Wehrle *et al.*, 2002).

The above data indicate that the mechanism of ATP hydrolysis is similar between F- and V-type ATPases. Accordingly, it was suggested that the energy of ATP hydrolysis in the catalytic A subunits is converted into torque, which drives the " $\gamma$ -like" subunit D (Murata *et al.*, 2001). It is unknown so far, how the rotation is coupled to ion translocation across the membrane. In the *E. coli* F-ATPase evidence exists that subunit  $\gamma$  rotates together with subunit  $\epsilon$  and the c-oligomer (Sambongi *et al.*, 1999; Pänke *et al.*, 2000). The c-oligomer together with subunit a accomplishes ion translocation (Dmitriev *et al.*, 1995; Kaim & Dimroth, 1998c). As the V-type subunit a is also suggested to be involved in ion translocation (Kawasaki-Nishi *et al.*, 2001), and the V-type c subunits are homologous to those of F-type ATPases, it could be speculated that a hexamer of V-type c subunits acts as a rotor and that ions are transported in a similar way as proposed for the F-type ATPase (Stevens & Forgac, 1997). Interestingly, the V-type ATPase comprises only half the number of protonatable sites as the F-type ATPase in the c-oligomer (Arai *et al.*, 1988), which directly affects the stoichiometry of translocated protons per ATP hydrolysed. Lowering the  $H^+$ /ATP ratio might enable ATP-driven  $H^+$ -pumping to generate greater electrochemical gradients. Thereby the protons are energised to a greater extent and could be pumped against a higher proton motive force (Perzov *et al.*, 2001). However, it was found that the  $H^+$ /ATP ratio was variable in V-ATPases and thus, ATP hydrolysis and ion translocation are not tightly coupled. This might be determined by a further regulatory element of the c-oligomer of V-type ATPases termed 'slippage'. During slip, ATP is hydrolysed at the catalytic sites without being coupled to  $H^+$  transport. A probable explanation for this change in the stoichiometry of pumped protons per hydrolysed ATP might be the limited production of proton motive force by the energy of ATP hydrolysis. This results in a decrease of the proton pumping rate with increasing internal pH, possibly to prevent overacidification of internal organella (Nelson *et al.*, 2000; Perzov *et al.*, 2001). The authors suggest that the distribution of ion binding sites in the proteolipids (one per hairpin in F-type ATPase and one per two hairpins in V-type ATPase, respectively) could be the determinant whether

slippage is generated or not. In V-type c subunits the distance between two negative charges is double the distance found in F-type c-oligomers. Perzov *et al.* (2001) postulate that in V-ATPases this longer spacing between the carboxylate residues might cause a flux of protons back to the cytoplasm when a positive potential is building up across the membrane.

### 5.1.3 A-type ATPases

Biochemical, immunological, and molecular characterisation revealed that the ATPase enzymes from archaea share structural features with the V-type ATPases and functional features with F-type ATPase (Figure 3) (Schäfer & Meyering-Vos, 1992). The archaeal  $A_1A_o$ -ATPase, like the F-type ATPase perform both, ATP synthesis and ATP hydrolysis (Wieczorek *et al.*, 2000). A-type ATPases comprise ten subunits with unknown stoichiometry (Table 1) and are like  $F_1F_o$  and  $V_1V_o$ -ATPase composed of a peripheral head and a membrane embedded base connected by two stalks. The dimensions of the domains and the entire complex are comparable to V- and F- type ATPases, but the subunit composition of each domain is still speculative. The only hydrophobic subunits in  $A_1A_o$ -ATPases are subunits I and K, which are likely to build  $A_o$ .

Archaeal I subunits have a high degree of sequence conservation compared to the 100 kDa subunit of  $V_1V_o$ -ATPases (Manolson *et al.*, 1992; Manolson *et al.*, 1994). They are composed of a hydrophobic and a hydrophilic domain that potentially correspond to subunits a and b from the  $F_1F_o$ -ATPase. Interestingly, the hydrophilic domain of the I subunit and subunit b share a considerable sequence identity of 20 % to 30 %, whereas the similarity between subunit a and the hydrophobic domain was below 20 % (Müller *et al.*, 1999). As the hydrophobic domain of the yeast Vph1p as well as subunit a from  $F_1F_o$ -ATPases are known to be involved in ion translocation (Deckers-Hebestreit & Altendorf, 1996; Leng *et al.*, 1996; Kaim & Dimroth, 1998b; Leng *et al.*, 1998) it is speculated that the hydrophobic, membrane spanning part of subunit I is participating in the ion translocation process, whereas the hydrophilic domain of subunit I could serve as part of the peripheral stalk. Subunit K from *Methanosarcina mazei* Gö1 is a proteolipid with two transmembrane helices and corresponds by size to subunit c from F-type ATPases. However, the size of the archaeal proteolipids is variable among species comprising two, four or six

transmembrane helices and a variable number of conserved ionisable groups per monomer. The larger proteolipid types were predicted from published genome sequences and could be verified by MALDI. Apparently, those proteolipids arose from gene duplication/triplication and subsequent fusion of the genes (Müller *et al.*, 1999). In analogy to  $F_1F_0$ -ATPase, the proteolipids are arranged as a ring. Recently, an oligomeric c-ring harbouring a mixture of 8 kDa and 16 kDa proteolipids was also detected in the  $F_1F_0$ -ATPase of *Acetobacterium woodii* (Müller *et al.*, 2001), and in addition genetically engineered *E. coli* c-rings containing duplicated proteolipids yielded functional ATP synthases (Jones & Fillingame, 1998). These findings suggest that the size of the proteolipid monomer is not the determinant, whether an enzyme complex is able to synthesise ATP or not. This could be rather determined by the number of carboxylate residues per c-oligomer participating in ion translocation. As mentioned above, in the four- and five-helix proteolipids of  $V_1V_0$ -ATPases only one carboxylate residue is found, whereas in A-type ATPases one carboxylate residue is found in the single and duplicated form of the proteolipids and two carboxylates per triplicated form (Müller *et al.*, 1999). In F-type ATPases every proteolipid contains a carboxylate residue, except that from *A. woodii*, which contains a mixture of two proteolipid types harbouring one hairpin and one carboxylate, and one type that comprising two hairpins that contain one carboxylate (Müller *et al.*, 2001).

From the overall similarity it was concluded that the  $A_1A_0$ -ATPase is a rotary enzyme like the  $F_1F_0$ -ATPase. Since the membrane domain of the A-type ATPase is composed of two subunits only, it is assumed that subunit K rotates relative to subunit I (Müller *et al.*, 1999).

## 5.2 Coupling mechanism of the $F_1F_0$ -ATPases

The above described ATPases are thought to operate in a similar way as the  $F_1F_0$ -ATPase. The similarities in the overall structure and the sequence homologies suggest a common ancestor of these ATPases (Gogarten *et al.*, 1992). Despite these structural similarities, one open question remains: how are the catalytic processes coupled to ion translocation in V-type and A-type ATPases? Interestingly, there is experimental evidence for rotational coupling in the F-type ATPase (Noji *et al.*, 1997; Sambongi *et al.*, 1999; Pänke *et al.*, 2000; Tanabe *et al.*, 2001) and different models for ion translocation and torque generation in  $F_0$  were proposed so far.

### 5.2.1 Coupling models of $F_1F_0$ -ATPases

#### Two channel model

For the proton translocation through  $F_0$  of *E. coli* a model was suggested (Vik & Antonio, 1994; Junge *et al.*, 1997) comprising the following properties. (i) Subunit a is part of the stator and contains two half channels, each in contact with a different side of the membrane. (ii) A ring-like oligomer of c subunits constitutes the rotor part and harbours an ion binding site in the core of the membrane (Figure 6A).

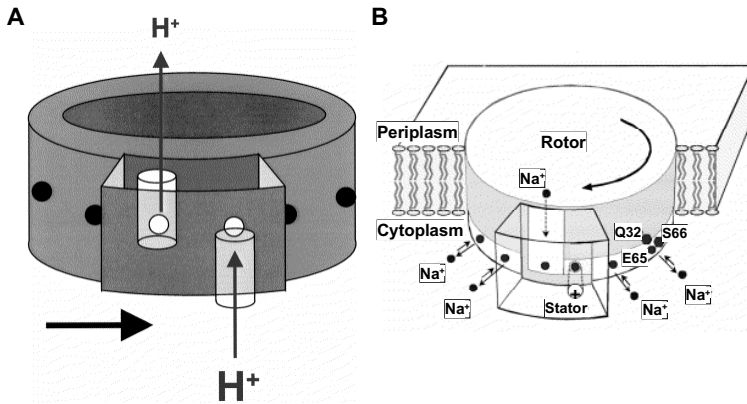


**Figure 6: A Schematic cartoon of the two-channel model.** A rotating ring of c subunits transports the protons from one half channel in subunit a facing the cytoplasm to the other half channel in subunit a facing the periplasm. In this model, all c subunits entering the lipid phase are occupied by a proton (black circles) and all c subunits in contact with subunit a are empty (white circles). The direction of the rotation is driven by the pH gradient. **B One-channel model for torque generation by the  $F_0$  motor from *P. modestum*.** The rotor contains 11  $Na^+$  binding sites near the cytoplasmic membrane surface. The stator contains an aqueous channel that conducts ions from the periplasmic reservoir to the level of the rotor sites. This channel is laterally connected with the cytoplasm by a hydrophilic strip. The positive stator charge (aArg227) prevents leakage of ions along this strip to the cytoplasm. Rotation during ATP synthesis is to the left.  $Na^+$  ions from the periplasm can only exit to the cytoplasm having bound to a rotor site and passing through the dielectric barrier forming the left wall of the channel. If the occupied rotor site moves to the right, it loses its ion back to the channel when it approaches the positive stator charge.

All c subunit binding sites are occupied with protons, except those c subunits, which are in contact with subunit a. In order to cross the membrane, a proton enters one half channel on subunit a, moves to the centre of the membrane and binds to the carboxyl

group of a c subunit. It is then carried to the second half channel on subunit a by a complete turn of the rotor and is released to the other side of the membrane. During ion translocation, it is presumed that  $F_o$  operates as a stochastically driven motor and the direction of the c-oligomer rotation is entirely determined by the orientation of the proton gradient. This gradient enforces the occupation of c subunits with protons *via* the subunit a half channel facing the membrane side of high proton concentration, whereas the dissociation of protons is favoured to the side of the membrane with low proton potential. According to this model, unoccupied c subunits bearing a negative charge are repelled from entering the lipid phase and thus, all c subunits must be occupied with a proton while passing from one subunit a channel to the other.

### One channel model

A different model regarding ion translocation through the  $F_o$  part was described for the  $Na^+$ -translocating ATPase from *P. modestum* (Figure 6B) (Dimroth *et al.*, 1999). The counter-rotating assembly of the  $F_o$  motor is composed of the rotor, consisting of the c-ring, and the stator subunit a. The c-oligomer contains 11  $Na^+$  binding sites near the cytoplasmic membrane surface having direct access to the cytoplasmic reservoir. Subunit a harbours an aqueous blind channel conducting ions from the periplasm to the level of the  $Na^+$  binding sites of the c-ring. The direction of rotation is determined by asymmetric features of the a subunit. (i) A hydrophilic strip connects the subunit a channel laterally with the cytoplasmic reservoir and allows unoccupied, charged rotor sites to enter the rotor-stator interface. Leakage of ions along this strip is prevented by the positive stator charge (aArg227). (ii) The stator channel admits  $Na^+$  from the periplasm, but these ions can only exit to the cytoplasm by boarding a rotor site and passing through the dielectric barrier forming the left wall of the channel. In contrast to the stochastic one-channel model, in this model the membrane potential plays an important role in torque generation. Basically, the rotor turns within a limited angle driven by the Brownian motion. A negatively charged rotor site entering the hydrophilic strip is attracted by the positive stator charge and the membrane potential biases the thermal escape of the rotor site from aArg227 towards the stator channel. Thus, the membrane potential imposes a directed rotation to the basically stochastic Brownian motion, which would allow rotation with equal probability to either side.

### 1a+11-channel model

Based on the experimental data supporting the one-channel model (Kaim & Dimroth, 1998b; Kaim & Dimroth, 1998c; Kaim & Dimroth, 1998a) and a more recent structure of the *I. tartaricus* oligomer together with crosslinking data (von Ballmoos *et al.*, 2002) a revised two-channel model was postulated (Vonck *et al.*, 2002). In this model, the sodium binding site is located within the core of the membrane. As in the one-channel model, access from the periplasmic surface to cGlu65 would be accomplished by a subunit a half channel. From the cytoplasmic side, the binding sites in the middle of the membrane are accessible *via* half channels on the c subunit ring. These half channels are lined with polar and charged residues that allow direct accessibility for the sodium ions. Ion translocation would then take place essentially as described in the one-channel model.

### 5.2.2 *In vitro* re-assembled ATPase offers a powerful tool to investigate mutants of *P. modestum* ATPase

The sodium translocating ATPase of *P. modestum* offers favourable possibilities to investigate the ion translocation mechanism of F<sub>1</sub>F<sub>o</sub>-ATPases: (i) in contrast to the H<sup>+</sup> concentration, the Na<sup>+</sup> concentration can be varied over a broad range without severe damage of the enzyme, and (ii) the path of Na<sup>+</sup> ions through F<sub>o</sub> across the membrane can easily be traced and quantitatively measured by using the radioactive isotope <sup>22</sup>Na<sup>+</sup>. Since the hybrid ATPase from *E. coli* PEF42 harbouring F<sub>o</sub> and subunit  $\delta$  from *P. modestum* and the remaining F<sub>1</sub> subunits from *E. coli* (Kaim & Dimroth, 1993) could not be purified to homogeneity, individual F<sub>o</sub> subunits from *P. modestum* were expressed in *E. coli* and purified. An *in vitro* system was established allowing the reconstitution of a functional F<sub>o</sub> part from individual subunits a, b, and c. This new reconstitution procedure enabled us to study the properties of F<sub>o</sub> complexes containing mixtures of mutant and wild-type subunits. Furthermore, amino acid residues that are considered to be essential for ion translocation and do not allow growth of the mutant strains, can be examined thoroughly by this approach.



### 5.3 Role of the positive stator charge in the coupling process of $F_1F_0$ -ATPase

In recent models of torque generation in  $F_1F_0$  ATP synthases, a key role was ascribed to a highly conserved arginine residue on subunit a (Elston *et al.*, 1998; Dimroth *et al.*, 1999; Oster *et al.*, 2000). In *E. coli*, this key residue was identified to be aArg210 (Cain & Simoni, 1986; Lightowers *et al.*, 1987; Cain & Simoni, 1989; Valiyaveetil & Fillingame, 1997), and the corresponding residue in *P. modestum* is aArg227 (Kaim & Dimroth, 1998b). In the preceding chapters, several point mutations of *P. modestum* subunit a were designed and constructed in order to obtain a more detailed understanding of the ion translocation mechanism. These mutants strongly confirm the functional importance of aArg227. Mutant aArg227Ala was of particular importance as it was unidirectionally uncoupled. The enzyme containing an alanine at position 227 was able to synthesise ATP, whereas ATP hydrolysis was not coupled to sodium translocation.

The data obtained by the characterisation of wild-type ATPase and ATPase harbouring mutant aArg227Ala allow us to draw a more concise model of the participation of the positive stator charge in the ion translocation process. We discuss the mechanism of ATP synthesis and ATP hydrolysis (Figure 7) on the basis of the model suggested by Dimroth *et al.* (1999).

#### 5.3.1 ATP synthesis

During ATP synthesis, torque must be generated by the  $F_0$  portion (Figure 7A). To achieve this, the sodium ions enter a channel in subunit a and pass through until they attain their binding sites on the c-oligomer within the core of the membrane (Dimroth *et al.*, 1999; von Ballmoos *et al.*, 2002). Leakage of  $Na^+$  ions towards the cytoplasm is prevented by the positive charge of aArg227. This positively charged site attracts negatively charged, empty rotor sites (cGlu65) into the rotor-stator interface. The membrane potential facilitates the escape of the rotor site from the electrostatic attraction of the positive stator charge towards the periplasmic channel. There, this rotor site picks up a sodium ion from the periplasm. The occupied c subunit is now able to pass the hydrophobic barrier on the left side of the rotor-stator interface, and the sodium ion gains access to the cytoplasm.

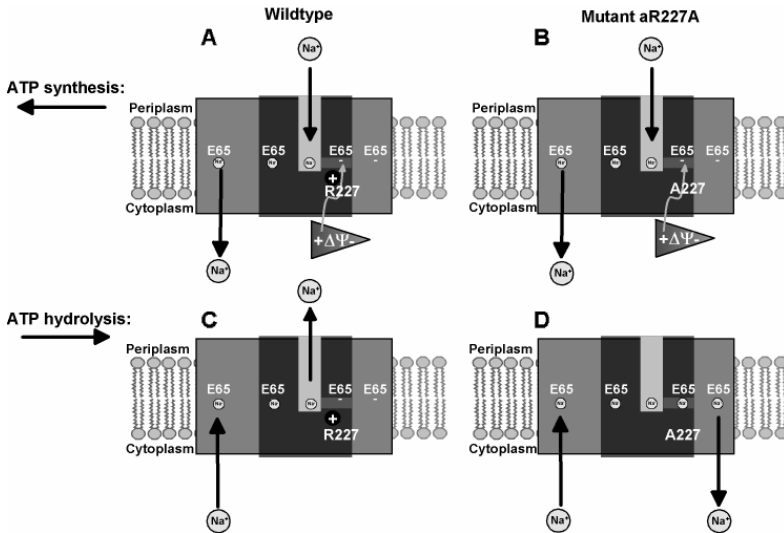


**Figure 7: Schematic model of the interactions between the stator subunit a (dark grey) and the c-oligomer (light grey) during ATP synthesis (A/B) or ATP hydrolysis (C/D).** The stator is equipped with an aqueous channel that connects the sodium binding sites on subunit c, which are freely accessible from the cytoplasm, to the periplasm. **A** During ATP synthesis rotation is to the left and the  $\text{Na}^+$  binding sites are occupied from the periplasm. The positive charge of aR227 prevents leakage of sodium ions through the hydrophilic strip and attracts negatively charged rotor sites into the rotor/stator interface, from where the membrane potential ( $\Delta\Psi$ ) facilitates the thermal escape of cGlu65 into the stator channel. After having bound a  $\text{Na}^+$  from the channel the occupied subunit c can pass the hydrophobic barrier forming the left wall of the channel and the sodium ion is released into the cytoplasm. **B** ATP synthesis in mutant aArg227Ala is similar as described for the wild-type. The membrane potential still attracts the rotor sites toward the subunit a channel, where the sodium ions can bind and pass to the cytoplasmic side of the membrane. However, a constraint of this model is the requirement of empty rotor sites entering the rotor/stator interface in order to be attracted by the membrane potential that is necessary for torque generation. This demand is only fulfilled at low cytoplasmic  $\text{Na}^+$  concentration allowing the dissociation of the sodium ions without the help of the positive stator charge. In the wild-type enzyme ATP synthesis is not affected by increasing internal sodium concentrations as the positive charge of aArg227 facilitates the dissociation of  $\text{Na}^+$ . **C** Rotation driven by ATP hydrolysis is to the right. Sodium ions enter the rotor/stator interface from the left after boarding a rotor site. After the  $\text{Na}^+$ -bound site has reached the subunit a channel, the  $\text{Na}^+$  dissociates facilitated by the positively charged aArg227 into the channel and passes to the periplasmic side of the membrane. **D** ATP hydrolysis in mutant aArg227Ala is uncoupled. Since in the mutant no positive charge is present in the hydrophilic strip,  $\text{Na}^+$  ions do not dissociate into the subunit a channel and remain bound to the rotor, thereby passing through the hydrophilic strip back to the cytoplasm.

With this model in mind we discuss mutant aArg227Ala, with the important positive charge missing (Figure 7B). During ATP synthesis the sodium ions are translocated from the periplasm to the cytoplasm essentially as in the wild-type. This works well as long as the cytoplasmic sodium concentration is low and the Na<sup>+</sup> ions can dissociate from their binding sites into the cytoplasm. With increasing sodium concentrations in the cytoplasm, the c subunits entering the rotor-stator interface are increasingly occupied. In this situation, the rotor site is no longer electrostatically attracted by the membrane potential, torque is not generated and ATP synthesis is not catalysed. In the wild-type enzyme, however, ATP synthesis is not affected by the internal sodium concentration due to the fact that sodium ions bound to the rotor, which enter the rotor-stator interface, dissociate when they approach the positive aArg227 residue.

### 5.3.2 ATP hydrolysis

*Vice versa*, torque at F<sub>1</sub> is generated by ATP hydrolysis and the rotor turns in the opposite direction. The sodium ions enter the channel from the left side through the hydrophobic barrier in subunit a bound to the c-ring (Figure 7C). Once there, aArg227 lowers the binding affinity of the rotor sites, and the sodium ions dissociate into the channel. If the positive stator charge is missing (as in mutant aArg227Ala) the Na<sup>+</sup> ions remain on their binding sites, pass the rotor-stator interface and diffuse back to the cytoplasm (Figure 7D). This model accounts for the observed phenotype of the alanine mutant, which is able to synthesise ATP at low sodium concentrations at the cytoplasmic side of the enzyme and shows an ATP hydrolysing activity that is uncoupled from ion translocation. The model is also in agreement with the growth phenotype of the *E. coli* aArg210Ala mutant. The mutant was reported to lack growth on succinate as sole carbon source (Valiyaveetil & Fillingame, 1997). This seems to be contradictory to our ATP synthesis data. However, taken into consideration that the dissociation of sodium ions from the c-ring is lowered with increasing sodium concentrations the result from growth experiments with *E. coli* fits nicely. Since *E. coli* possesses a proton pumping ATP synthase, it can be assumed that the concentration of H<sup>+</sup> in the cytoplasm is above the critical concentration where ATP synthesis is permitted.

## 5.4 Outlook

During many years much effort was performed to investigate the  $F_1F_0$  ATP synthases from various organisms. Detailed knowledge about structure and mechanism is available for the catalytic  $F_1$  portion. Extensive biochemical studies deliver insights into the ion transport processes in  $F_0$ , but structural details of the  $F_0$  complex are rare. Recently the stoichiometry of the c-oligomer of *I. tartaricus* was determined and an electron crystallographic model from 2-D crystals was calculated. Despite this progress, a lot of open questions remain. One of these involves the location of the ion channel in subunit a. This could be investigated by testing the accessibility of genetically engineered cysteine residues for thiol specific reagents. The expression and reconstitution procedure presented in the preceding chapters would provide a suitable tool to perform site directed mutagenesis as well as to determine the amino acids that are exposed to the channel. Furthermore, to understand the ion translocation process through  $F_0$ , the knowledge of the structural organisation of subunit a is a prerequisite. To realise these kind of structural investigations, efforts should be promoted to obtain an expression system that allows higher yield of the recombinant a subunit and to purify subunit a to homogeneity. With this purified subunit a or with the  $F_0$  complex 2-D and 3-D crystallisation trials can be undertaken. The structural data received from 2-D or 3-D crystals would provide a tremendous amount of detailed knowledge, and in combination with the information already available would allow creating a fairly complete model of the structure and function of the  $F_1F_0$ -ATPase.

## 5.5 References

- ARAI, H., TERRES, G., PINK, S. & FORGAC, M. (1988). Topography and subunit stoichiometry of the coated vesicle proton pump. *J. Biol. Chem.* 263(18), 8796-8802.
- BERG, H. C. (2000). Constraints on models for the flagellar rotary motor. *Phil. Trans. R. Soc. Lond. B.* 355(1396), 491-501.
- BLAIR, D. F. & BERG, H. C. (1988). Restoration of torque in defective flagellar motors. *Science* 242(4886), 1678-1681.
- BLAIR, D. F. & BERG, H. C. (1991). Mutations in the MotA protein of *Escherichia coli* reveal domains critical for proton conduction. *J. Mol. Biol.* 221(4), 1433-1442.
- BOEKEMA, E. J. UBBINK-KOK T., Lolkema J. S., BRISSON A. & KONINGS WN (1997). Visualization of a peripheral stalk in V-type ATPase: evidence for the stator structure essential to rotational catalysis. *Proc. Natl. Acad. Sci. USA* 94(26), 14291-14293.

- BRAUN, T. F., POULSON, S., GULLY, J. B., EMPEY, J. C., VAN WAY, S., PUTNAM, A. & BLAIR, D. F. (1999). Function of proline residues of MotA in torque generation by the flagellar motor of *Escherichia coli*. *J. Bacteriol.* 181(11), 3542-3551.
- CAIN, B. D. & SIMONI, R. D. (1986). Impaired proton conductivity resulting from mutations in the a subunit of F<sub>1</sub>F<sub>o</sub>-ATPase in *Escherichia coli*. *J. Biol. Chem.* 261(22), 10043-10050.
- CAIN, B. D. & SIMONI, R. D. (1989). Proton translocation by the F<sub>1</sub>F<sub>o</sub>-ATPase of *Escherichia coli*. Mutagenic analysis of the a subunit. *J. Biol. Chem.* 264(6), 3292-3300.
- CHUN, S. Y. & PARKINSON, J. S. (1988). Bacterial motility: membrane topology of the *Escherichia coli* MotB protein. *Science* 239(4837), 276-278.
- DEAN, G. E., MACNAB, R. M., STADER, J., MATSUMURA, P. & BURKS, C. (1984). Gene sequence and predicted amino acid sequence of the MotA protein, a membrane-associated protein required for flagellar rotation in *Escherichia coli*. *J. Bacteriol.* 159(3), 991-999.
- DECKERS-HEBESTREIT, G. & ALTENDORF, K. (1996). The F<sub>o</sub>F<sub>1</sub>-type ATP synthase of bacteria: Structure and function of the F<sub>o</sub> complex. *Annu. Rev. Microbiol.* 50, 791-824.
- DIMROTH, P., WANG, H., GRABE, M. & OSTER, G. (1999). Energy transduction in the sodium F-ATPase of *Propionigenium modestum*. *Proc. Natl. Acad. Sci. USA* 96(9), 4924-4929.
- DMITRIEV, O. Y., ALTENDORF, K. & FILLINGAME, R. H. (1995). Reconstitution of the F<sub>o</sub> complex of *Escherichia coli* ATP synthase from isolated subunits. Varying the number of essential carboxylates by co-incorporation of wild-type and mutant subunit c after purification in organic solvent. *Eur. J. Biochem.* 233(2), 478-483.
- DSCHIDA, W. J. & BOWMAN B. J. (1992). Structure of the vacuolar ATPase from *Neurospora crassa* as determined by electron microscopy. *J. Biol. Chem.* 267(26), 18783-18789.
- ELSTON, T., WANG, H. & OSTER, G. (1998). Energy transduction in ATP synthase. *Nature* 391, 510-513.
- FORGAC, M. (1989). Structure and function of vacuolar class of ATP-driven proton pumps. *Physiol. Rev.* 69(3), 765-796.
- GOGARTEN, J. P., STARKE T., KIBAK H., FISHMAN J. & TAIZ L. (1992). Evolution and isoforms of V-ATPase subunits. *J. Exp. Biol.* 172, 137-147.
- HIRATA, R., GRAHAM, L. A., TAKATSUKI, A., STEVENS, T. H. & ANRAKU, Y. (1997). *VMA11* and *VMA16* encode second and third proteolipid subunits of the *Saccharomyces cerevisiae* vacuolar membrane H<sup>+</sup>-ATPase. *J. Biol. Chem.* 272(8), 4795-4803.
- HIROTA, N. & IMAE, Y. (1983). Na<sup>+</sup>-driven flagellar motors of an alkaliphilic *Bacillus strain YN-1*. *J. Biol. Chem.* 258(17), 10577-10581.
- IMAE, Y. & ATSUMI, T. (1989). Na<sup>+</sup>-driven bacterial flagellar motors. *J. Bioenerg. Biomembr.* 21(6), 705-716.
- IMAE, Y., MATSUKURA, H. & KOBAYASI, S. (1986). Sodium-driven flagellar motors of alkaliphilic *Bacillus*. *Methods Enzymol.* 125, 582-592.
- JÄGER, H., BIRKENHÄGER, R., STALZ, W.-D., ALTENDORF, K. & DECKERS-HEBESTREIT, G. (1998). Topology of subunit a of the *Escherichia coli* ATP synthase. *Eur. J. Biochem.* 251(1-2), 122-132.
- JONES, P. C. & FILLINGAME, R. H. (1998). Genetic fusions of subunit c in the F<sub>o</sub> sector of the H<sup>+</sup>-transporting ATP synthase. Functional dimers and trimers and determination of stoichiometry by crosslinking analysis. *J. Biol. Chem.* 273(45), 29701-29705.
- JUNGE, W., LILL, H. & ENGELBRECHT, S. (1997). ATP synthase: An electrochemical transducer with rotary mechanics. *Trends Biochem. Sci.* 22(11), 420-423.
- KAIM, G. & DIMROTH, P. (1993). Formation of a functionally active sodium-translocating hybrid F<sub>1</sub>F<sub>o</sub>-ATPase in *Escherichia coli* by homologous recombination. *Eur. J. Biochem.* 218(3), 937-944.
- KAIM, G. & DIMROTH, P. (1998a). ATP synthesis by the F<sub>1</sub>F<sub>o</sub> ATP synthase of *Escherichia coli* is obligatorily dependent on the electric potential. *FEBS Lett.* 434(1-2), 57-60.

- KAIM, G. & DIMROTH, P. (1998b). A triple mutation in the a subunit of the *Escherichia coli*/*Propionigenium modestum* F<sub>1</sub>F<sub>0</sub>-ATPase hybrid causes a switch from Na<sup>+</sup> stimulation to Na<sup>+</sup> inhibition. *Biochemistry* 37(13), 4626-4634.
- KAIM, G. & DIMROTH, P. (1998c). Voltage-generated torque drives the motor of the ATP synthase. *EMBO J.* 17(20), 5887-5895.
- KAWASAKI-NISHII, S., NISHII, T. & FORGAC, M. (2001). Arg-735 of the 100-kDa subunit a of the yeast V-ATPase is essential for proton translocation. *Proc. Natl. Acad. Sci. USA* 98(22), 12397-12402.
- KHAN, S. & BERG, H. C. (1983). Isotope and thermal effects in chemiosmotic coupling to the flagellar motor of *Streptococcus*. *Cell* 32(3), 913-919.
- KOJIMA, S. & BLAIR, D. F. (2001). Conformational change in the stator of the bacterial flagellar motor. *Biochemistry* 40(43), 13041-13050.
- KOJIMA, S., KURODA, M., KAWAGISHI, I. & HOMMA, M. (1999). Random mutagenesis of the *pomA* gene encoding a putative channel component of the Na<sup>+</sup>-driven polar flagellar motor of *Vibrio alginolyticus*. *Microbiology* 145(7), 1759-1767.
- LENG, X. H., NISHII, T. & FORGAC, M. (1999). Transmembrane topography of the 100-kDa subunit (Vph1p) of the yeast vacuolar proton-translocating ATPase. *J. Biol. Chem.* 274(21), 14655-14661.
- LENG, X. H., MANOLSON, M. F. & FORGAC, M. (1998). Function of the COOH-terminal domain of Vph1p in activity and assembly of the yeast V-ATPase. *J. Biol. Chem.* 273(12), 6717-6723.
- LENG, X. H., MANOLSON, M. F., LIU, Q. & FORGAC, M. (1996). Site-directed mutagenesis of the 100-kDa subunit (Vph1p) of the yeast vacuolar H<sup>+</sup>-ATPase. *J. Biol. Chem.* 271(37), 22487-22493.
- LIGHTOWLERS, R. N., HOWITT, S. M., HATCH, L., GIBSON, F. & COX, G. B. (1987). The proton pore in *Escherichia coli* F<sub>0</sub>F<sub>1</sub>-ATPase: A requirement of arginine at position 210 of the a-subunit. *Biochim. Biophys. Acta* 894(3), 399-406.
- LLOYD, S. A. & BLAIR, D. F. (1997). Charged residues of the rotor protein FliG essential for torque generation in the flagellar motor of *Escherichia coli*. *J. Mol. Biol.* 266(4), 733-744.
- LONG, J. C., WANG, S. & VIK, S. B. (1998). Membrane topology of subunit a of the F<sub>1</sub>F<sub>0</sub> ATP synthase as determined by labelling of unique cysteine residues. *J. Biol. Chem.* 273(26), 16235-16240.
- MACNAB, R. M. (1996). *Flagella and motility. Cellular and molecular biology.* ASM Press, Washington, D.C., Washington, D.C.
- MANDEL, M., MORIYAMA, Y., HULMES, J. D., PAN, Y. C., NELSON, H. & NELSON, N. (1988). cDNA sequence encoding the 16-kDa proteolipid of chromaffin granules implies gene duplication in the evolution of H<sup>+</sup>-ATPases. *Proc. Natl. Acad. Sci. USA* 85(15), 5521-5524.
- MANOLSON, M. F., PROTEAU, D., PRESTON, R. A., STENBIT, A., ROBERTS, B. T., HOYT, M. A., PREUSS, D., MULHOLLAND, J., BOTSTEIN, D. & JONES, E. W. (1992). The VPH1 gene encodes a 95-kDa integral membrane polypeptide required for *in vivo* assembly and activity of the yeast vacuolar H<sup>+</sup>-ATPase. *J. Biol. Chem.* 267(20), 14294-14303.
- MANOLSON, M. F., WU, B., PROTEAU, D., TAILLON, B. E., ROBERTS, B. T., HOYT, M. A. & JONES, E. W. (1994). STV1 gene encodes functional homologue of 95-kDa yeast vacuolar H<sup>+</sup>-ATPase subunit Vph1p. *J. Biol. Chem.* 269(19), 14064-14074.
- MEISTER, M., CAPLAN, S. R. & BERG, H. C. (1989). Dynamics of a tightly coupled mechanism for flagellar rotation. Bacterial motility, chemiosmotic coupling, protonmotive force. *Biophys. J.* 55(5), 905-914.
- MÜLLER, V., AUFURTH, S. & RAHLFS, S. (2001). The Na<sup>+</sup> cycle in *Acetobacterium woodii*: identification and characterization of a Na<sup>+</sup>-translocating F<sub>1</sub>F<sub>0</sub>-ATPase with a mixed oligomer of 8 and 16 kDa proteolipids. *Biochim. Biophys. Acta* 1505(1), 108-120.
- MÜLLER, V., RUPPERT, C. & LEMKER, T. (1999). Structure and function of the A<sub>1</sub>A<sub>0</sub>-ATPases from methanogenic Archaea. *J. Bioenerg. Biomembr.* 31(1), 15-27.

- MURATA, T., KAWANO, M., IGARASHI, K., YAMATO, I. & KAKINUMA, Y. (2001). Catalytic properties of Na<sup>+</sup>-translocating V-ATPase in *Enterococcus hirae*. *Biochim. Biophys. Acta* 1505(1), 75-81.
- NELSON, N., PERZOV, N., COHEN, A., HAGAI, K., PADLER, V. & NELSON, H. (2000). The cellular biology of proton-motive force generation by V-ATPases. *J. Exp. Biol.* 203(1), 89-95.
- NOJI, H., YASUDA, R., YOSHIDA, M. & KINOSITA, K. (1997). Direct observation of the rotation of F<sub>1</sub>-ATPase. *Nature* 386, 299-302.
- OSTER, G., WANG, H. & GRABE, M. (2000). How F<sub>o</sub>-ATPase generates rotary torque. *Philos. Trans. R. Soc. Lond.* 355(1396), 523-528.
- PÄNKE, O., GUMBIOWSKI, K., JUNGE, W. & ENGELBRECHT, S. (2000). F-ATPase: specific observation of the rotating c subunit oligomer of EF<sub>0</sub>EF<sub>1</sub>. *FEBS Lett.* 472(1), 34-38.
- PERIN, M. S., FRIED, V. A., STONE, D. K., XIE, X. S. & SUDHOF, T. C. (1991). Structure of the 116-kDa polypeptide of the clathrin-coated vesicle/synaptic vesicle proton pump. *J. Biol. Chem.* 266(6), 3877-3881.
- PERZOV, N., PADLER-KARAVANI, V., NELSON, H. & NELSON, N. (2001). Features of V-ATPases that distinguish them from F-ATPases. *FEBS Lett.* 504(3), 223-228.
- POWELL, B., GRAHAM, L. A. & STEVENS, T. H. (2000). Molecular characterization of the yeast vacuolar H<sup>+</sup>-ATPase proton pore. *J. Biol. Chem.* 275(31), 23654-23660.
- SAMBONGI, Y., IKO, Y., TANABE, M., OMOTE, H., IWAMOTO-KIHARA, A., UEDA, I., YANAGIDA, T., WADA, Y. & FUTAI, M. (1999). Mechanical rotation of the c subunit oligomer in ATP synthase F<sub>1</sub>F<sub>o</sub>: direct observation. *Science* 286(5445), 1722-1724.
- SATO, K. & HOMMA, M. (2000). Multimeric structure of PomA, a component of the Na<sup>+</sup>-driven polar flagellar motor of *Vibrio alginolyticus*. *J. Biol. Chem.* 275(26), 20223-20228.
- SCHÄFER, G. & MEYERING-VOS, M. (1992). F-type or V-type? The chimeric nature of the archaeobacterial ATP synthase. *Biochim. Biophys. Acta* 1101(2), 232-235.
- STADER, J., MATSUMURA, P., VACANTE, D., DEAN, G. E. & MACNAB, R. M. (1986). Nucleotide sequence of the *Escherichia coli* *motB* gene and site-limited incorporation of its product into the cytoplasmic membrane. *J. Bacteriol.* 166(1), 244-252.
- STEVENS, T. H. & FORGAC, M. (1997). Structure, function and regulation of the vacuolar H<sup>+</sup>-ATPase. *Ann. Rev. Cell Dev. Biol.* 13, 779-808.
- SUGIYAMA, S., MATSUKURA, H. & IMAE, Y. (1985). Relationship between Na<sup>+</sup>-dependent cytoplasmic pH homeostasis and Na<sup>+</sup>-dependent flagellar rotation and amino acid transport in alkalophilic *Bacillus*. *FEBS Lett.* 182(2), 265-268.
- TANABE, M., NISHIO, K., IKO, Y., SAMBONGI, Y., IWAMOTO-KIHARA, A., WADA, Y. & FUTAI, M. (2001). Rotation of a complex of the gamma subunit and c ring of *Escherichia coli* ATP synthase. The rotor and stator are interchangeable. *J. Biol. Chem.* 276(18), 15269-15274.
- THOMAS, D., MORGAN, D. G. & DEROSIER, D. J. (2001). Structures of bacterial flagellar motors from two FliF-FliG gene fusion mutants. *J. Bacteriol.* 183(21), 6404-6412.
- VALIYAVEETIL, F. I. & FILLINGAME, R. H. (1997). On the role of Arg-210 and Glu-219 of subunit a in proton translocation by the *Escherichia coli* F<sub>o</sub>F<sub>1</sub>-ATP synthase. *J. Biol. Chem.* 272(51), 32635-32641.
- VIK, S. B. & ANTONIO, B. J. (1994). A mechanism of proton translocation by F<sub>1</sub>F<sub>o</sub> ATP synthases by double mutants of the a subunit. *J. Biol. Chem.* 269(48), 30364-30369.
- VON BALLMOOS, C., APPOLDT, Y., BRUNNER, J., GRANIER, T., VASELLA, A. & DIMROTH, P. (2002). Membrane topography of the coupling ion binding site in Na<sup>+</sup>-translocating F<sub>1</sub>F<sub>o</sub> ATP synthase. *J. Biol. Chem.* 277(5), 3504-3510.
- VONCK, J., KRUG VON NIDDA, T., MEIER, T., MATTHEY, U., MILLS, D. J., KÜHLBRANDT, W. & DIMROTH, P. (2002). Molecular architecture of the undecameric rotor of a bacterial Na<sup>+</sup>-ATP synthase. *J. Mol. Biol.* 321(2), 307-316.

- WADA, W., LONG, J. C., ZHANG, D. & VIK, S. B. (1999). A novel labeling approach supports the five-transmembrane model of subunit a of the *Escherichia coli* ATP synthase. *J. Biol. Chem.* 274(24), 17353-17357.
- WALZ, D. & CAPLAN, S. R. (2002). Bacterial flagellar motor and H<sup>+</sup>/ATP synthase: two proton-driven rotary molecular devices with different functions. *Bioelectrochemistry* 55(1-2), 89-92.
- WEHRLE, F., KAIM, G. & DIMROTH, P. (2002). Molecular mechanism of the ATP synthase's F<sub>o</sub> motor probed by mutational analysis. *J. Mol. Biol.* 322(2), 369-381.
- WELCH, M., OOSAWA K., AIZAWA S. & EISENBACH M. (1993). Phosphorylation-dependent binding of a signal molecule to the flagellar switch of bacteria. *Proc. Natl. Acad. Sci. USA* 90(19), 8787-8791.
- WIECZOREK, H., BROWN, D., GRINSTEIN, S., EHRENFELD, J. & HARVEY, W. R. (1999). Animal plasma membrane energization by proton-motive V-ATPases. *Bioessays* 21(8), 637-648.
- WIECZOREK, H., GRUBER, G., HARVEY, W. R., HUSS, M., MERZENDORFER, H. & ZEISKE, W. (2000). Structure and regulation of insect plasma membrane H<sup>+</sup> V-ATPase. *J. Exp. Biol.* 203 Pt 1, 127-135.
- YAMAGUCHI, S., AIZAWA S., KIHARA M., ISOMURA M., JONES C. J. & MACNAB R. M. (1986). Genetic evidence for a switching and energy-transducing complex in the flagellar motor of *Salmonella typhimurium*. *J. Bacteriol.* 168(3), 1172-1179.
- YORIMITSU, T. & HOMMA, M. (2001). Na<sup>+</sup>-driven flagellar motor of *Vibrio*. *Biochim. Biophys. Acta* 1505(1), 82-93.
- YORIMITSU, T., SATO, K., ASAI, Y., KAWAGISHI, I. & HOMMA, M. (1999). Functional interaction between PomA and PomB, the Na<sup>+</sup>-driven flagellar motor components of *Vibrio alginolyticus*. *J. Bacteriol.* 181(16), 5103-5106.
- ZHOU, J., FAZZIO, R. T. & BLAIR, D. F. (1995). Membrane topology of the MotA protein of *Escherichia coli*. *J. Mol. Biol.* 251(2), 237-242.
- ZHOU, J., LLOYD, S. A. & BLAIR, D. F. (1998a). Electrostatic interactions between rotor and stator in the bacterial flagellar motor. *Proc. Natl. Acad. Sci. USA* 95(11), 6436-6441.
- ZHOU, J., SHARP, L. L., TANG, H. L., LLOYD, S. A., BILLINGS, S., BRAUN, T. F. & BLAIR, D. F. (1998b). Function of protonatable residues in the flagellar motor of *Escherichia coli*: a critical role for Asp32 of MotB. *J. Bacteriol.* 180(10), 2729-2735.
- ZHOU, Y., DUNCAN, T. M. & CROSS, R. L. (1997). Subunit rotation in *Escherichia coli* F<sub>o</sub>F<sub>1</sub>-ATP synthase during oxidative phosphorylation. *Proc. Natl. Acad. Sci. USA* 94(20), 10583-10587.



## APPENDIX

### Transport activities of mutants at cGlu65 from *P. modestum* ATPase

#### Experimental Procedures

Plasmids pT7c(ED) and pT7c(EQ) harbouring mutations cE65D and cE65Q, respectively were constructed using the Quick Change Site Directed Mutagenesis Kit as described by the manufacturer (Stratagene) and plasmid pT7c as template (Matthey *et al.*, 1997). The primers used for site-directed mutagenesis are listed in Table 1. The resulting plasmids were sequenced according to the dideoxynucleotide chain-termination method (Sanger *et al.*, 1977) using a *Taq* DyeDeoxy terminator cycle sequencing kit and the ABI Prism 310 genetic analyzer from Applied Biosystems. Synthesis of the mutant c subunits and purification was performed as described (Matthey *et al.*, 1997; Matthey *et al.*, 1999). *In vitro* assembly of F<sub>o</sub> from single subunits, reconstitution of F<sub>o</sub> and F<sub>1</sub>F<sub>o</sub> liposomes and <sup>22</sup>Na<sup>+</sup> transport measurements followed the procedures described in Wehrle *et al.* (2002).

Primer	Sequence (5'-3')	Restriction site
Mpc65Q V	GACAAGCGATCGCGCA <b>AT</b> CAACTG	<i>PvuI</i>
Mpc65Q R	CAGTTGAT <b>TTG</b> CGCGATCGCTTGTC	<i>PvuI</i>
Mpc65D V	ACAAGCGATCGCG <b>GA</b> CTCAACTGGT	<i>PvuI</i>
Mpc65D R	ACCAGTTGAG <b>GT</b> CCGCGATCGCTTGT	<i>PvuI</i>

**Table 1: Primers used for site directed mutagenesis.** The mutated codons are shown in bold and the newly introduced *PvuI* site is in italics.

#### Results

Together with purified subunits a and b, the mutant c subunits were reconstituted into F<sub>o</sub> liposomes and ΔΨ-driven <sup>22</sup>Na<sup>+</sup> transport was determined. The results of figure 1A show that mutant cE65D translocates <sup>22</sup>Na<sup>+</sup> ions with a velocity of about 56 % of the wild-type activity, whereas mutant cE65Q was not active. Sodium transport stopped after incubation of the proteoliposomes with DCCD. ATP-driven

$^{22}\text{Na}^+$  uptake was determined with  $\text{F}_1\text{F}_0$  liposomes from mutant cE65D and from wild-type. The mutant was only marginally active at approximately 30 % of the wild-type enzyme. ATP-driven sodium pumping was inhibited by the incubation of the proteoliposomes with DCCD, indicating that in the mutant ATP hydrolysis and sodium transport were coupled.

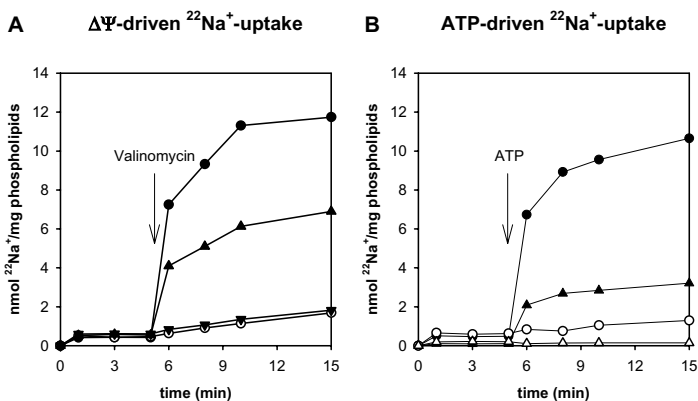


**Figure 1:**  $^{22}\text{Na}^+$  transport activities of proteoliposomes containing mutant cE65D (▲), mutant cE65Q (▼) or wild-type subunit c (●). **A**  $\Delta\Psi$ -driven  $^{22}\text{Na}^+$  uptake into  $\text{F}_0$  liposomes. The incubation mixture contained in 1 ml at 25 °C: 2 mM Tricine, pH 7.4, 100 mM cholinechlorid, 5 mM  $\text{MgCl}_2$ , 2 mM NaCl (0.47  $\mu\text{Ci}$ ) and 50  $\mu\text{l}$  proteoliposomes (10 mg phospholipids) loaded with 200 mM KCl.  $^{22}\text{Na}^+$ -uptake was initiated by the addition of 5  $\mu\text{M}$  valinomycin. Samples were taken at the indicated time points and  $^{22}\text{Na}^+$ -uptake was determined by  $\gamma$ -counting. As a control, wild-type proteoliposomes were measured after incubation with 100  $\mu\text{M}$  DCCD for 20 min (○). **B** For the determination of ATP-driven  $^{22}\text{Na}^+$  uptake 50  $\mu\text{l}$   $\text{F}_1\text{F}_0$  liposomes (10 mg phospholipids) were diluted into 1 ml of 20 mM potassium phosphate buffer, pH 7.4, 5 mM  $\text{MgCl}_2$ , 2 mM NaCl (0.47  $\mu\text{Ci}$ ), 6 mM phosphoenolpyruvate and 20 U pyruvate kinase. Five min after starting the incubation, sodium uptake was initiated by the addition of 1.25 mM ATP. Control experiments were performed after incubation of the  $\text{F}_1\text{F}_0$  liposomes with 100  $\mu\text{M}$  DCCD for 20 min (open symbols).  $^{22}\text{Na}^+$  uptake was subsequently determined as described above.

Our data corroborate earlier results from the *E. coli* enzyme. It was found that after replacing cAsp61 from *E. coli* by a glutamate about 30 % of ATP-driven proton transport remained, whereas no  $\text{H}^+$ -quenching was measured with mutant cD61N (Miller *et al.*, 1990). The transfer of the aspartate of position 61 to the position of cAla24 also yielded an active enzyme complex. The conclusion from these data

suggests that the presence of a carboxyl group at the ion binding site is important for a functional  $F_0$  complex.

## References

- MATTHEY, U., KAIM, G., BRAUN, D., WÜTHRICH, K. & DIMROTH, P. (1999). NMR studies of subunit c of the ATP synthase from *Propionigenium modestum* in dodecylsulfate micelles. *Eur. J. Biochem.* 261(2), 459-467.
- MATTHEY, U., KAIM, G. & DIMROTH, P. (1997). Subunit c from the sodium-ion-translocating  $F_1F_3$ -ATPase of *Propionigenium modestum*. Production, purification and properties of the protein in dodecylsulfate solution. *Eur. J. Biochem.* 247(3), 820-825.
- MILLER, M. J., OLDENBURG, M. & FILLINGAME, R. H. (1990). The essential carboxyl group in subunit c of the  $F_1F_0$  ATP synthase can be moved and  $H^+$ -translocating function retained. *Proc. Natl. Acad. Sci. USA* 87(13), 4900-4904.
- SANGER, F., NICKLEN, S. & COULSON, A. R. (1977). DNA sequencing with chain-terminating inhibitors. *Proc. Natl. Acad. Sci. USA* 74(12), 5463-5467.
- WEHRLE, F., APPOLDT, Y., KAIM, G. & DIMROTH, P. (2002). Reconstitution of  $F_0$  of the ATP synthase of *Propionigenium modestum* from its heterologously expressed and purified subunits. *Eur. J. Biochem.* 269(10), 2567-2573.

## CURRICULUM VITAE

### **Franziska Wehrle**

born May 10, 1972 in Uznach (SG), Switzerland

citizen of Muolen (SG), Switzerland

1978 – 1984 Primary education in Kaltbrunn (SG), Switzerland

1984 – 1986 Secondary education in Kaltbrunn (SG), Switzerland

1986 – 1992 Gymnasium; Kantonsschule Wattwil (SG), Switzerland  
Final examination: Matura type B

1992 – 1997 Studies of Biology at the Swiss Federal Institute of Technology (ETH),  
Zürich  
Diploma Thesis at the Institute of Microbiology, ETH Zürich

1997 – 2002 Assistant researcher at the institute of Microbiology, ETH Zürich  
Ph. D. Thesis

## LIST OF PUBLICATIONS

- WEHRLE, F., KAIM, G. & DIMROTH, P. (2002) Molecular mechanism of the ATP synthase's  $F_0$  motor probed by mutational analyses of subunit a, *J. Mol. Biol.* 322(2):369-381.
- WEHRLE, F., APPOLDT, Y., KAIM, G. & DIMROTH, P. (2002) Reconstitution of  $F_0$  of the sodium ion translocating ATP synthase of *Propionigenium modestum* from its heterologously expressed and purified subunits, *Eur. J. Biochem.* 269(10):2567-2573.
- KAIM G., WEHRLE F., GERIKE U. & DIMROTH P. (1997) Molecular basis for the coupling ion selectivity of  $F_1F_0$  ATP synthases: probing the liganding groups for  $Na^+$  and  $Li^+$  in the c subunit of the ATP synthase from *Propionigenium modestum*, *Biochemistry* 36(30):9185-9194